

Zirconocene Dichlorides as Catalysts in Alkene Carbo- and Cyclometalation by AlEt_3 : Intermediate Structures and Dynamics

Lyudmila V. Parfenova,^{*,a} Pavel V. Kovyazin,^a Olesia V. Mukhamadeeva,^a Pavel V. Ivchenko,^{b,c}
Ilya E. Nifant'ev,^{b,c} Leonard M. Khalilov,^a and Usein M. Dzhemilev^a

^aInstitute of Petrochemistry and Catalysis of Russian Academy of Sciences, 450075 Ufa, prosp. Oktyabrya, 141, Russian Federation

^bDepartment of Chemistry, Lomonosov Moscow State University, 119991 Moscow, 1-3 Leninskiye Gory, Russian Federation

^cA.V. Topchiev Institute of Petrochemical Synthesis, Russian Academy of Sciences, Leninsky prosp. 29, 119991 Moscow, Russian Federation

Supporting Information

The procedure for the evaluation of the exchange constants using the line- shape analysis	4
Figure S1. VT ^{13}C NMR of $(\text{AlEt}_3)_2$:	4
Figure S2. Plots of $\ln(k/T)$ vs $1/T$ for the ethyl group exchange in $(\text{AlEt}_3)_2$ obtained from line-shape analysis:.....	5
The procedure for the evaluation of the constants of the exchange in $\text{L}_2\text{Zr}(\mu\text{-Cl})\text{CH}_2\text{CH}_2\text{AlEt}_2$ (16m,n,p,q) using 2D EXSY	5
Figure S3. ^1H NMR of ClAlEt_2 in C_7D_8	6
Figure S4. ^{13}C NMR of ClAlEt_2 in C_7D_8	6
Figure S5. ^1H NMR of Cp_2ZrEtCl obtained by the reaction of $\text{Cp}_2\text{ZrHCl}+\text{C}_2\text{H}_4$ in C_7D_8 (270 K).	7
Figure S6. HSQC of Cp_2ZrEtCl obtained by the reaction of $\text{Cp}_2\text{ZrHCl}+\text{C}_2\text{H}_4$ in C_7D_8 (270 K).	7
Figure S7. ^1H NMR of system Cp_2ZrCl_2 (1a) - $(\text{AlEt}_3)_2$ (1:20) in C_7D_8 (5 min).	8
Figure S8. ^1H NMR of system Cp_2ZrCl_2 (1a) - $(\text{AlEt}_3)_2$ (1:20) in C_7D_8 (20 min).	8
Figure S9. ^{13}C NMR of system Cp_2ZrCl_2 (1a) - $(\text{AlEt}_3)_2$ (1:20) in C_7D_8	9
Figure S10. HSQC of system Cp_2ZrCl_2 (1a) - $(\text{AlEt}_3)_2$ (1:20) in C_7D_8 (20 min).	9
Figure S11. HMBC of system Cp_2ZrCl_2 (1a) - $(\text{AlEt}_3)_2$ (1:20) in C_7D_8	10
Figure S12. EXSY of system Cp_2ZrCl_2 (1a) - AlEt_3 at 290 in C_7D_8 ($\tau = 1$ s).	10
Figure S13. ^1H NMR of system $(\text{CpMe})_2\text{ZrCl}_2$ (1b) - $(\text{AlEt}_3)_2$ in C_7D_8	11
Figure S14. ^{13}C NMR of system $(\text{CpMe})_2\text{ZrCl}_2$ (1b) - $(\text{AlEt}_3)_2$ in C_7D_8	11
Figure S15. COSY HH of system $(\text{CpMe})_2\text{ZrCl}_2$ (1b) - $(\text{AlEt}_3)_2$ in C_7D_8	12
Figure S16. HSQC of system $(\text{CpMe})_2\text{ZrCl}_2$ (1b) - $(\text{AlEt}_3)_2$ in C_7D_8	12
Figure S17. ^1H NMR of complex 16a obtained by the reaction of Cp_2ZrEtCl with $(\text{AlEt}_3)_2$ in C_7D_8 (300 K).	13
Figure S18. ^{13}C NMR of complex 16a obtained by the reaction of Cp_2ZrEtCl with $(\text{AlEt}_3)_2$ in C_7D_8 (300 K).	13
Figure S19. HSQC of complex 16a in C_7D_8 (300 K).	14
Figure S20. ^{13}C NMR monitoring of reaction 16a + 1-hexene in C_7D_8	14
Figure S21. ^1H NMR of complex 16h obtained by the reaction of 1h with $(\text{AlEt}_3)_2$ (1:11) in C_7D_8 at 270 K.	15
Figure S22. COSY HH of complex 16h in C_7D_8 at 270 K.	15
Figure S23. EXSY of complex 16h in C_7D_8 at 298 K ($\tau = 0.3$ s).	16
Figure S24. HMBC of complex 16h in C_7D_8 at 298 K.	16

Figure S25. ^1H NMR of 16m obtained by the reaction of 1m with $(\text{AlEt}_3)_2$ (1:13) in C_7D_8 at 298 K.	17
Figure S26. COSY HH of 16m in C_7D_8 at 260 K.	17
Figure S27. ^{13}C NMR of 16m in C_7D_8 at 260 K.	18
Figure S28. HSQC of 16m in C_7D_8 at 260 K.	18
Figure S29. EXSY of 16m in C_7D_8 at 298 K ($\tau = 0.3$ s).	19
Figure S30. ^1H NMR of 16m obtained by the reaction of 1m with $(\text{AlEt}_3)_2$ (1:24) in CD_2Cl_2 at 270 K.	19
Figure S31. ^1H NMR of complex 16n obtained by the reaction of 1n with $(\text{AlEt}_3)_2$ (1:16) in C_7D_8 at 285 K.	20
Figure S32. COSY HH of 16n in C_7D_8 at 270 K.	20
Figure S33. ^{13}C NMR of 16n in C_7D_8 at 270 K.	21
Figure S34. HSQC of 16n in C_7D_8 at 270 K.	21
Figure S35. HMBC of 16n in C_7D_8 at 270 K.	22
Figure S36. EXSY spectrum of 16n in C_7D_8 at 293 K ($\tau = 0.3$ s).	22
Figure S37. ^1H NMR of 16p obtained by the reaction of 1p with $(\text{AlEt}_3)_2$ (1:13) in C_7D_8 at 280 K.	23
Figure S38. COSY HH of 16p in C_7D_8 at 260 K.	23
Figure S39. HSQC of 16p in C_7D_8 at 270 K.	24
Figure S40. HMBC of 16p in C_7D_8 at 270 K.	24
Figure S41. EXSY spectrum of 16p in C_7D_8 at 293 K ($\tau = 0.3$ s).	25
Figure S42. ^1H NMR of 16p obtained by the reaction of 1p with $(\text{AlEt}_3)_2$ (1:13) in CD_2Cl_2 at 280 K.	25
Figure S43. ^1H NMR of 16q obtained by the reaction of 1q with $(\text{AlEt}_3)_2$ (1:2) in C_7D_8 at 285 K.	26
Figure S44. COSY HH of 16q in C_7D_8 at 260 K.	26
Figure S45. ^{13}C NMR of 16q in C_7D_8 at 220 K.	27
Figure S46. HSQC of 16q in C_7D_8 at 220 K.	27
Figure S47. HMBC of 16q in C_7D_8 at 220 K.	28
Figure S48. EXSY of 16q in C_7D_8 at 290 K ($\tau = 0.3$ s).	28
Figure S49. ^1H NMR of 16q obtained by the reaction of 1q with $(\text{AlEt}_3)_2$ (1:13) in CD_2Cl_2 at 285 K.	29
Figure S50. ^1H NMR of 17l obtained by the reaction of 1l with $(\text{AlEt}_3)_2$ (1:24) in C_7D_8 at 298 K.	29
Figure S51. COSY HH of 17l in C_7D_8 at 298 K.	30
Figure S52. ^{13}C NMR of 17l in C_7D_8 at 298 K.	30
Figure S53. HSQC of 17l in C_7D_8 at 298 K.	31
Figure S54. HMBC of 17l in C_7D_8 at 298 K.	31
Figure S55. NOESY of 17l in C_7D_8 at 298 K.	32
Figure S56. ^1H NMR of 17m obtained by the reaction of 1m with $(\text{AlEt}_3)_2$ (1:13) in C_7D_8 at 299 K.	32
Figure S57. COSY HH of 17m in C_7D_8 at 299 K.	33
Figure S58. ^{13}C NMR of 17m in C_7D_8 at 299 K.	33
Figure S59. HSQC of 17m in C_7D_8 at 299 K.	34
Figure S60. HMBC of 17m in C_7D_8 at 299 K.	34
Figure S61. NOESY of 17m in C_7D_8 at 299 K.	35
Figure S62. ^1H NMR of system $\text{Cp}^*_2\text{ZrCl}_2$ (1c) - $(\text{AlEt}_3)_2$ (1:20) in C_7D_8 at 299 K.	35
Figure S63. COSY HH of system $\text{Cp}^*_2\text{ZrCl}_2$ (1c) - $(\text{AlEt}_3)_2$ (1:20) in C_7D_8	36

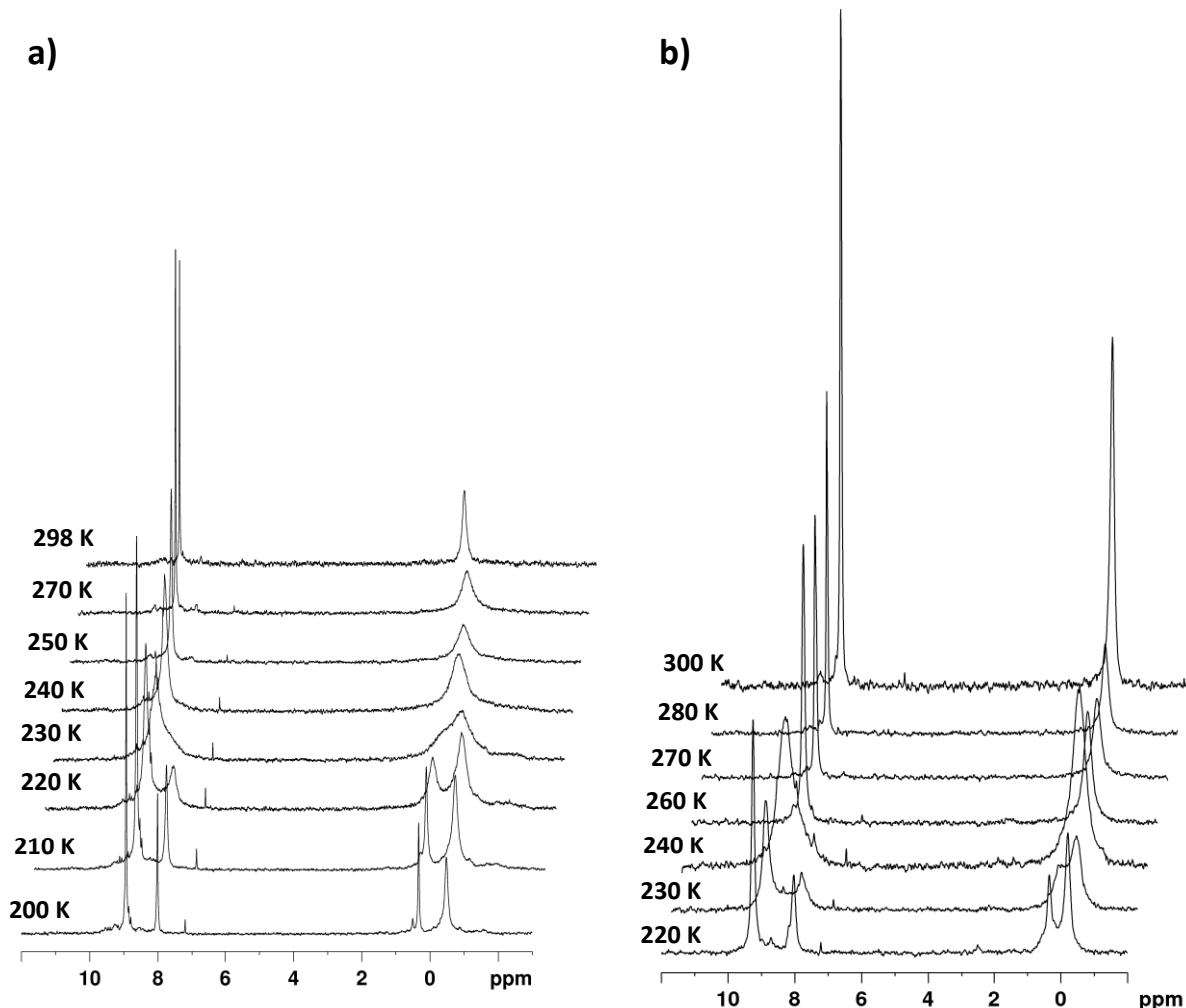
Figure S64. ^1H NMR of 20h obtained by the reaction of 1h with $(\text{AlEt}_3)_2$ (1:11) in C_7D_8 at 290 K.	36
Figure S65. COSY HH of 20h in C_7D_8 at 290 K.	37
Figure S66. ^{13}C NMR of 20h in C_7D_8 at 290 K.	37
Figure S67. HSQC of 20h in C_7D_8 at 290 K.	38
Figure S68. HMBC of 20h in C_7D_8 at 290 K.	38
Figure S69. ^1H NMR of 20p obtained by the reaction of 1p with $(\text{AlEt}_3)_2$ (1:13) in C_7D_8 at 305 K.	39
Figure S70. COSY HH of 20p in C_7D_8 at 299 K.	39
Figure S71. ^{13}C NMR of 20p in C_7D_8 at 299 K.	40
Figure S72. HSQC of 20p in C_7D_8 at 299 K.	40
Figure S73. HMBC of 20p in C_7D_8 at 299 K.	41
Figure S74. ^1H NMR of 20q obtained by the reaction of 1q with $(\text{AlEt}_3)_2$ (1:13) in CD_2Cl_2 at 298 K.	42
Figure S75. COSY HH of 20q in CD_2Cl_2 at 298 K.	42

The procedure for the evaluation of the exchange constants using the line- shape analysis.

The procedure is considered on the example of a solution of triethylaluminum in CD_2Cl_2 . Thus, the ^{13}C NMR spectra in the temperature range 200-300 K were recorded (Fig. S1).

Figure S1. VT ^{13}C NMR of $(\text{AlEt}_3)_2$:

a) 0.5 M/l in CD_2Cl_2 ; b) 0.6 M/l (AlEt_3) + 0.1 M/l (ClAlEt_2) in C_7D_8 .

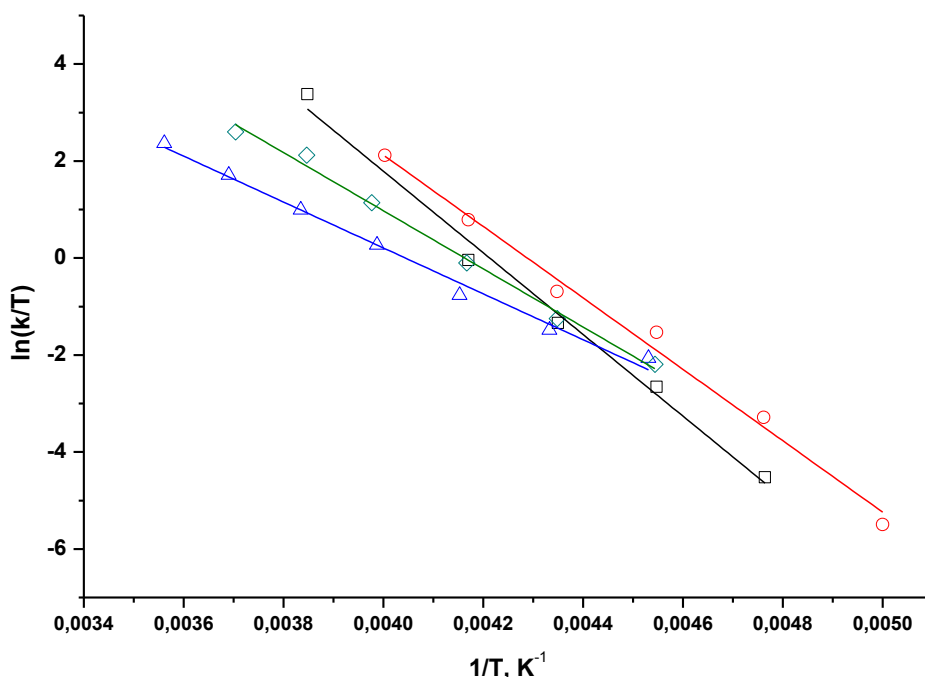


Line-shape analyses were carried out using Dynamic NMR module (version 1.1.2) implemented into the Bruker Topspin 3.2 program, which simulate 1D temperature dependent NMR spectra of coupled half spin nuclei, interactively set up and iteratively refine the model parameters to get the best fit of the measured and simulated 1D NMR spectra and to obtain the reaction speed parameters of exchange processes. The theory of the calculation, special features of the DNMR module (chemical exchange operators, fitting quality, etc.) and detailed procedure are described in the software manual "DNMR Lineshape Analysis" written by Dr. János Rohonczy, 2007.

The details on the constant evaluation via line-shape analysis are presented in the SI of Ref.[37].

Figure S2. Plots of $\ln(k/T)$ vs $1/T$ for the ethyl group exchange in $(AlEt_3)_2$ obtained from line-shape analysis:

□ - 4.8 M/l in CD_2Cl_2 , ○ - 0.5 M/l in CD_2Cl_2 , △ - 4.0 M/l in C_7D_8 , ◇ - 0.6 M/l $(AlEt_3)$ + 0.1 M/l $(ClAlEt_2)$ in C_7D_8 .



The procedure for the evaluation of the constants of the exchange in $L_2Zr(\mu-Cl)CH_2CH_2AlEt_2$ (16m,n,p,q) using 2D EXSY.

2D NMR EXSY (NOESY) spectra were recorded in the phase-sensitive mode using standard Bruker gradient pulse sequences with relaxation delay 1 s, 90° pulse - 8.0 μ s, mixing time $\tau=0.3$ -1 s. The mixing time was chosen in such a range that diagonal and cross- peaks were observed simultaneously. The areas of the diagonal and cross- peaks for the signals of the H^5 and H^6 atoms of the $ZrCH_2CH_2Al$ fragment in the -3 - 0 ppm region in the temperature range 290–310 K were determined. Constants of the exchange were calculated by the formula [Ch.L. Perrin, T.J. Dwyer, *Chem. Rev.*, 1990, **90**, 6, 935–967]:

$$k = \frac{1}{\tau} \ln \frac{r+1}{r-1}, \quad \text{where} \quad r = \frac{I_{AA} + I_{BB}}{I_{AB} + I_{BA}}$$

τ – mixing time, I_{AA} , I_{BB} – diagonal peak areas, I_{AB} , I_{BA} – cross-peak areas.

The values of ΔH^\ddagger , ΔG^\ddagger , ΔS^\ddagger were calculated according to the Eyring equation [J. Sandström, *Dynamic NMR Spectroscopy*. – NY: Academic Press, 1982. – 226p]:

$$\ln(k/T) = -\Delta H^\ddagger/RT + \Delta S^\ddagger/R + \ln(k_b/h),$$

where k_b – the Boltzmann constant, and h – the Planck constant.

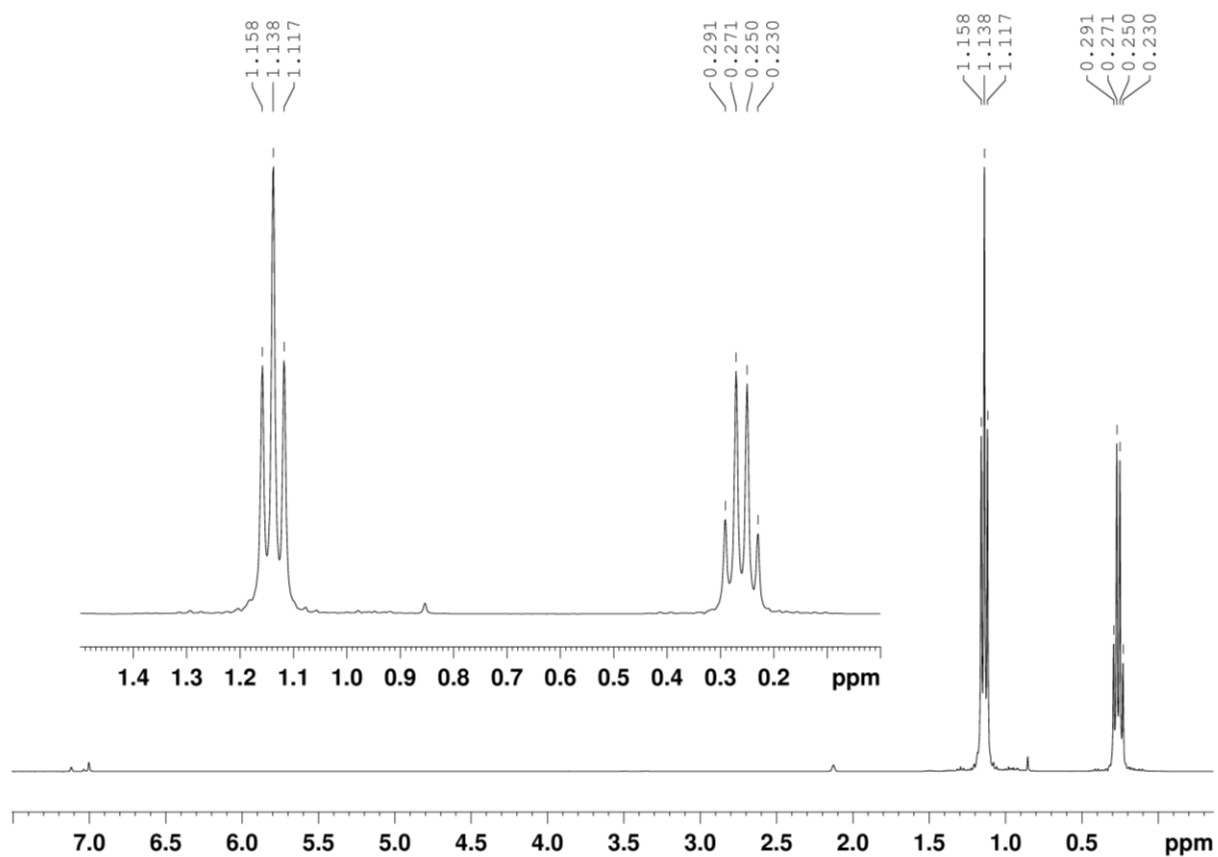
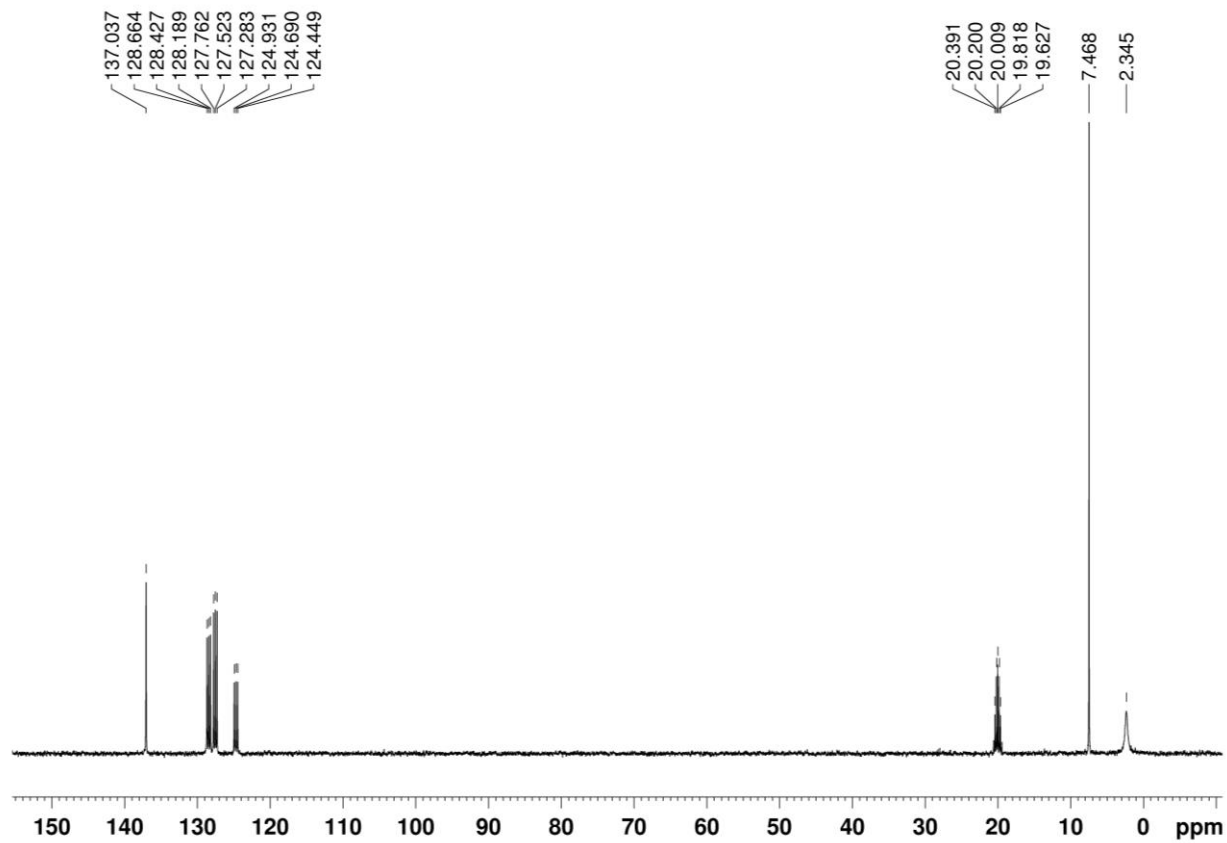
Figure S3. ^1H NMR of CIAIEt₂ in C₇D₈.**Figure S4.** ^{13}C NMR of CIAIEt₂ in C₇D₈.

Figure S5. ^1H NMR of Cp_2ZrEtCl obtained by the reaction of $\text{Cp}_2\text{ZrHCl} + \text{C}_2\text{H}_4$ in C_7D_8 (270 K).

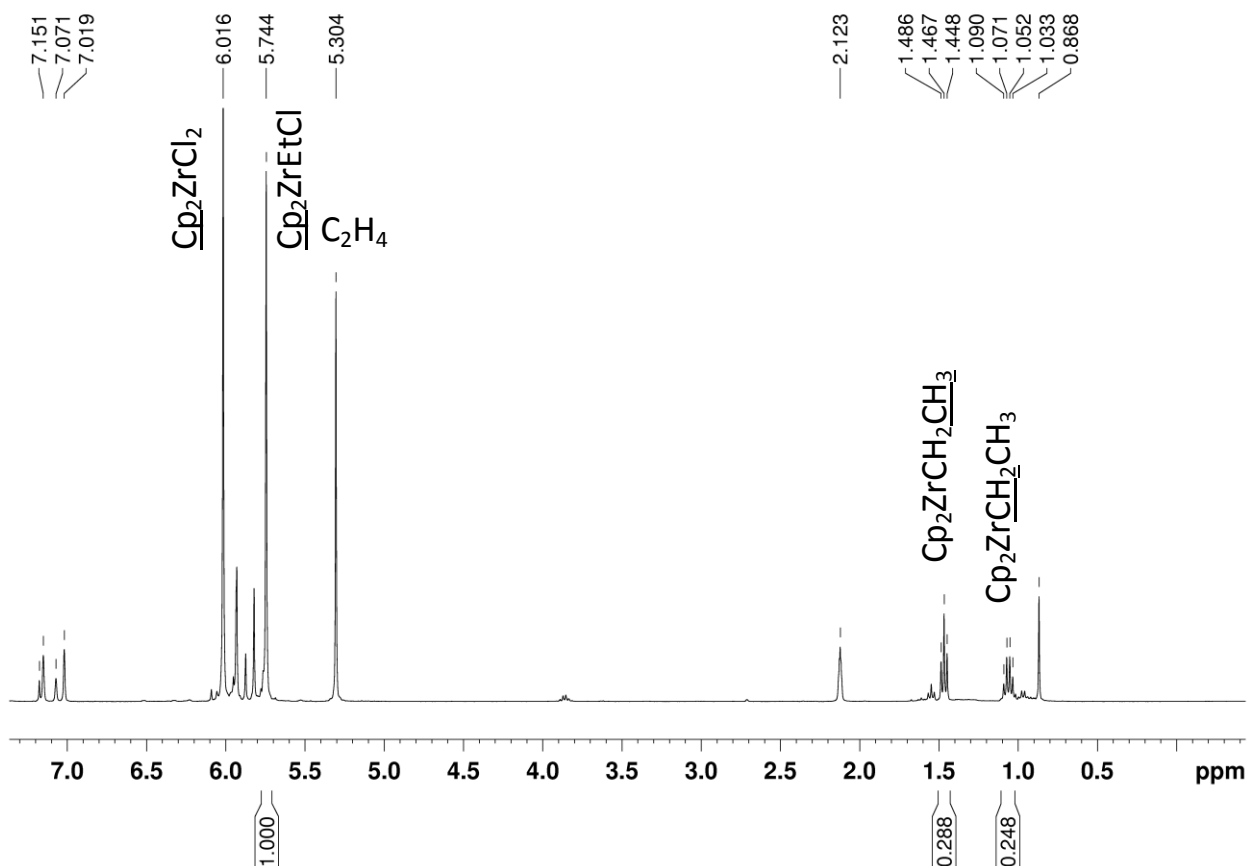


Figure S6. HSQC of Cp_2ZrEtCl obtained by the reaction of $\text{Cp}_2\text{ZrHCl} + \text{C}_2\text{H}_4$ in C_7D_8 (270 K).

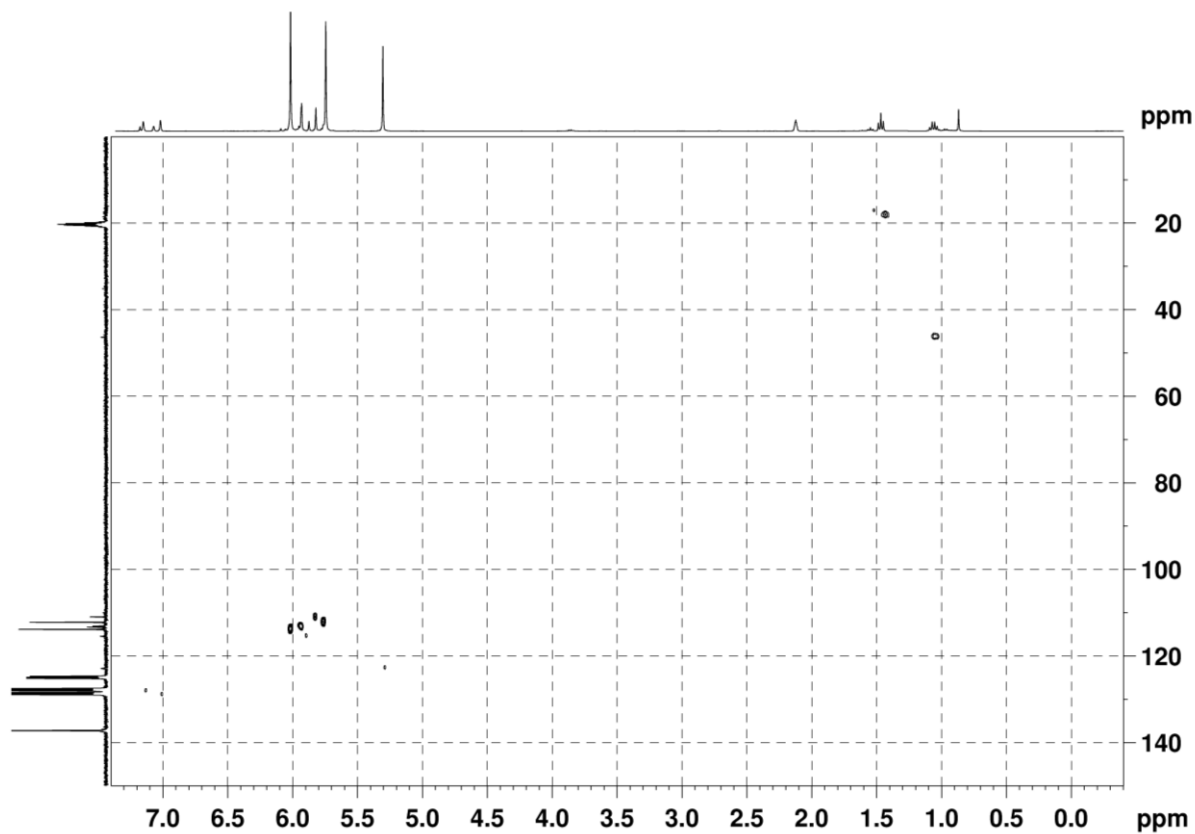


Figure S7. ^1H NMR of system Cp_2ZrCl_2 (**1a**) - $(\text{AlEt}_3)_2$ (1:20) in C_7D_8 (5 min).

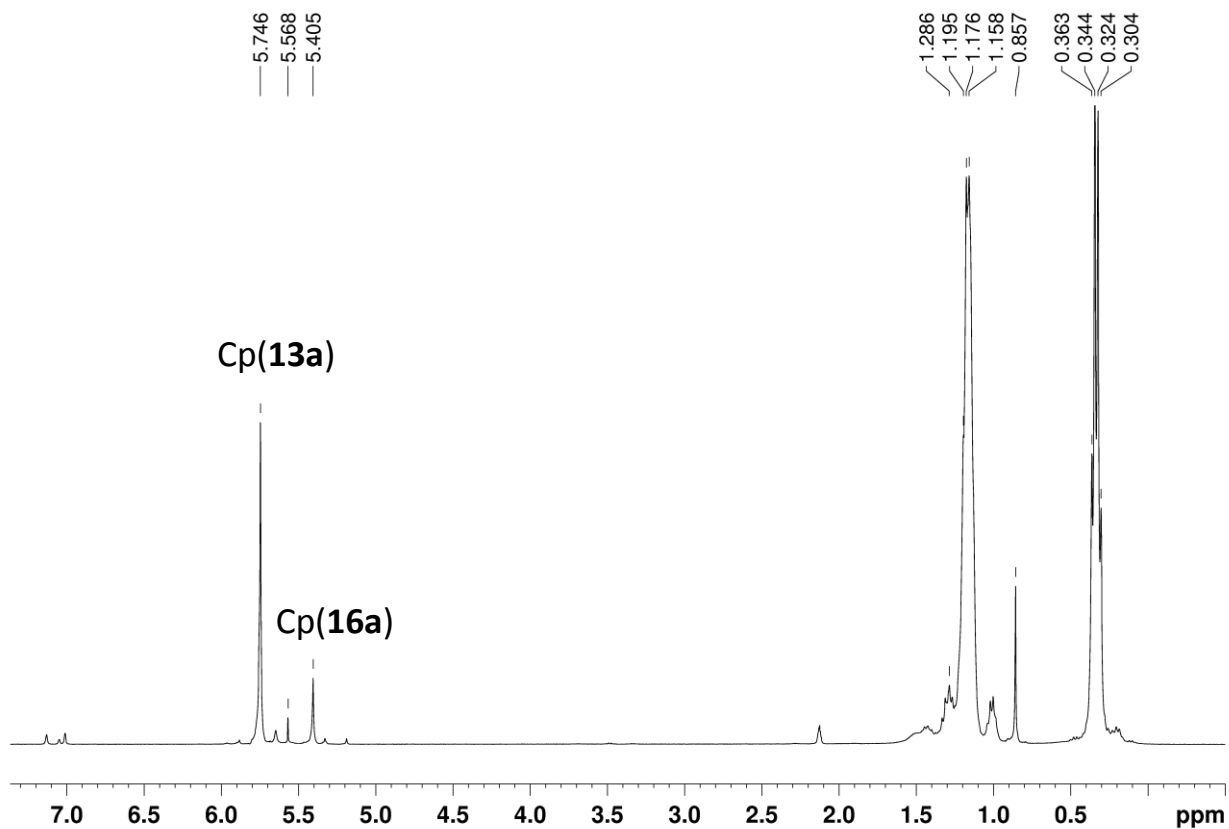


Figure S8. ^1H NMR of system Cp_2ZrCl_2 (**1a**) - $(\text{AlEt}_3)_2$ (1:20) in C_7D_8 (20 min).

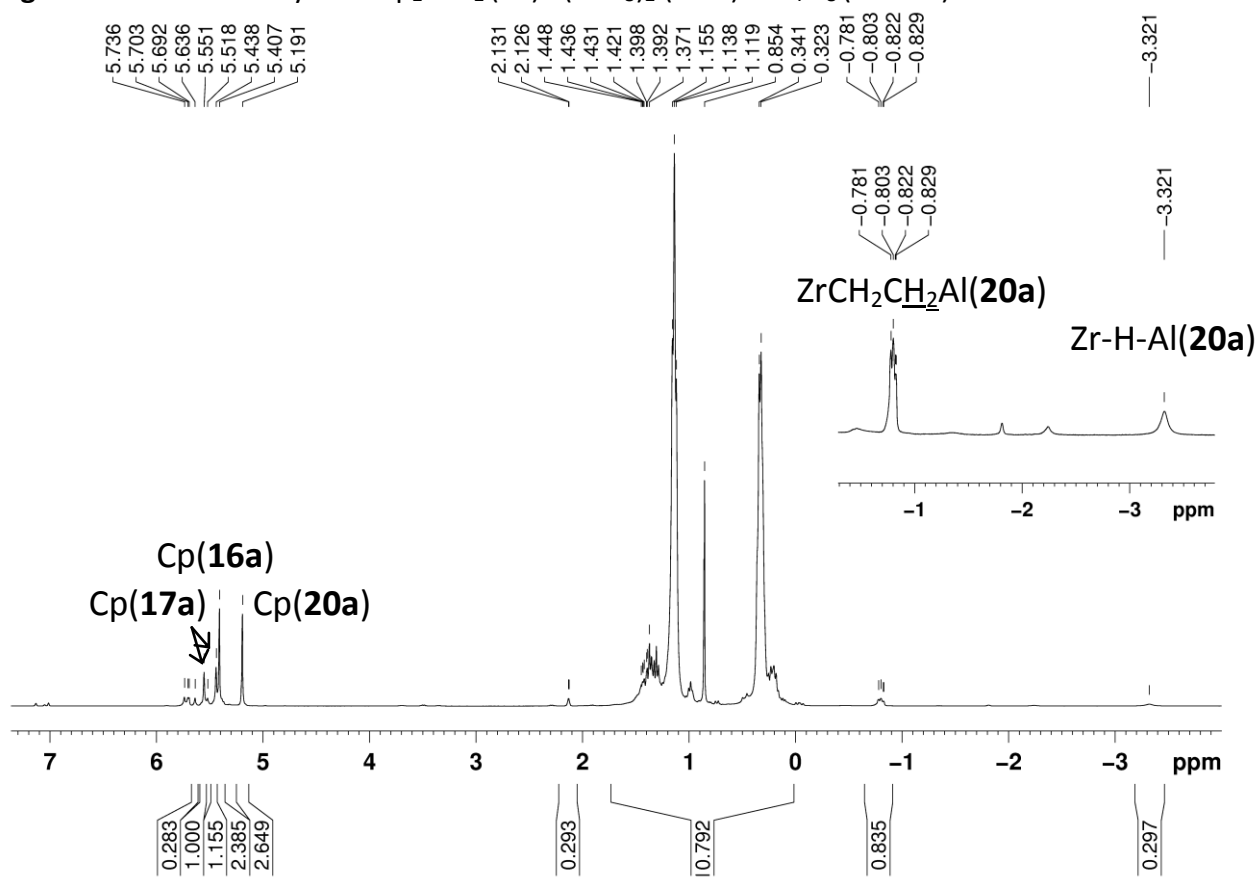


Figure S9. ^{13}C NMR of system Cp_2ZrCl_2 (**1a**) - $(\text{AlEt}_3)_2$ (1:20) in C_7D_8 .

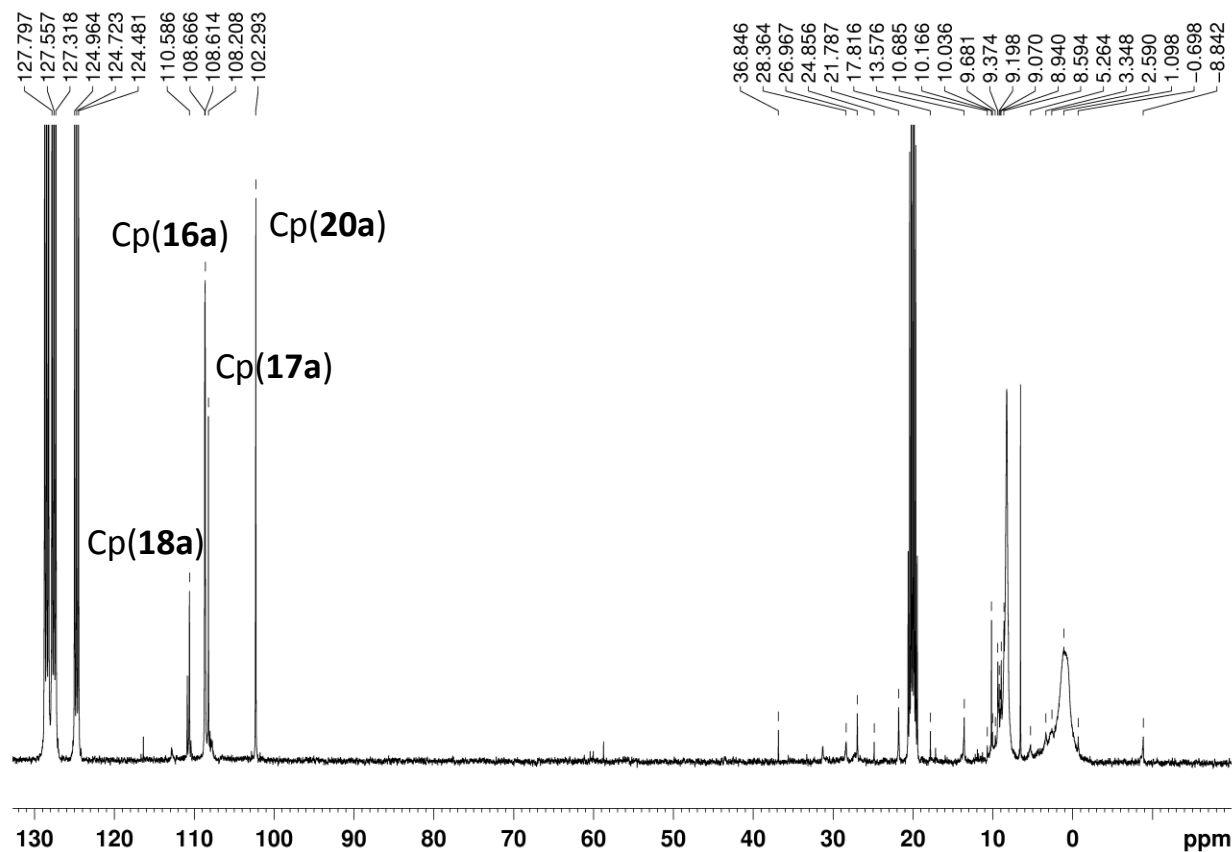


Figure S10. HSQC of system Cp_2ZrCl_2 (**1a**) - $(\text{AlEt}_3)_2$ (1:20) in C_7D_8 (20 min).

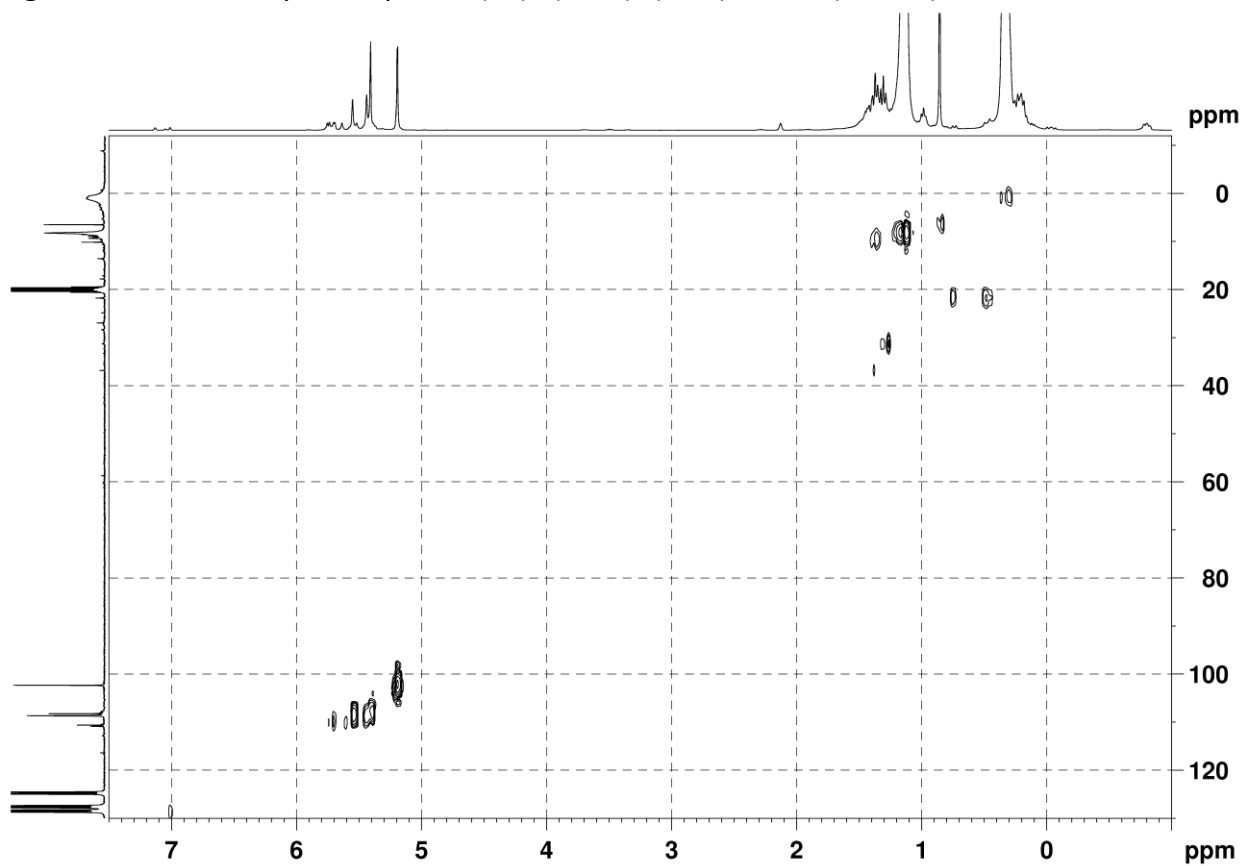


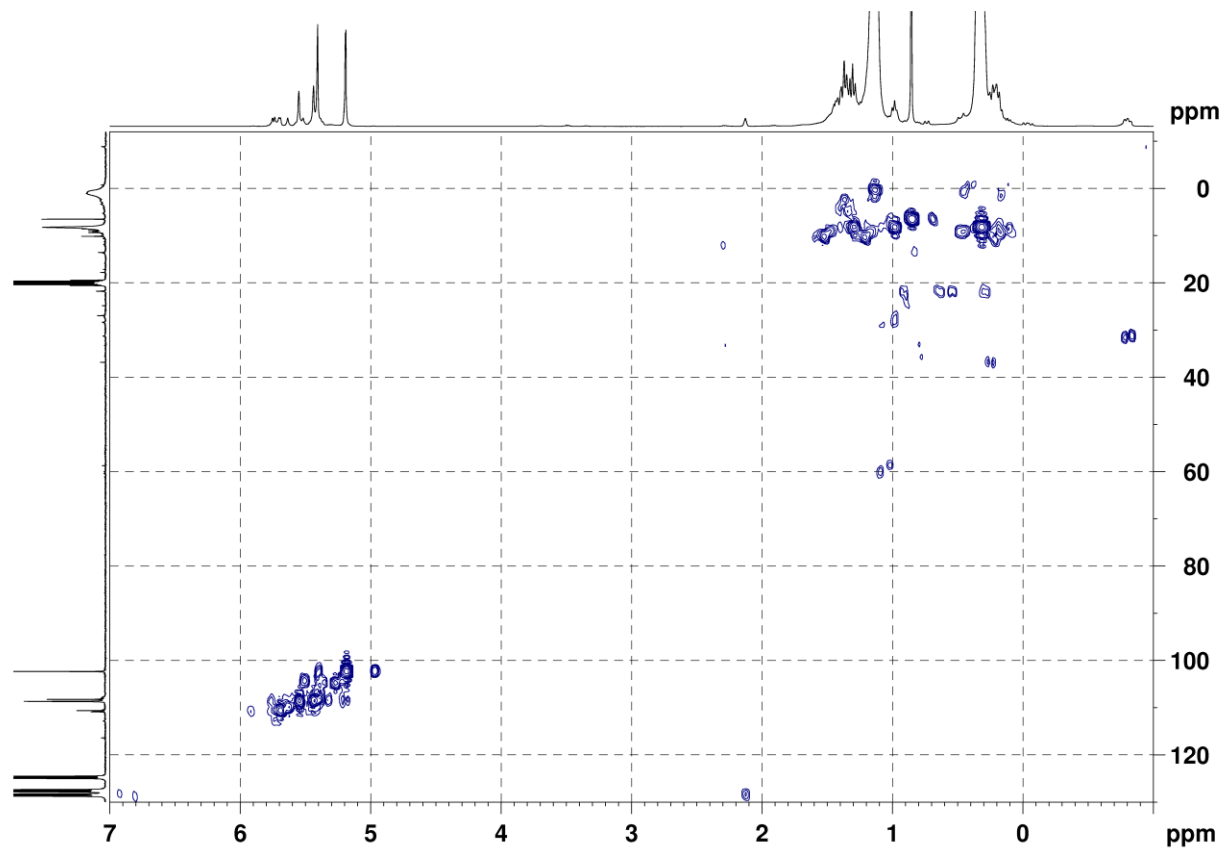
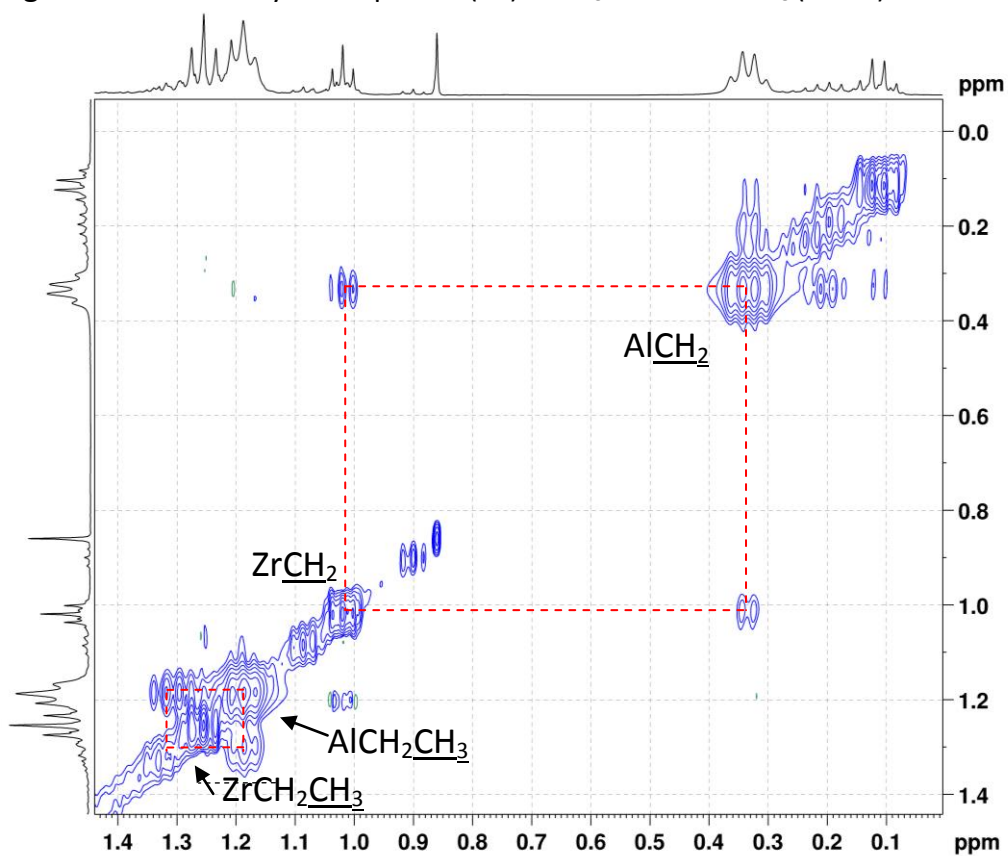
Figure S11. HMBC of system Cp_2ZrCl_2 (**1a**) - $(\text{AlEt}_3)_2$ (1:20) in C_7D_8 .**Figure S12.** EXSY of system Cp_2ZrCl_2 (**1a**) - AlEt_3 at 290 in C_7D_8 ($\tau = 1$ s).

Figure S13. ^1H NMR of system $(\text{CpMe})_2\text{ZrCl}_2$ (**1b**) - $(\text{AlEt}_3)_2$ (1:27) in C_7D_8 .

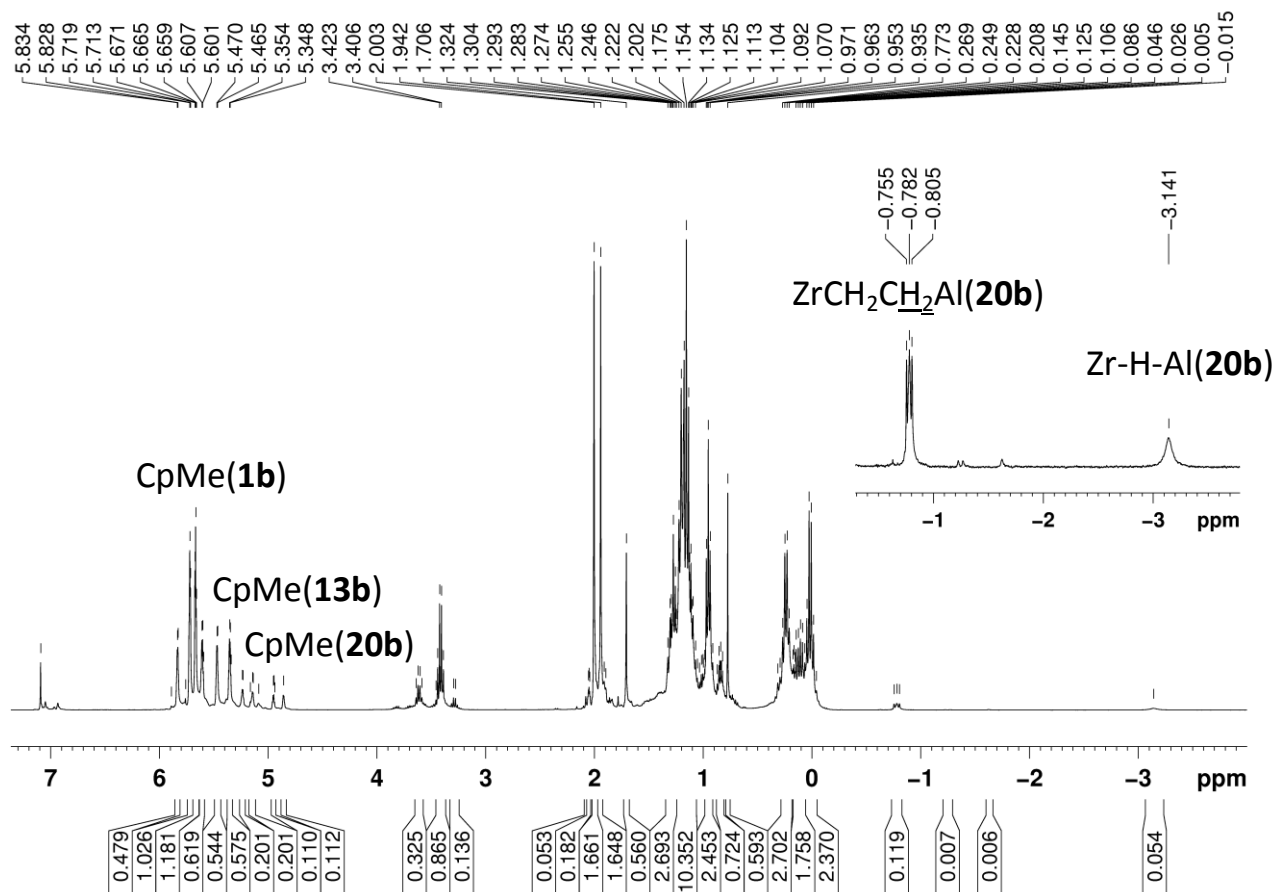


Figure S14. ^{13}C NMR of system $(\text{CpMe})_2\text{ZrCl}_2$ (**1b**) - $(\text{AlEt}_3)_2$ in C_7D_8 .

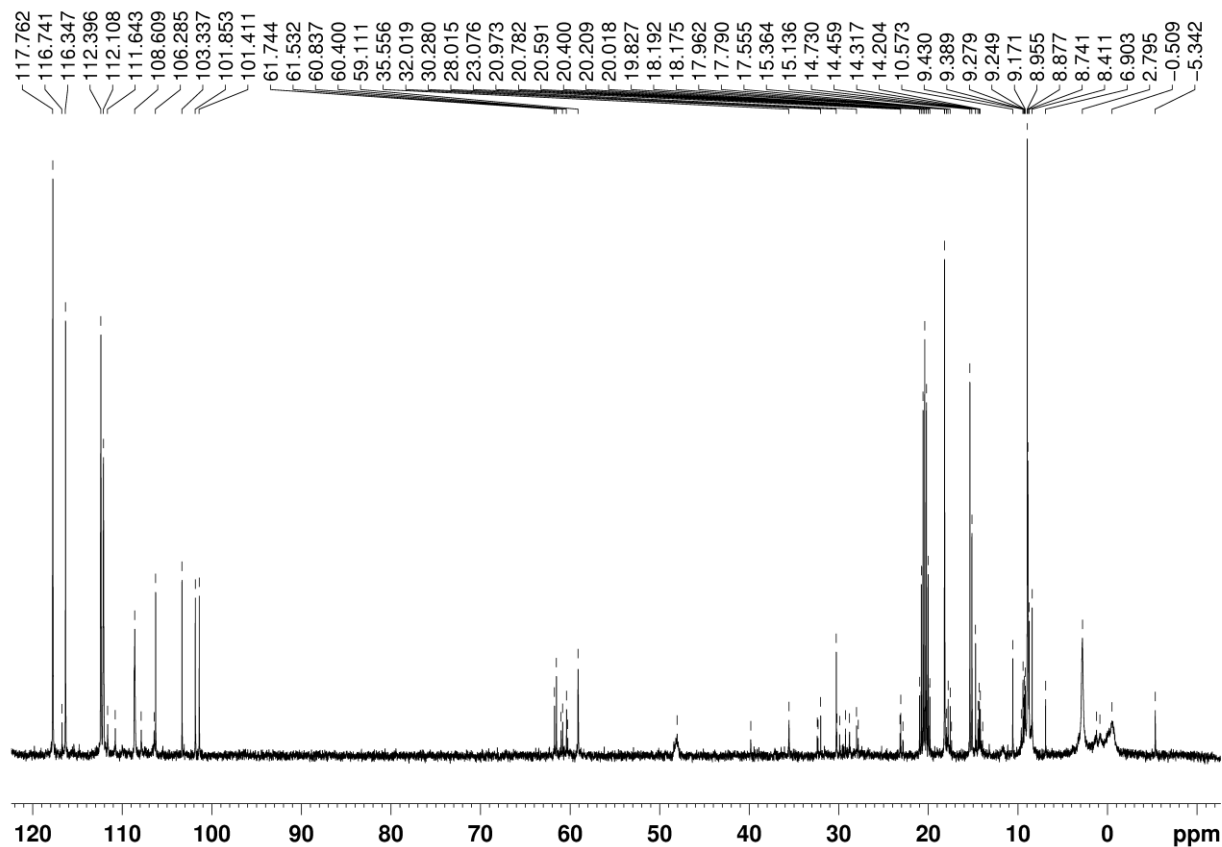


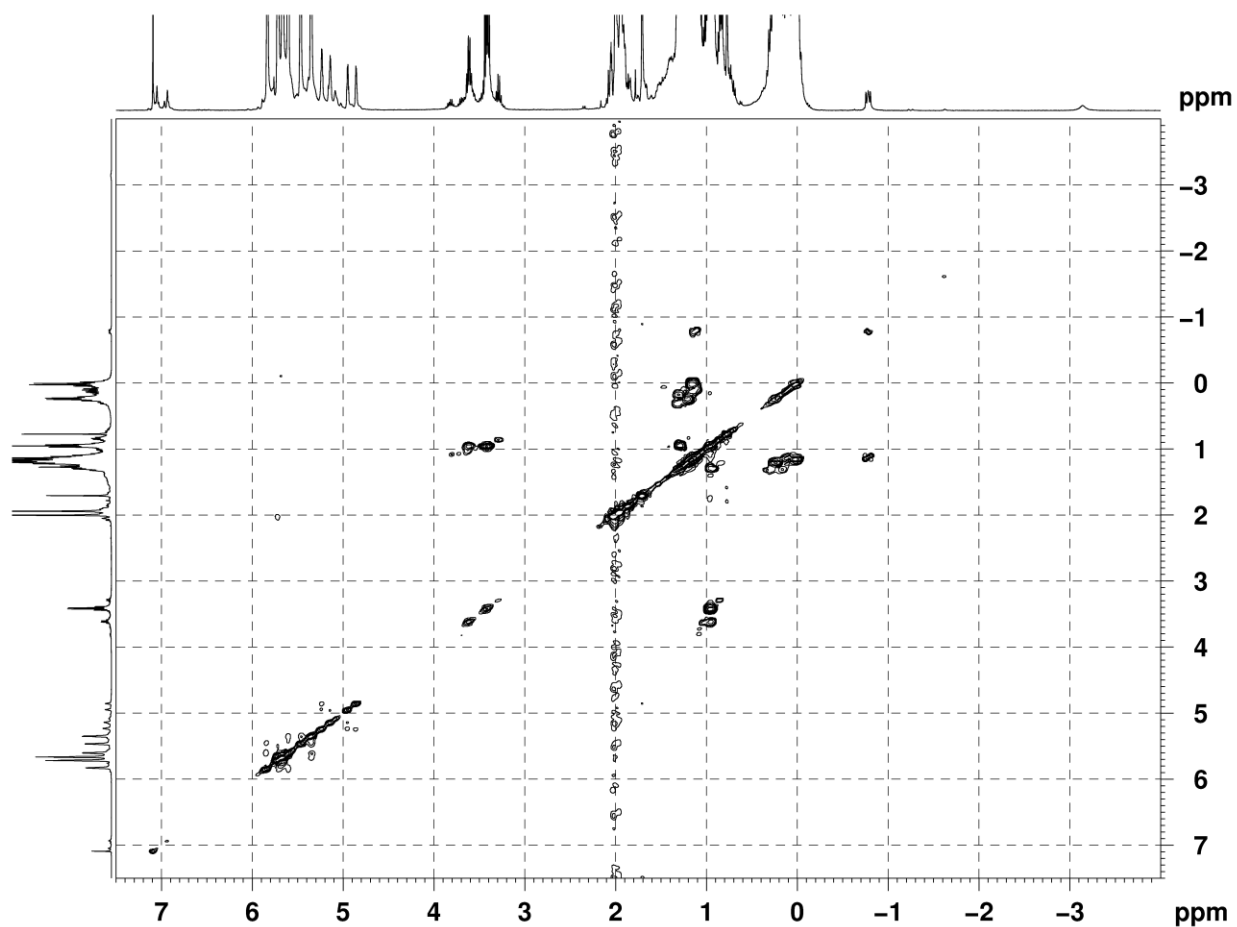
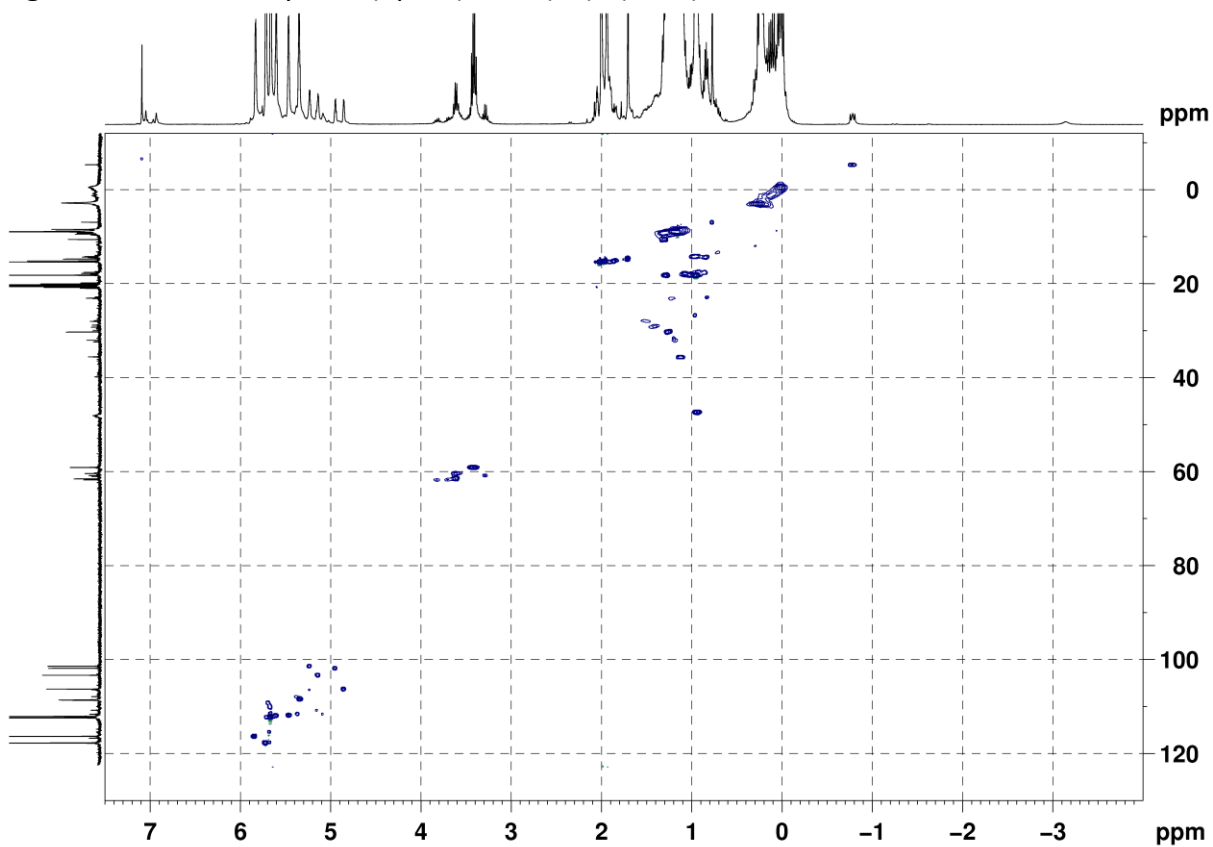
Figure S15. COSY HH of system $(\text{CpMe})_2\text{ZrCl}_2$ (**1b**) - $(\text{AlEt}_3)_2$ in C_7D_8 .**Figure S16.** HSQC of system $(\text{CpMe})_2\text{ZrCl}_2$ (**1b**) - $(\text{AlEt}_3)_2$ in C_7D_8 .

Figure S17. ^1H NMR of complex **16a** obtained by the reaction of Cp_2ZrEtCl with $(\text{AlEt}_3)_2$ in C_7D_8 (300 K).

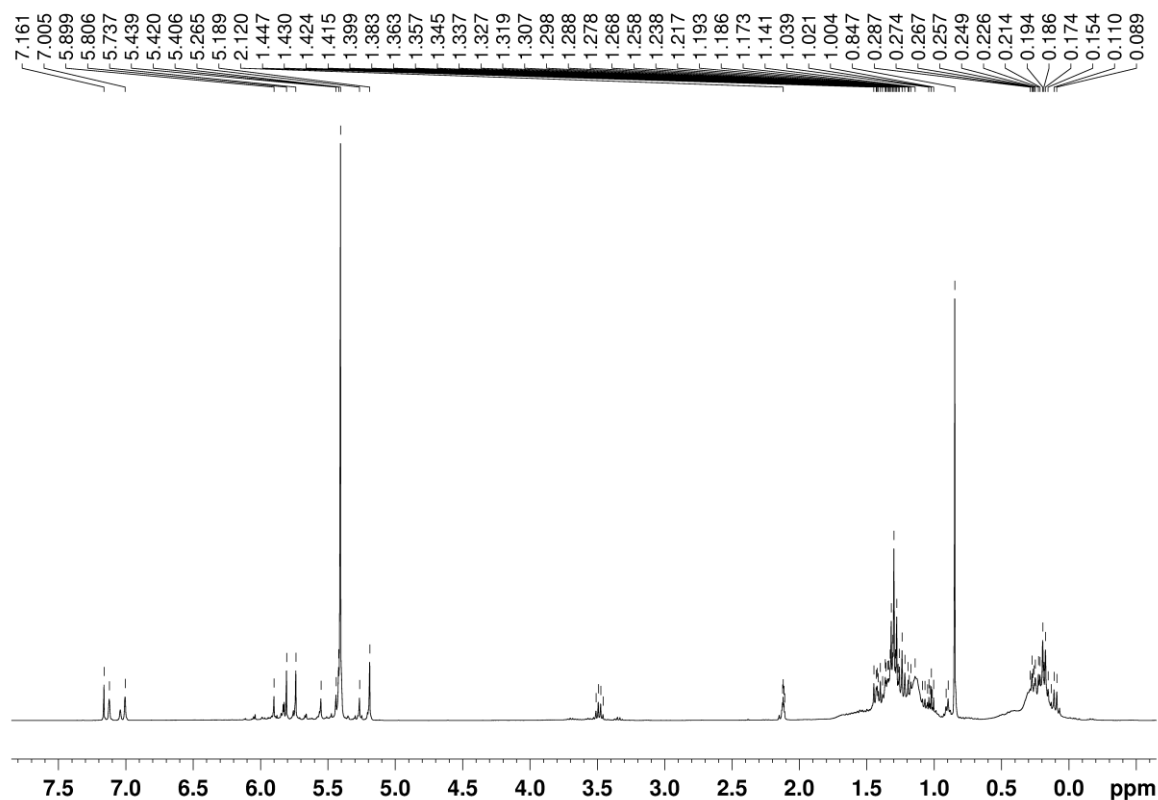


Figure S18. ^{13}C NMR of complex **16a** obtained by the reaction of Cp_2ZrEtCl with $(\text{AlEt}_3)_2$ in C_7D_8 (300 K).

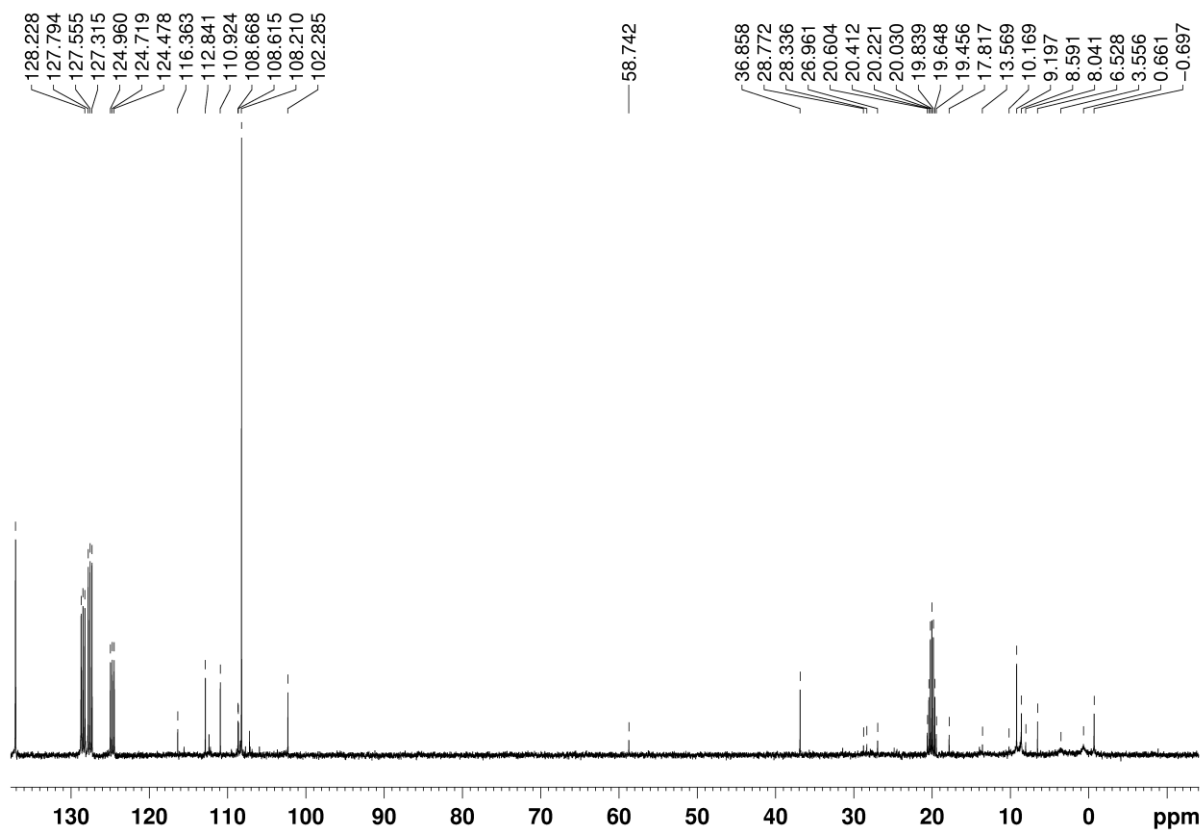


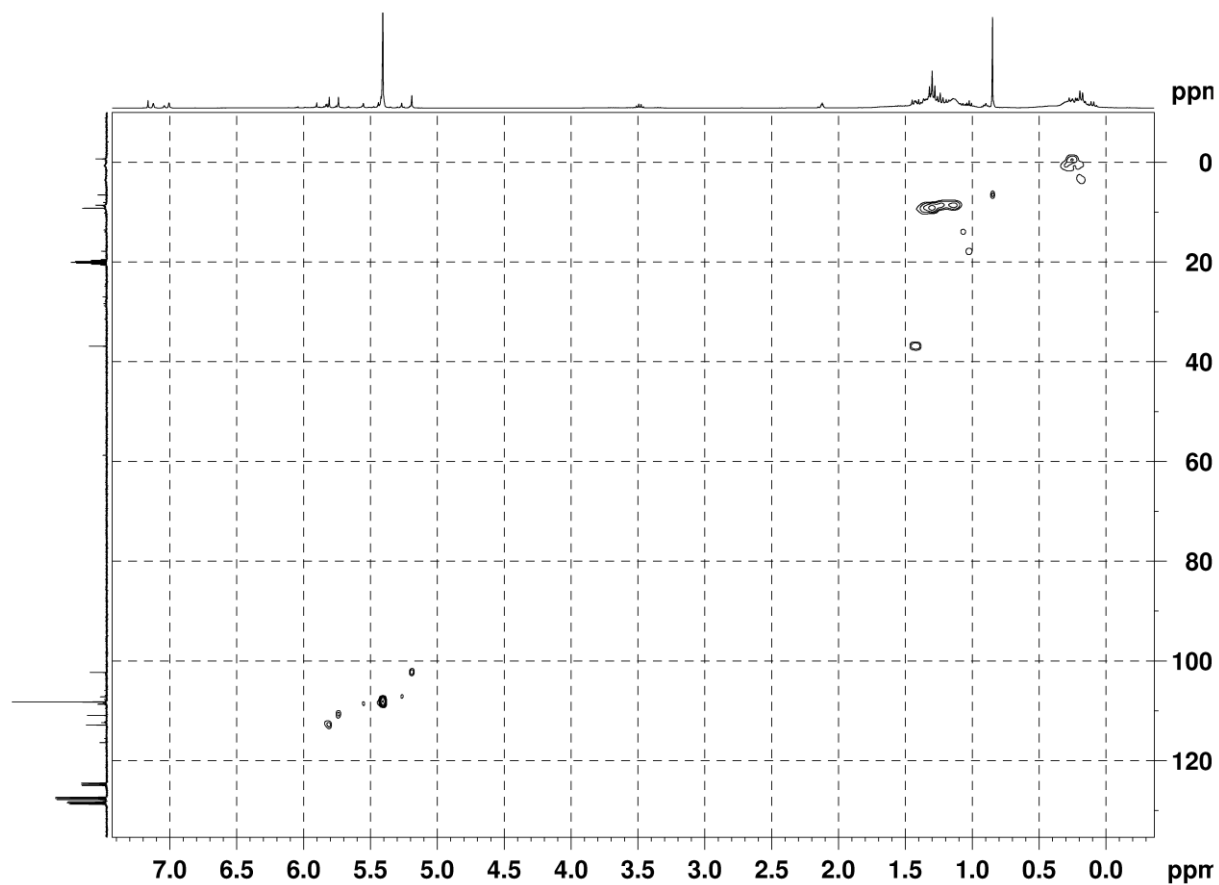
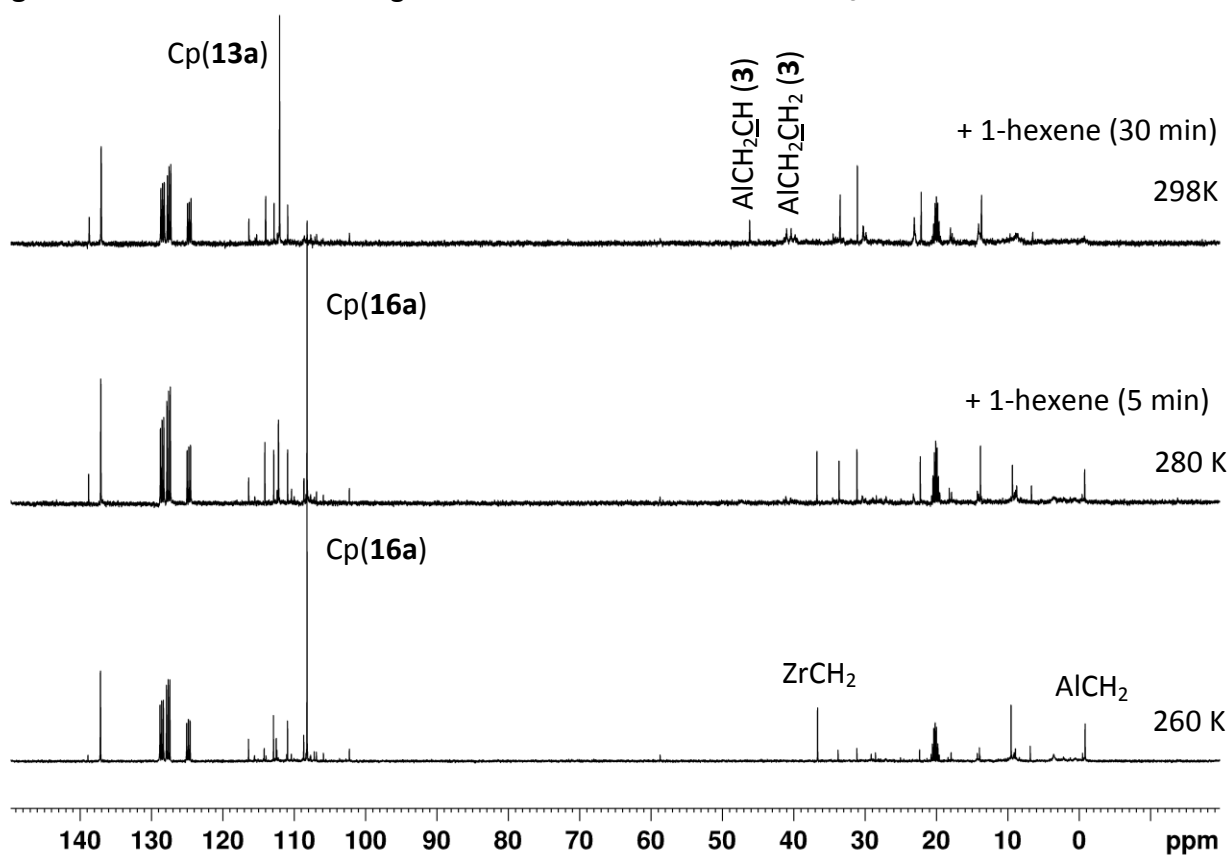
Figure S19. HSQC of complex **16a** in C_7D_8 (300 K).Figure S20. ^{13}C NMR monitoring of reaction **16a** + 1-hexene in C_7D_8 .

Figure S21. ^1H NMR of complex **16h** obtained by the reaction of **1h** with $(\text{AlEt}_3)_2$ (1:11) in C_7D_8 at 270 K.

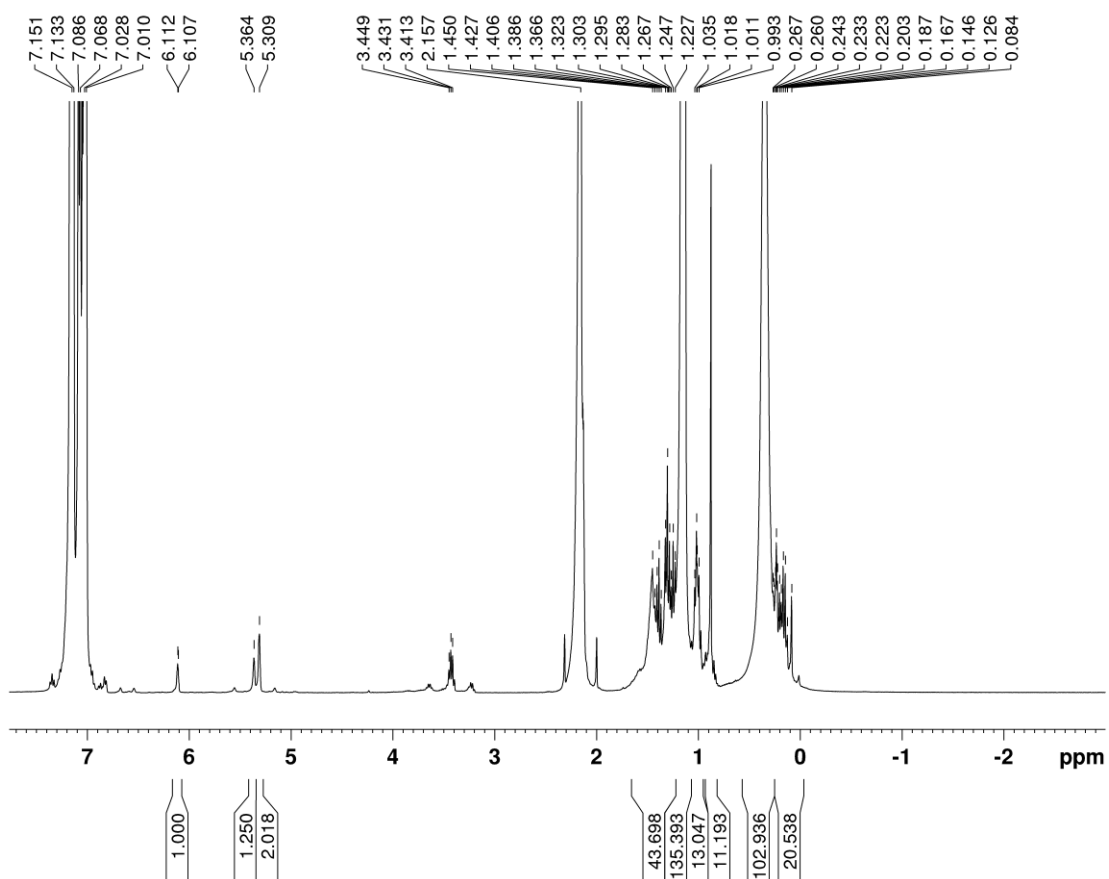


Figure S22. COSY HH of complex **16h** in C_7D_8 at 270 K.

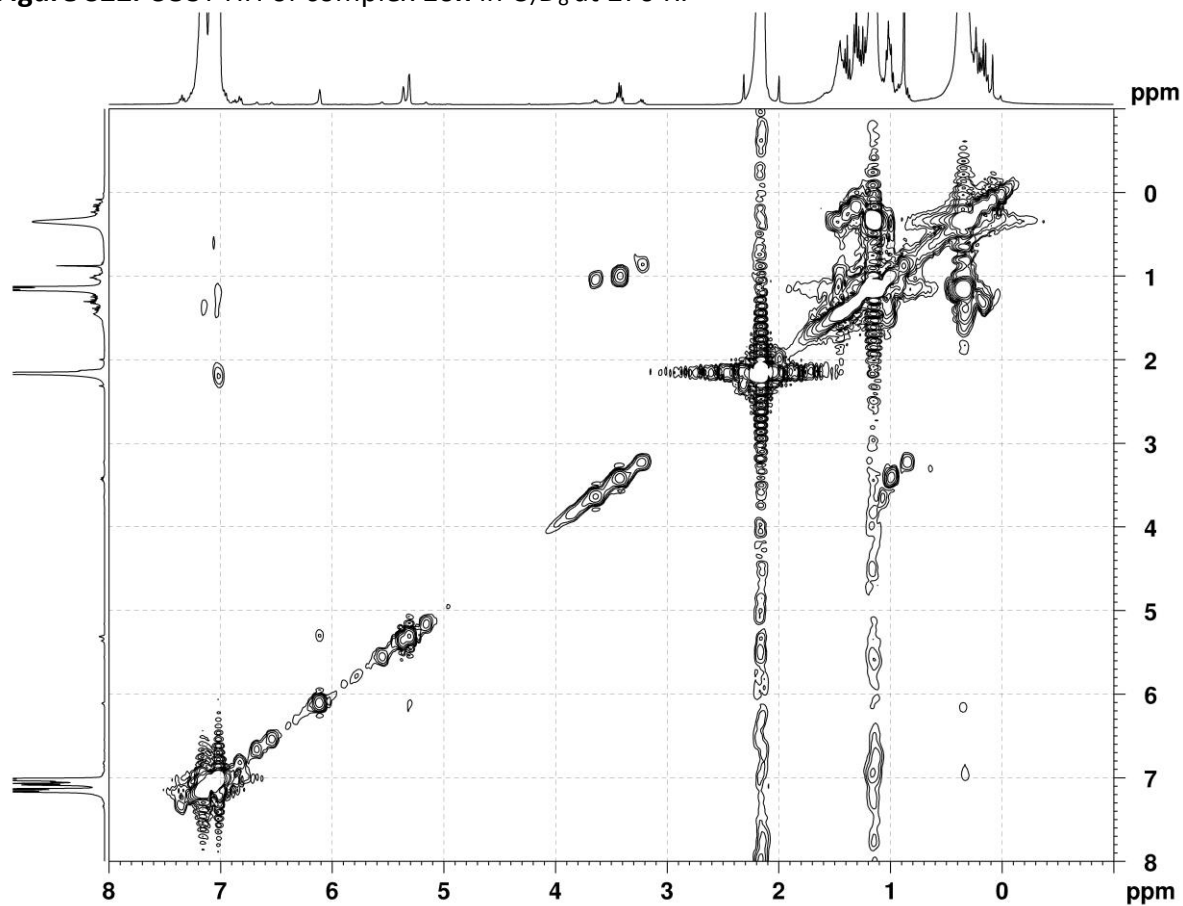


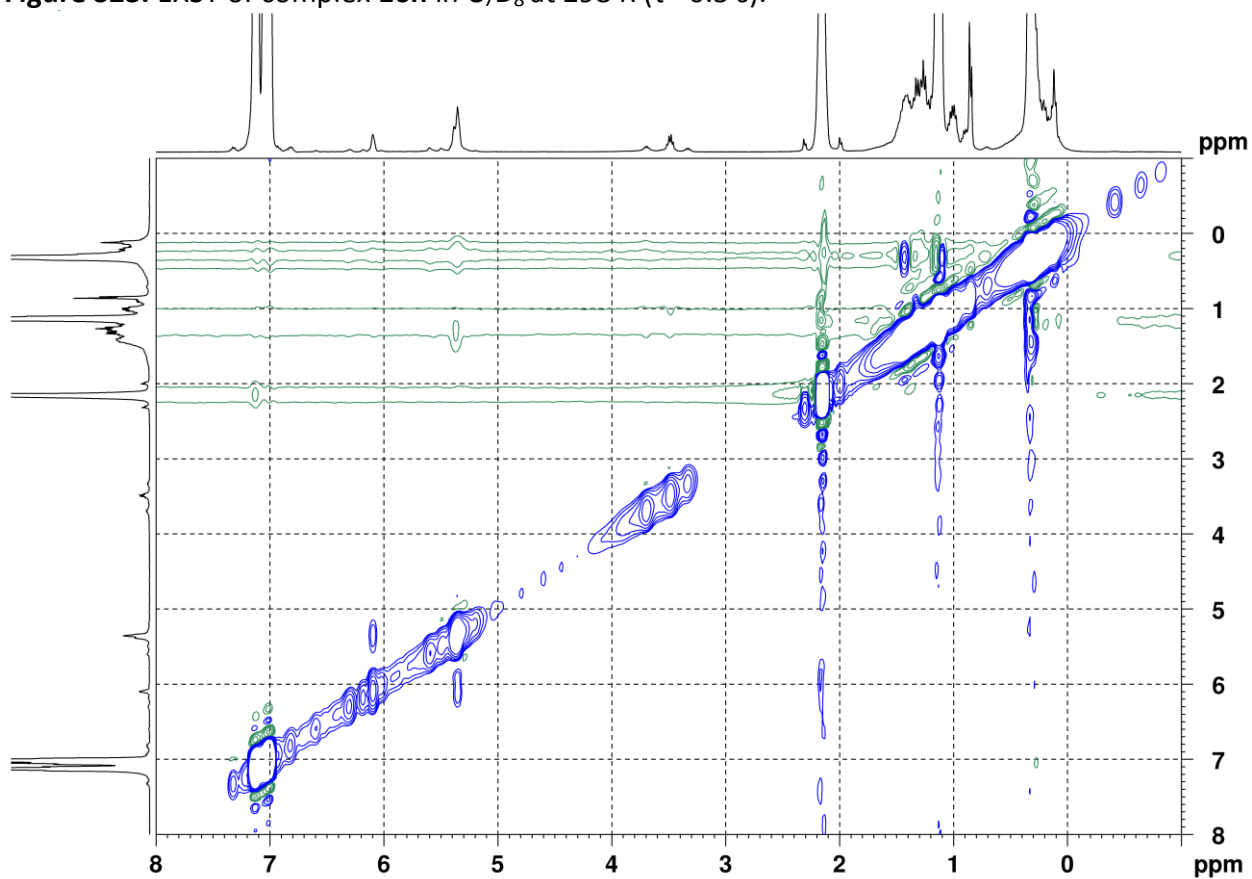
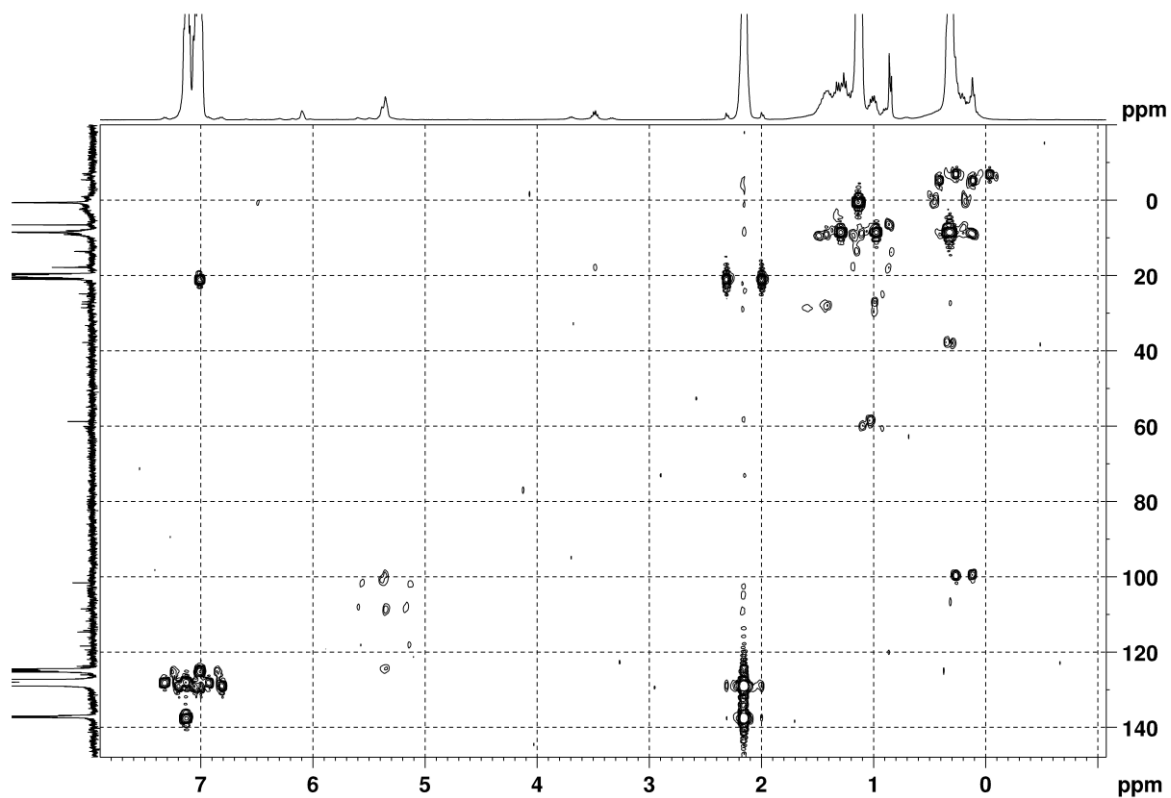
Figure S23. EXSY of complex **16h** in C_7D_8 at 298 K ($\tau = 0.3$ s).**Figure S24.** HMBC of complex **16h** in C_7D_8 at 298 K.

Figure S25. ^1H NMR of **16m** obtained by the reaction of **1m** with $(\text{AlEt}_3)_2$ (1:13) in C_7D_8 at 298 K.

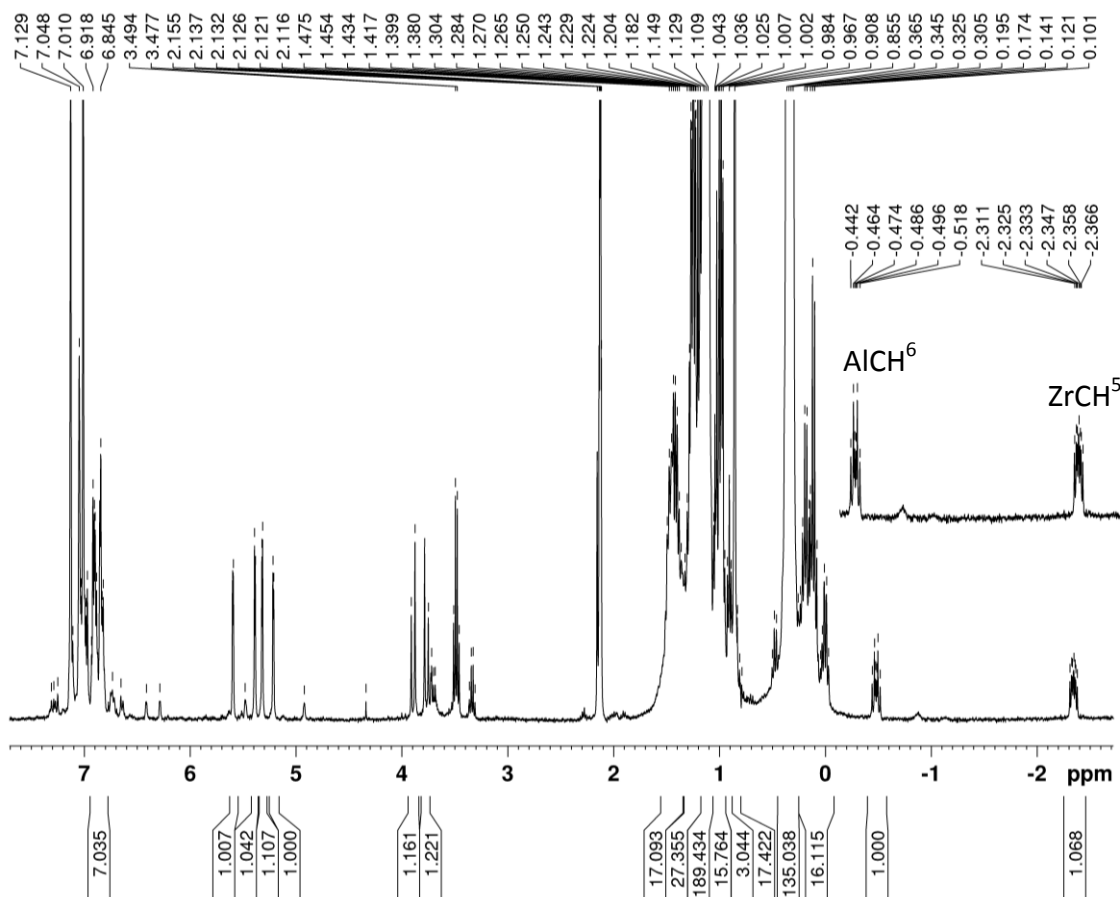


Figure S26. COSY HH of **16m** in C_7D_8 at 260 K.

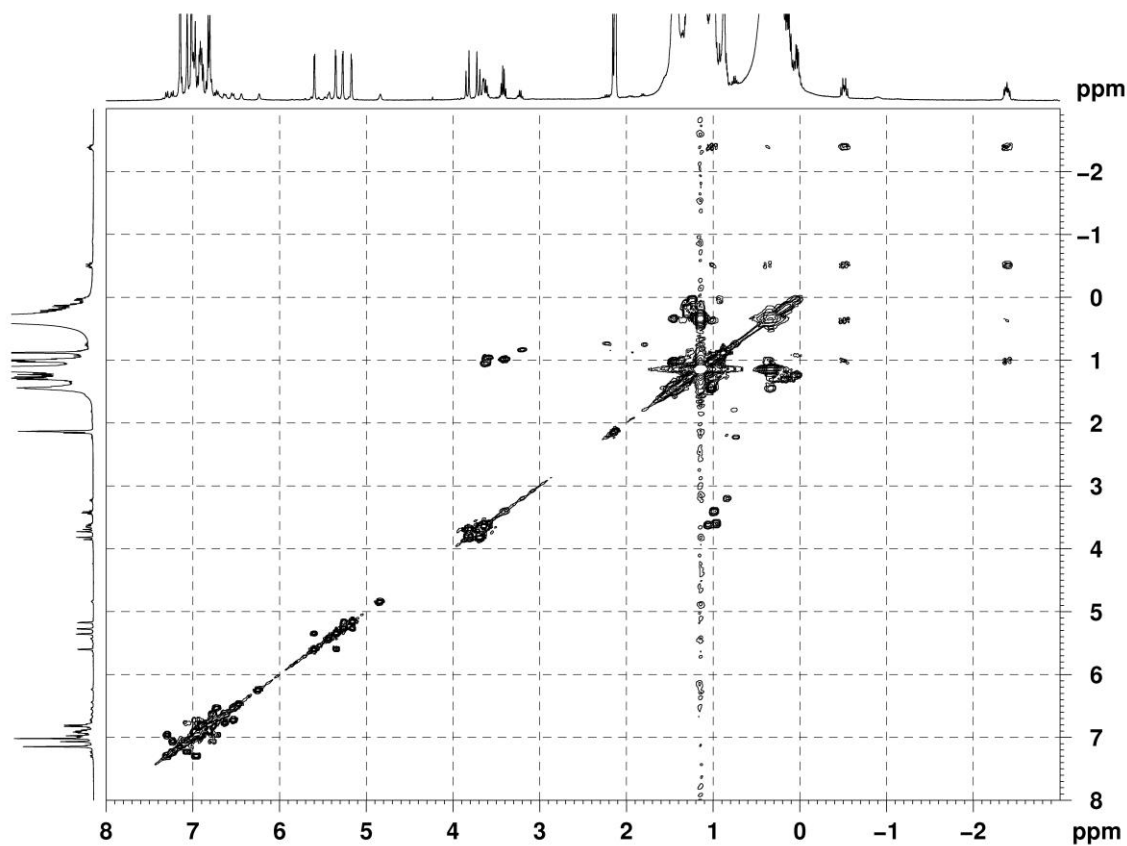


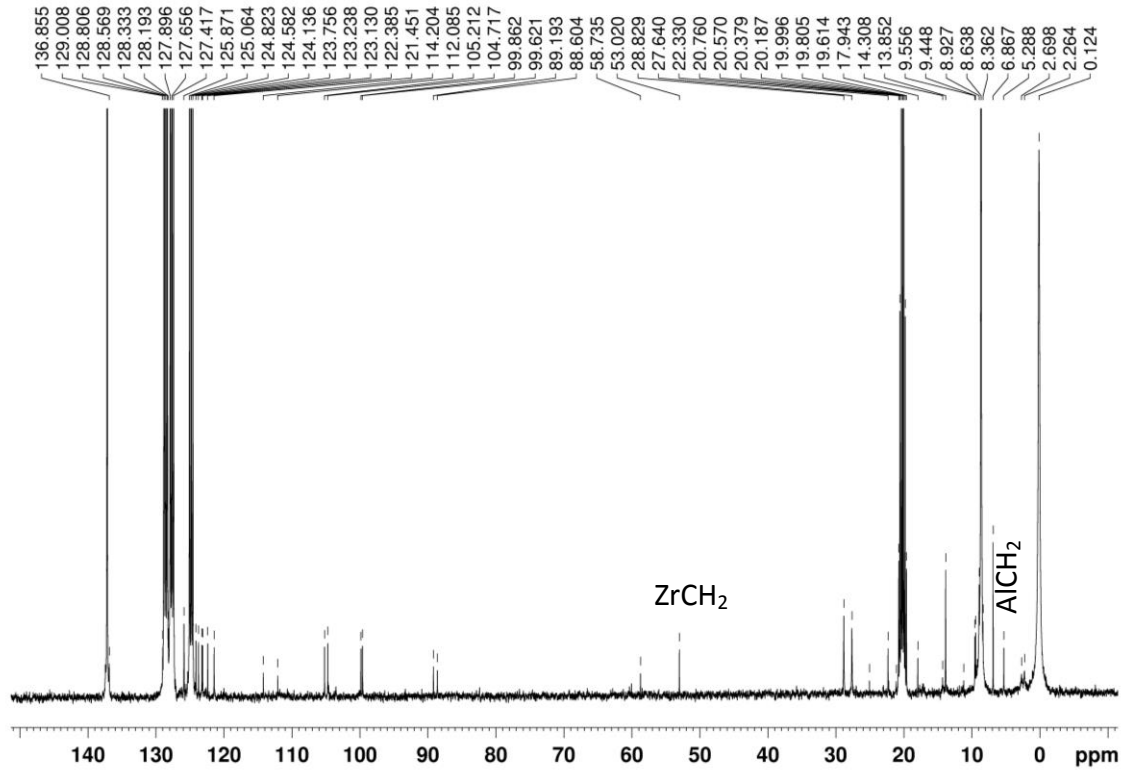
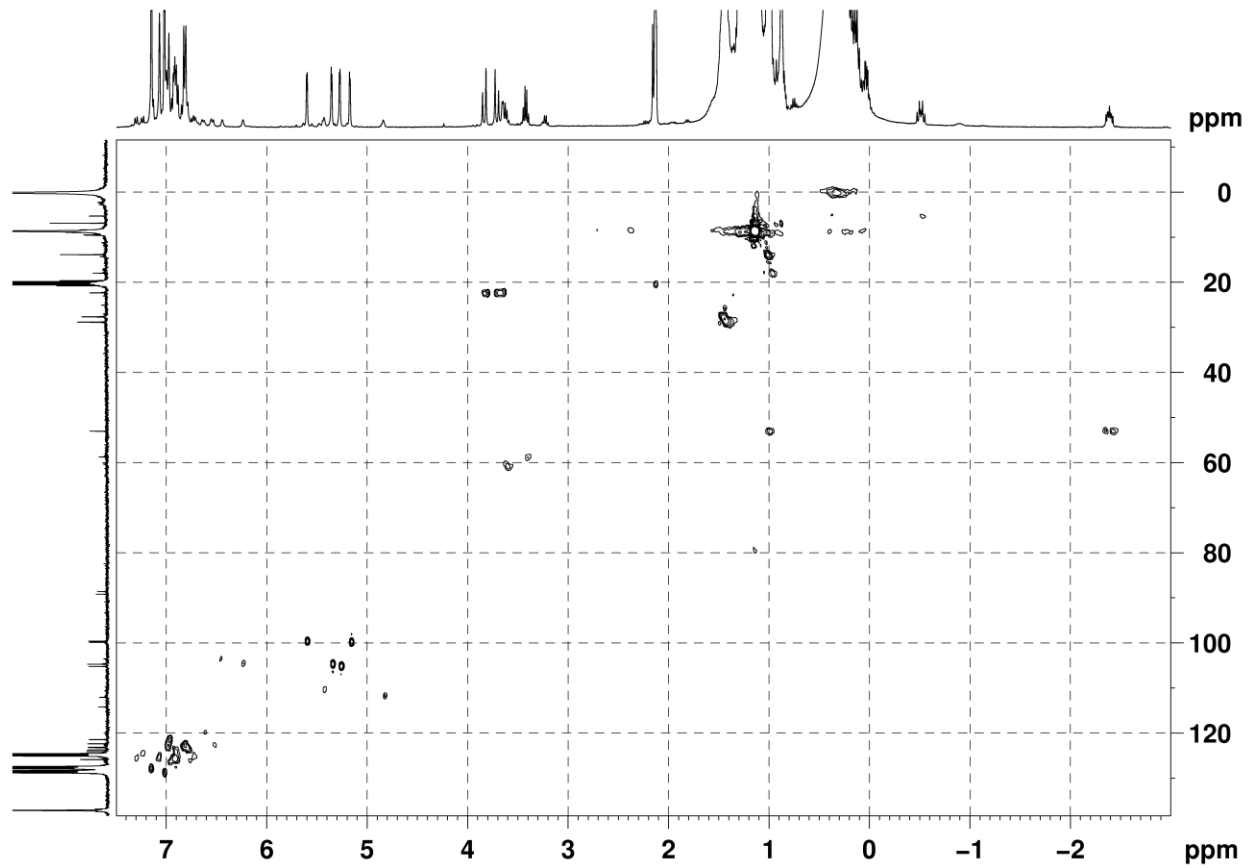
Figure S27. ^{13}C NMR of **16m** in C_7D_8 at 260 K.Figure S28. HSQC of **16m** in C_7D_8 at 260 K.

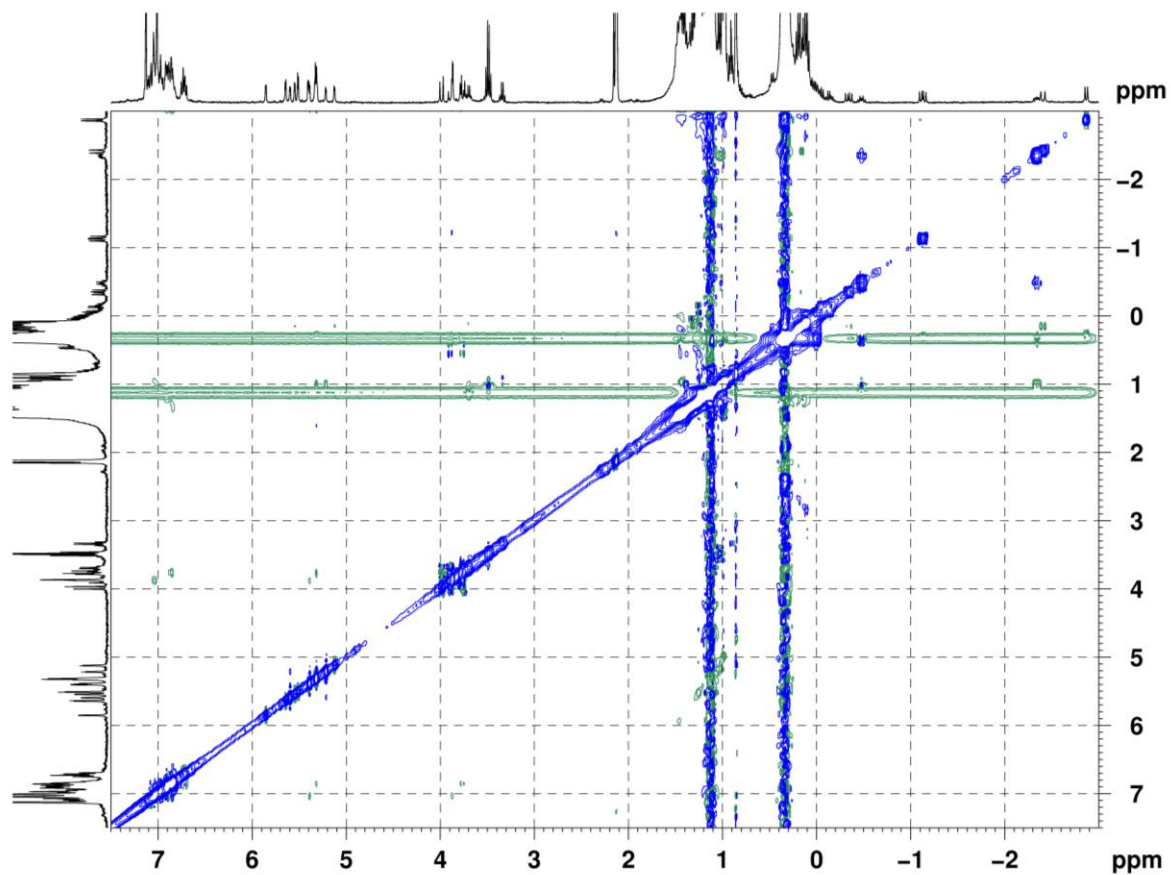
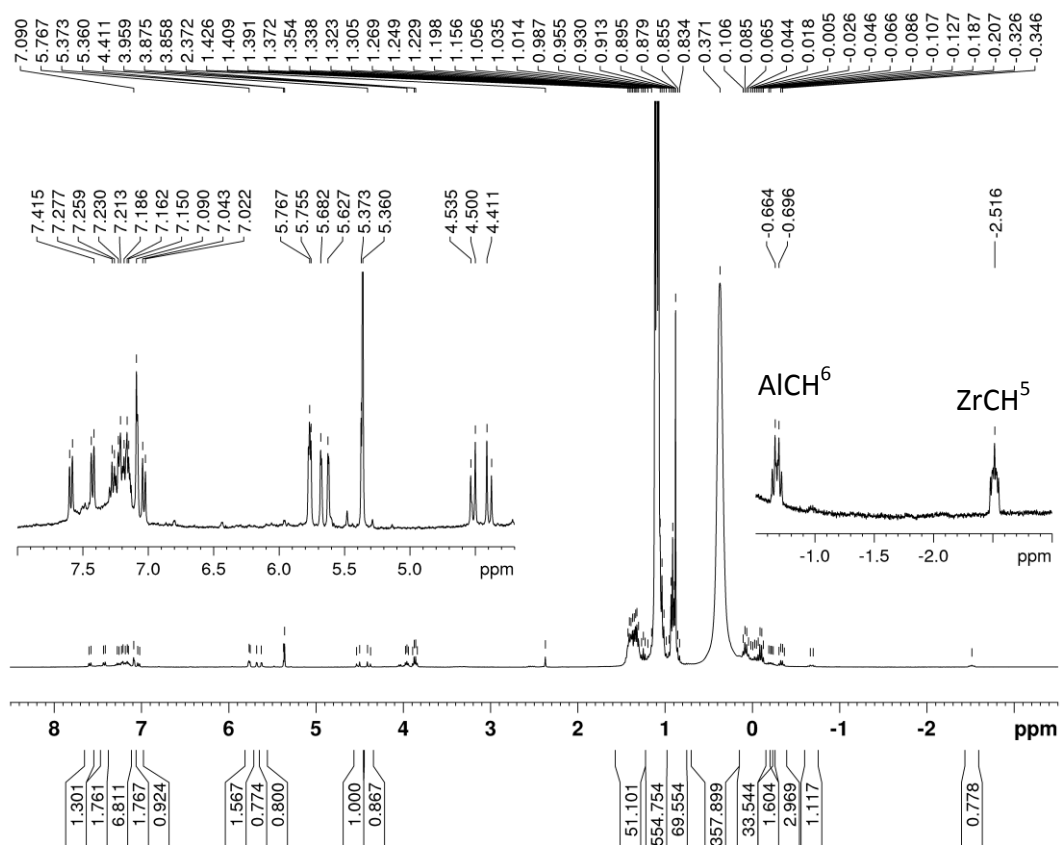
Figure S29. EXSY of **16m** in C_7D_8 at 298 K ($\tau = 0.3$ s).Figure S30. 1H NMR of **16m** obtained by the reaction of **1m** with $(AlEt_3)_2$ (1:24) in CD_2Cl_2 at 270 K.

Figure S31. ^1H NMR of complex **16n** obtained by the reaction of **1n** with $(\text{AlEt}_3)_2$ (1:16) in C_7D_8 at 285 K.

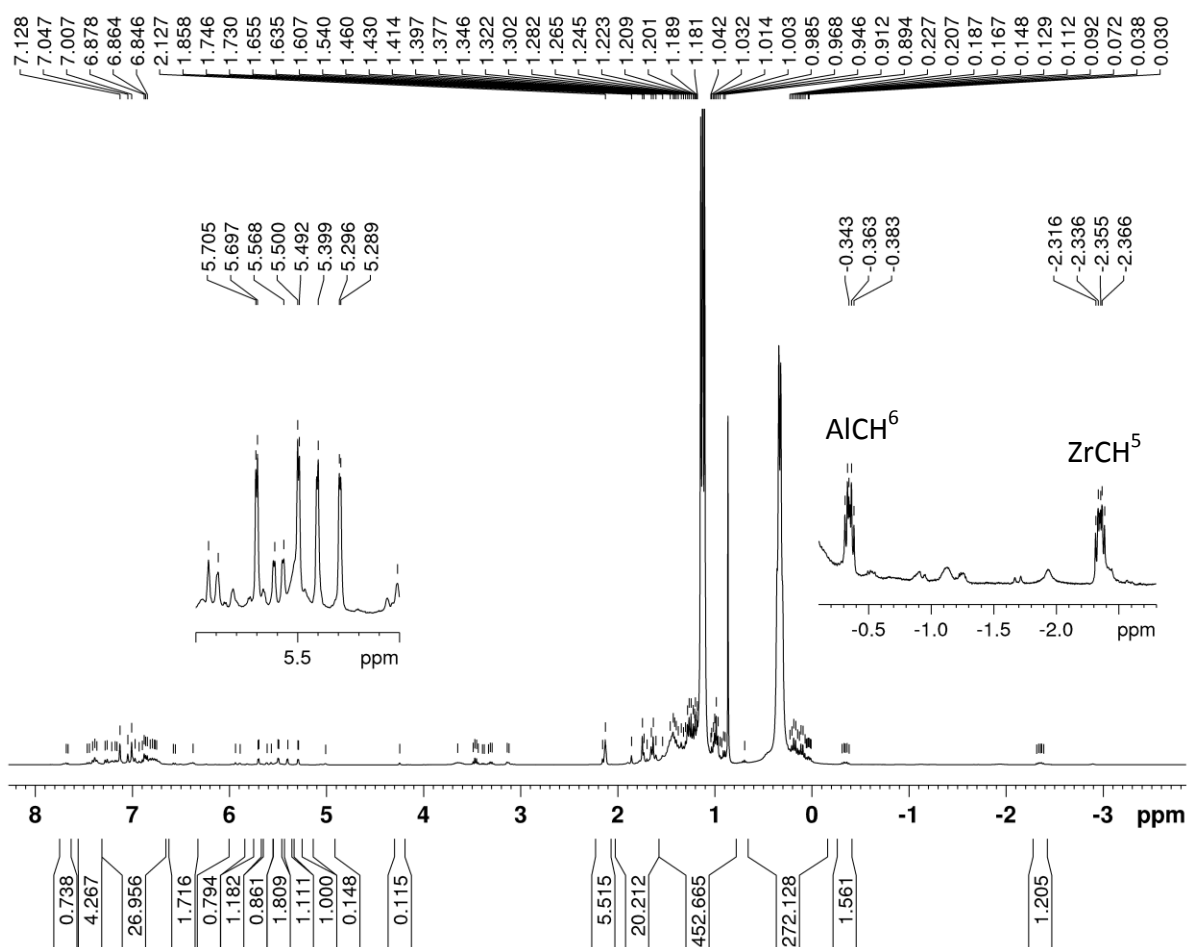


Figure S32. COSY HH of **16n** in C_7D_8 at 270 K.

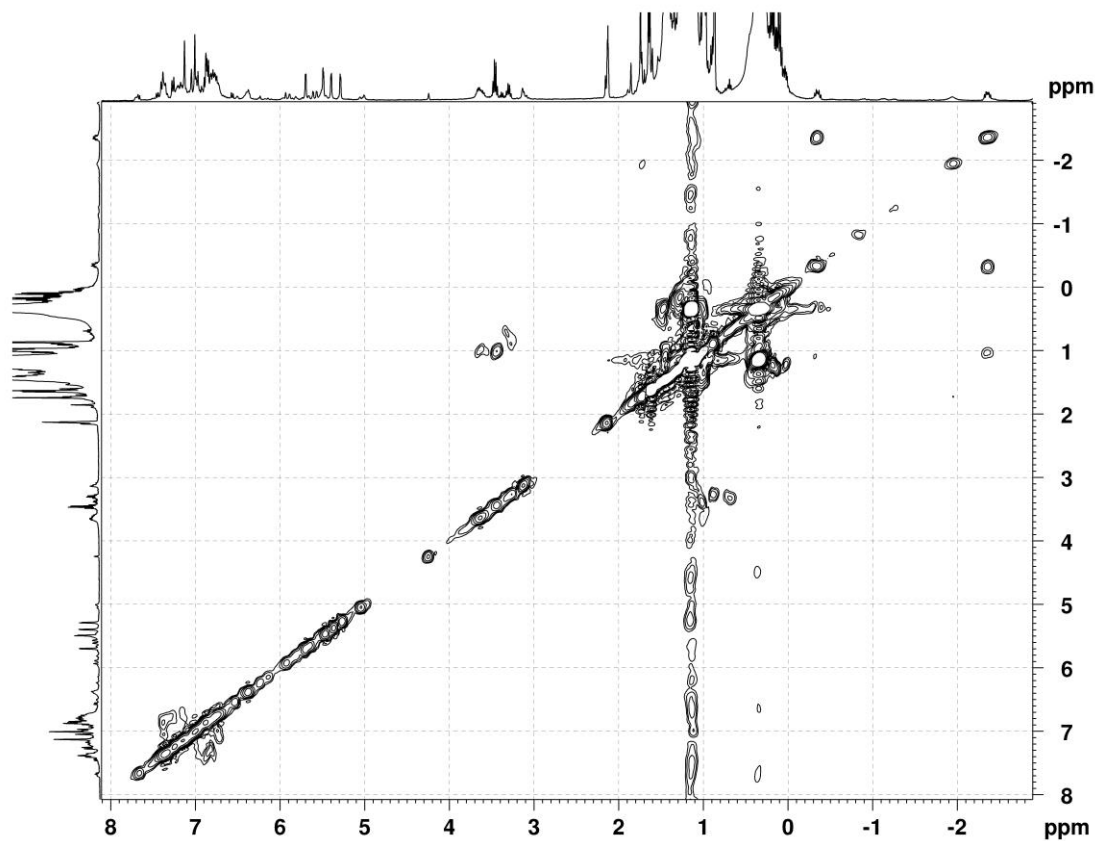


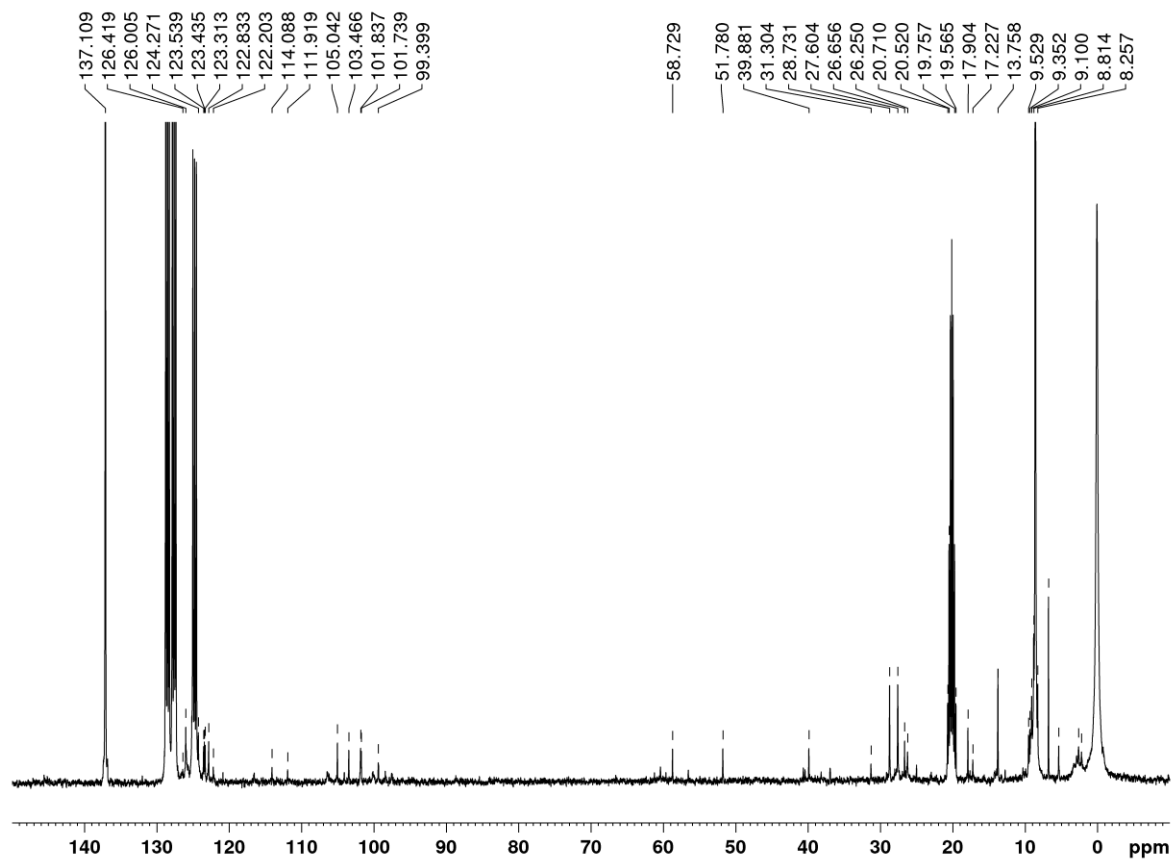
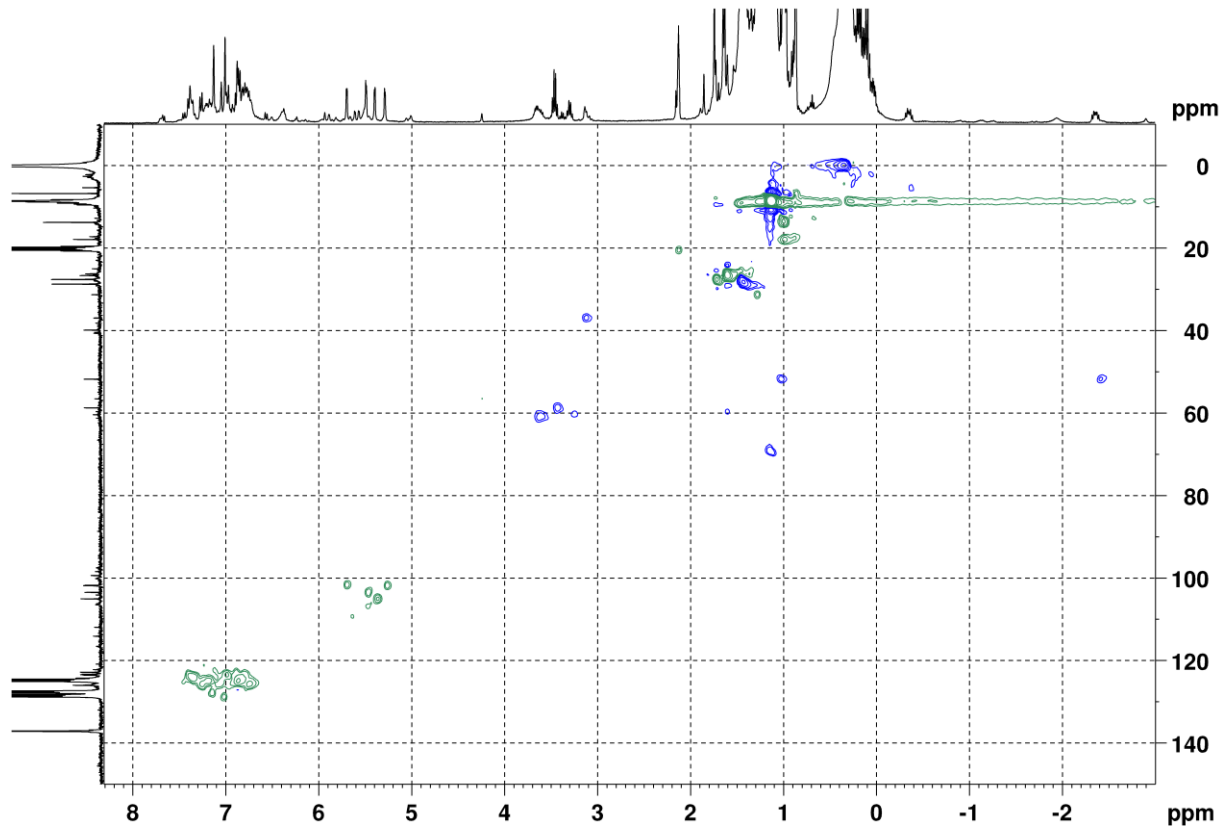
Figure S33. ^{13}C NMR of **16n** in C_7D_8 at 270 K.Figure S34. HSQC of **16n** in C_7D_8 at 270 K.

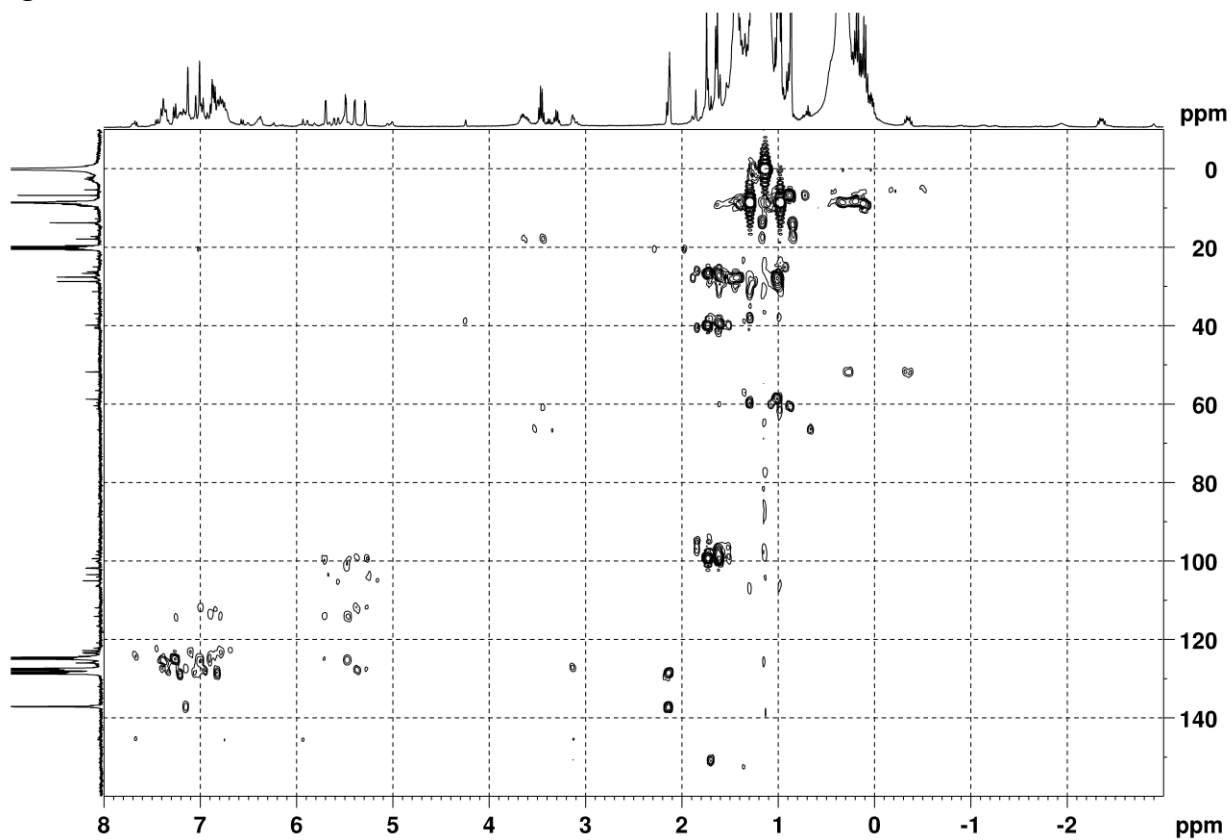
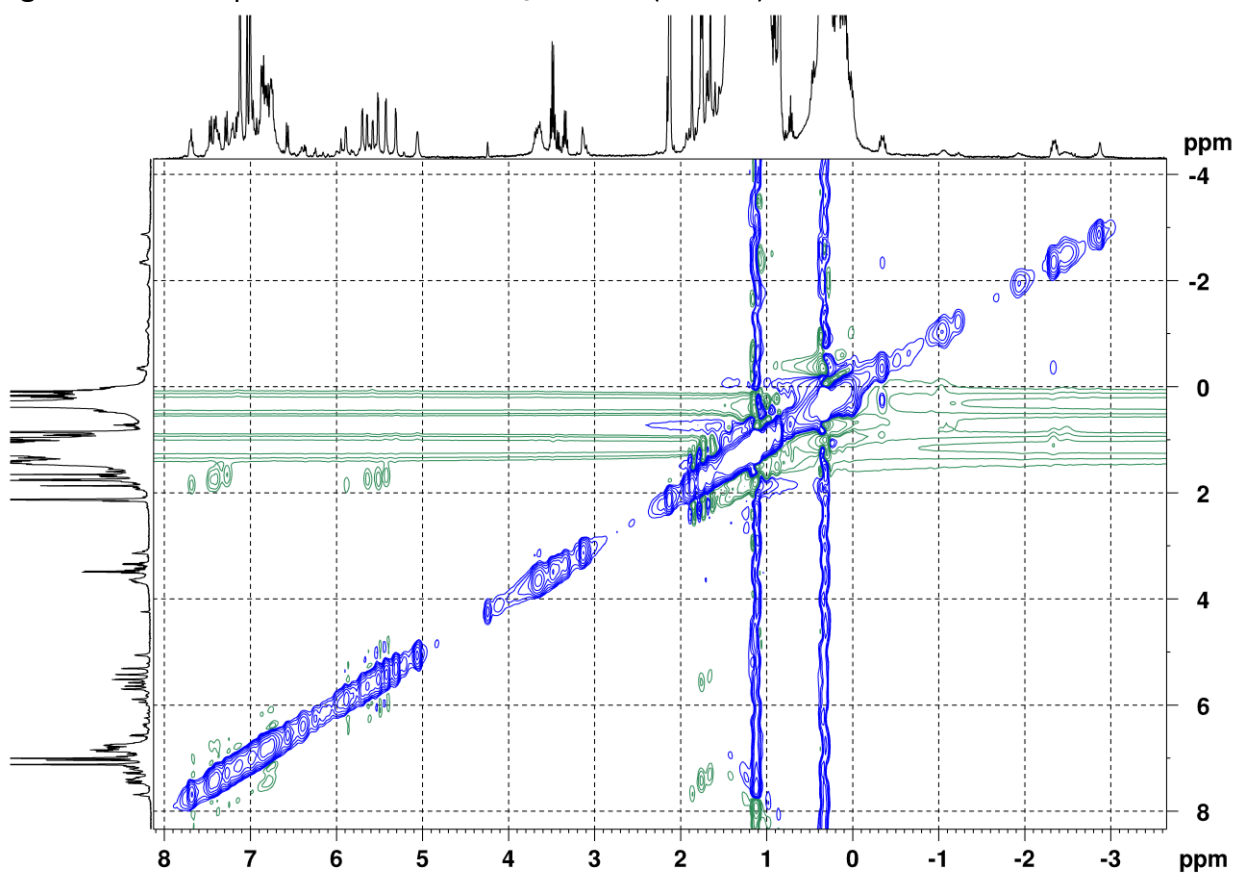
Figure S35. HMBC of **16n** in C_7D_8 at 270 K.Figure S36. EXSY spectrum of **16n** in C_7D_8 at 293 K ($\tau = 0.3$ s).

Figure S37. ^1H NMR of **16p** obtained by the reaction of **1p** with $(\text{AlEt}_3)_2$ (1:13) in C_7D_8 at 280 K.

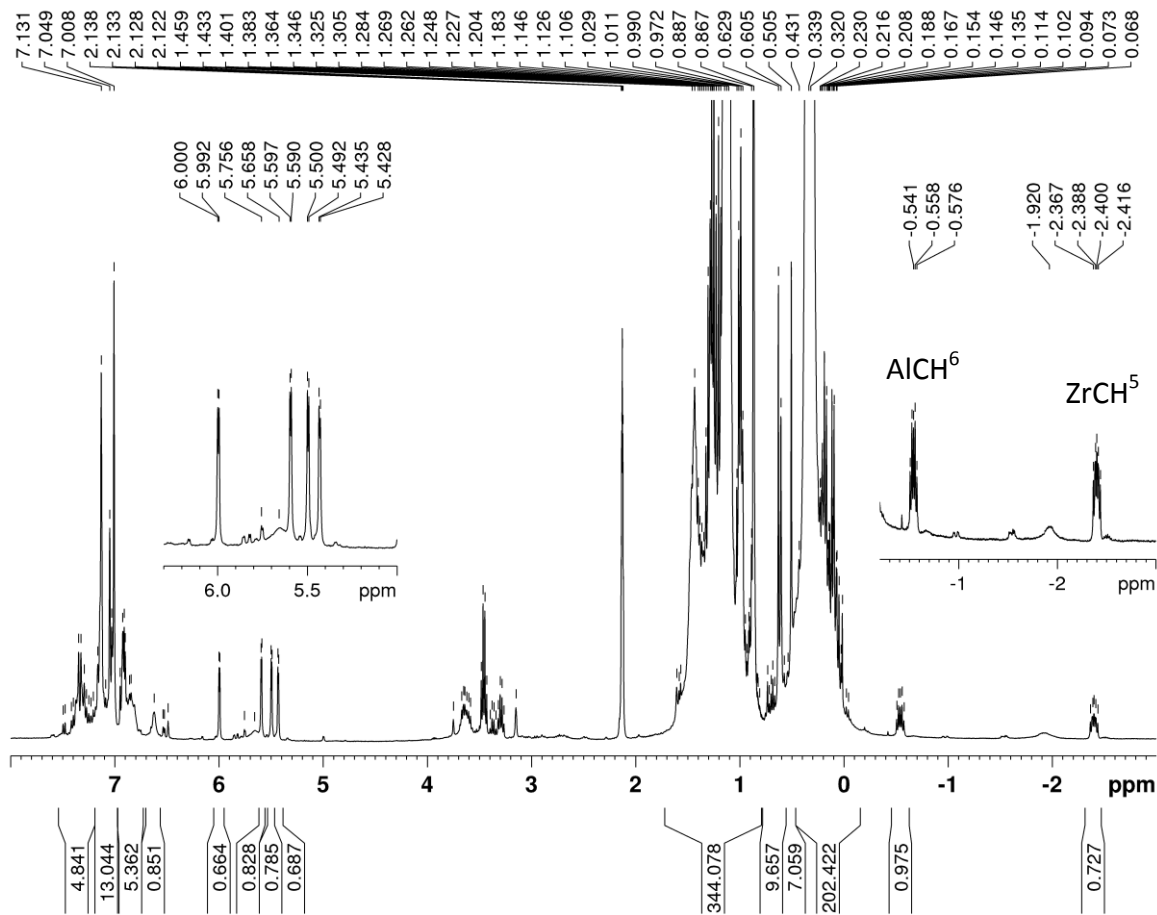


Figure S38. COSY HH of **16p** in C_7D_8 at 260 K.

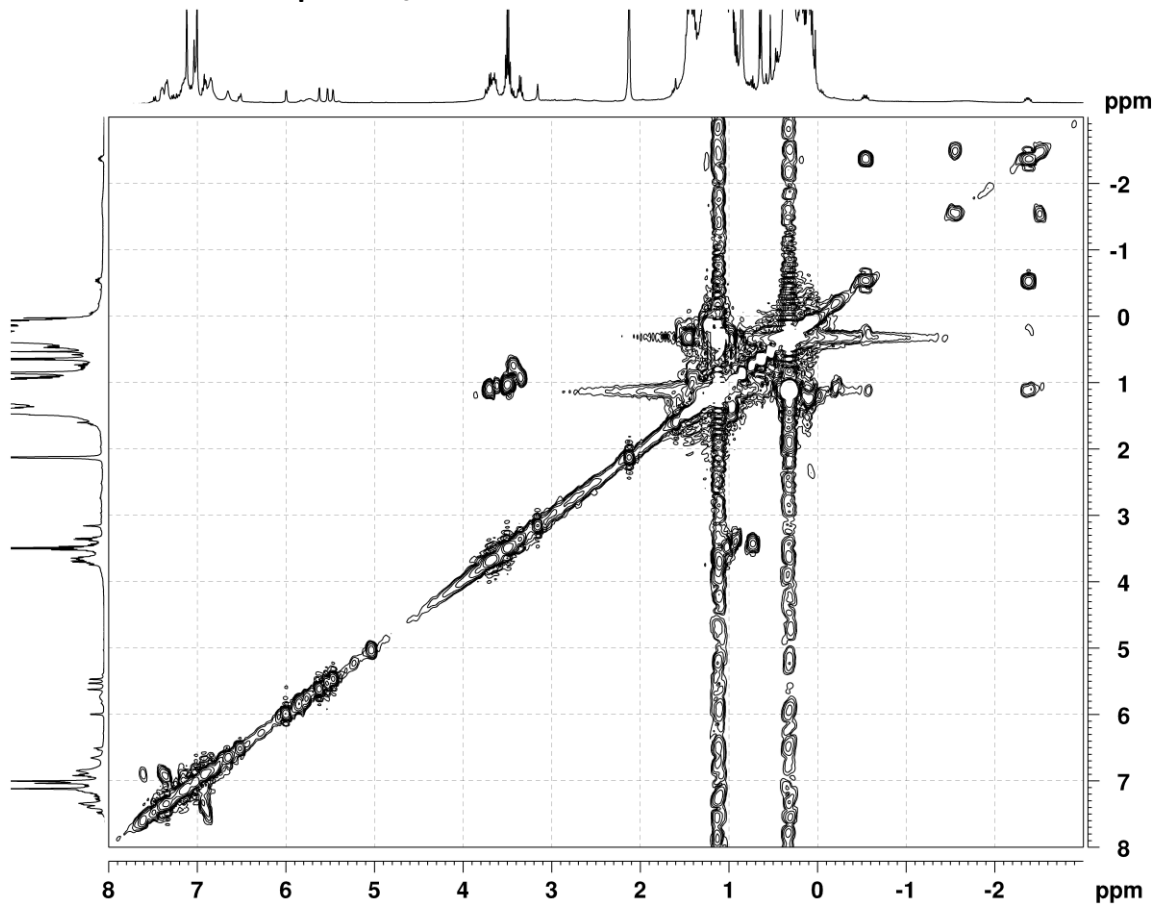


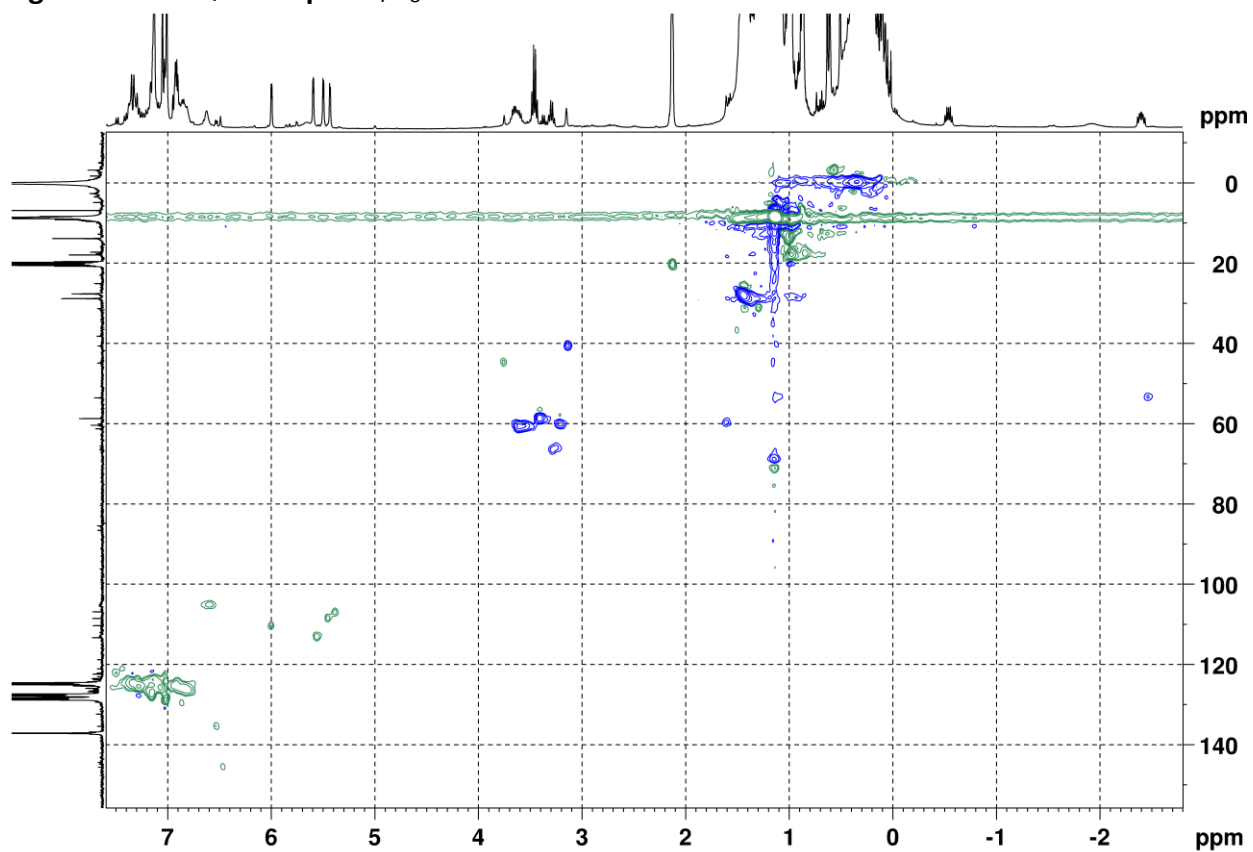
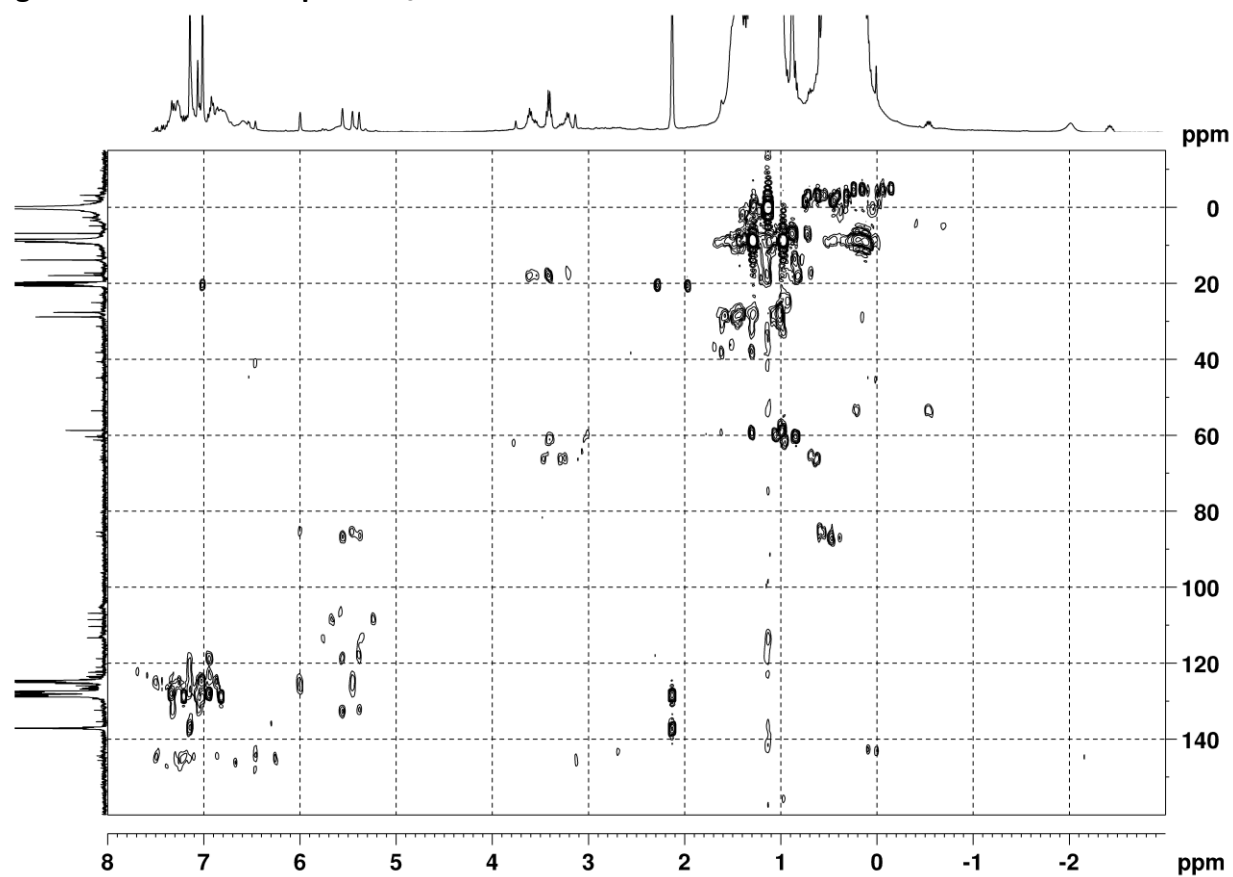
Figure S39. HSQC of **16p** in C_7D_8 at 270 K.Figure S40. HMBC of **16p** in C_7D_8 at 270 K.

Figure S41. EXSY spectrum of **16p** in C_7D_8 at 293 K ($\tau = 0.3$ s).

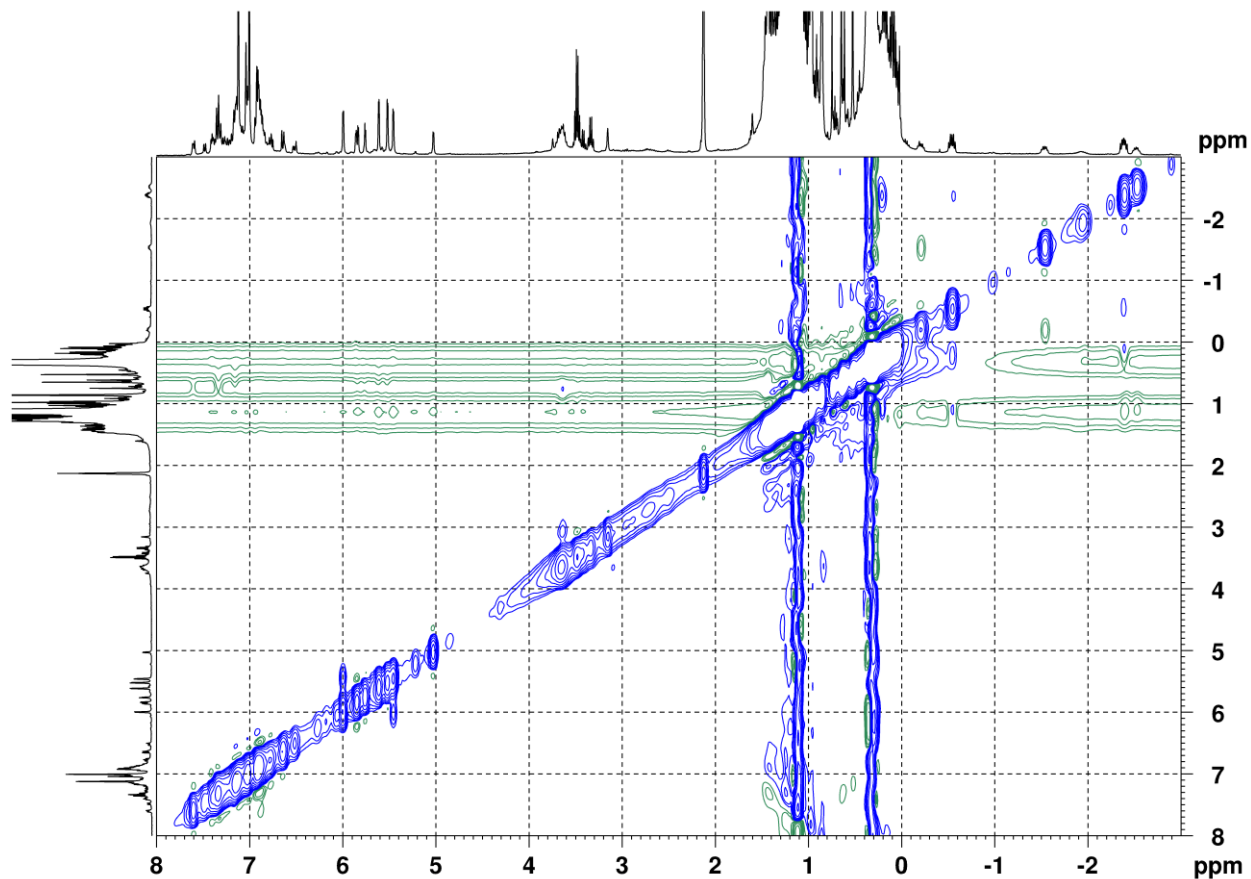


Figure S42. 1H NMR of **16p** obtained by the reaction of **1p** with $(AlEt_3)_2$ (1:13) in CD_2Cl_2 at 280 K.

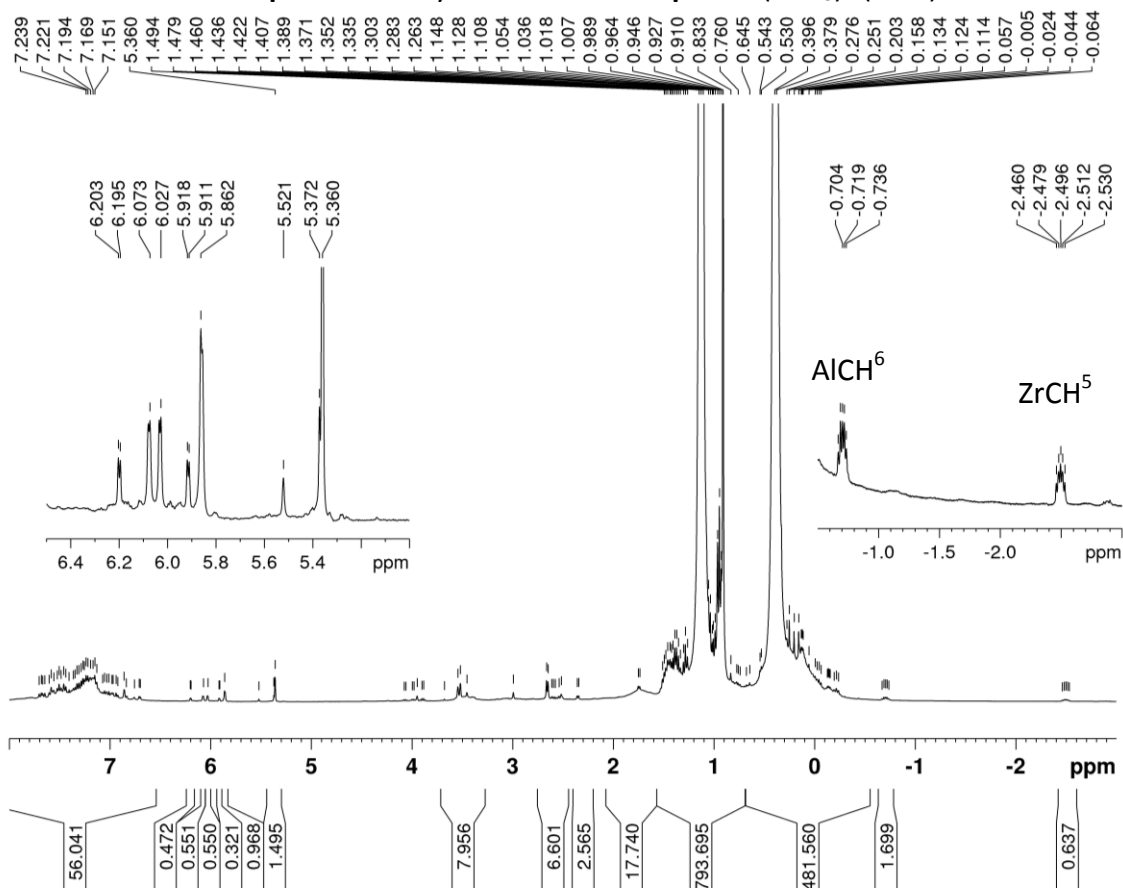


Figure S43. ^1H NMR of **16q** obtained by the reaction of **1q** with $(\text{AlEt}_3)_2$ (1:2) in C_7D_8 at 285 K.

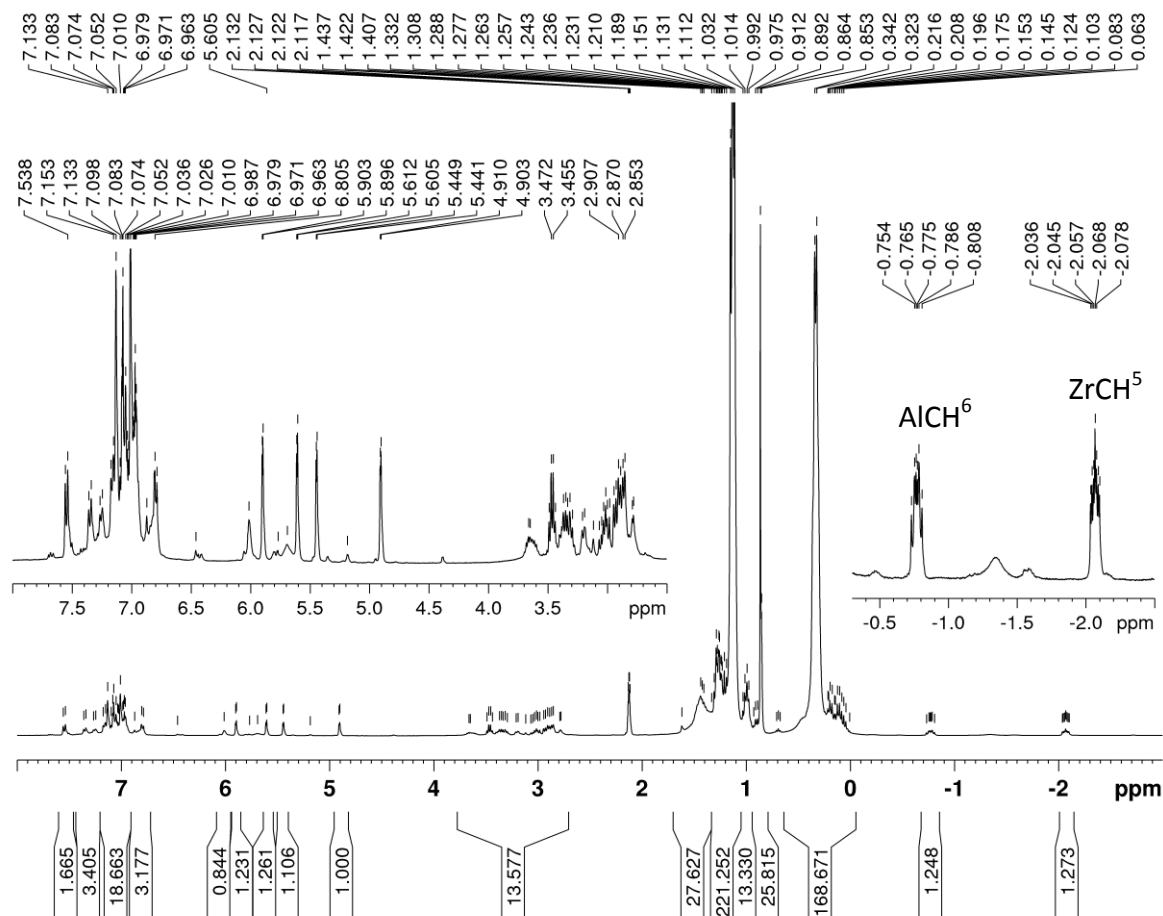


Figure S44. COSY HH of **16q** in C_7D_8 at 260 K.

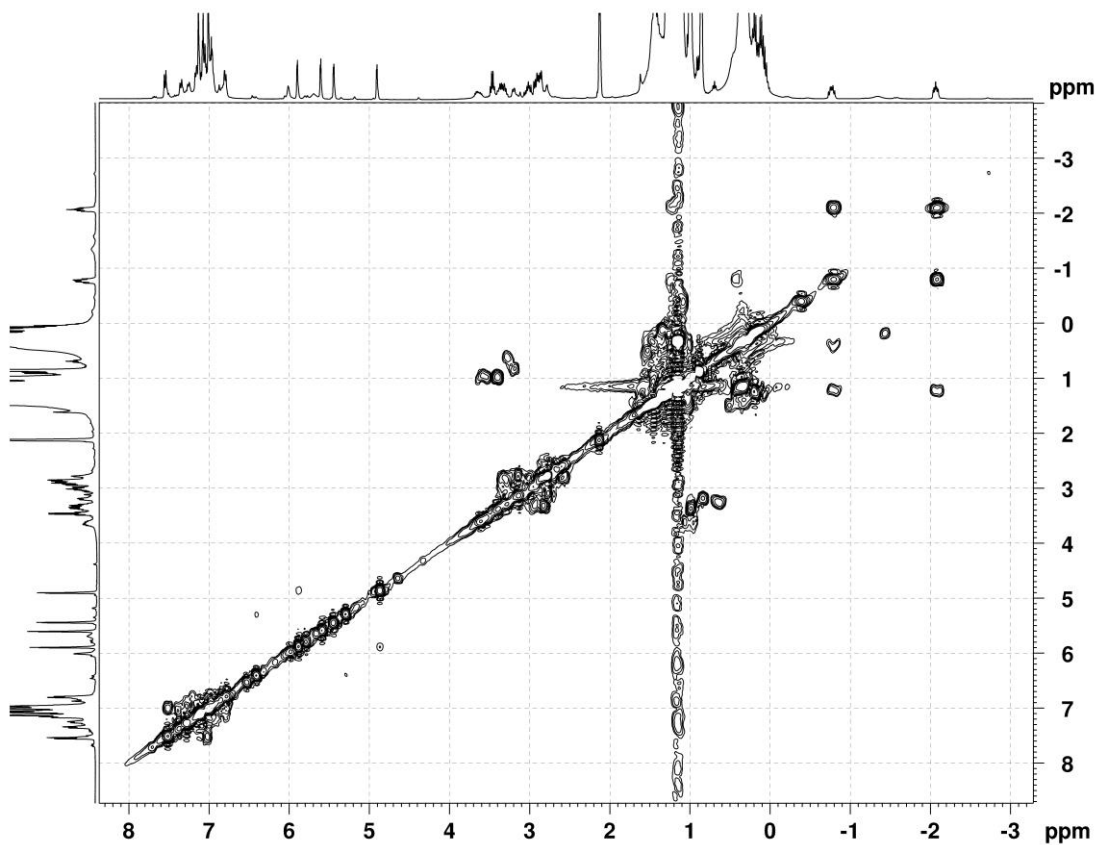


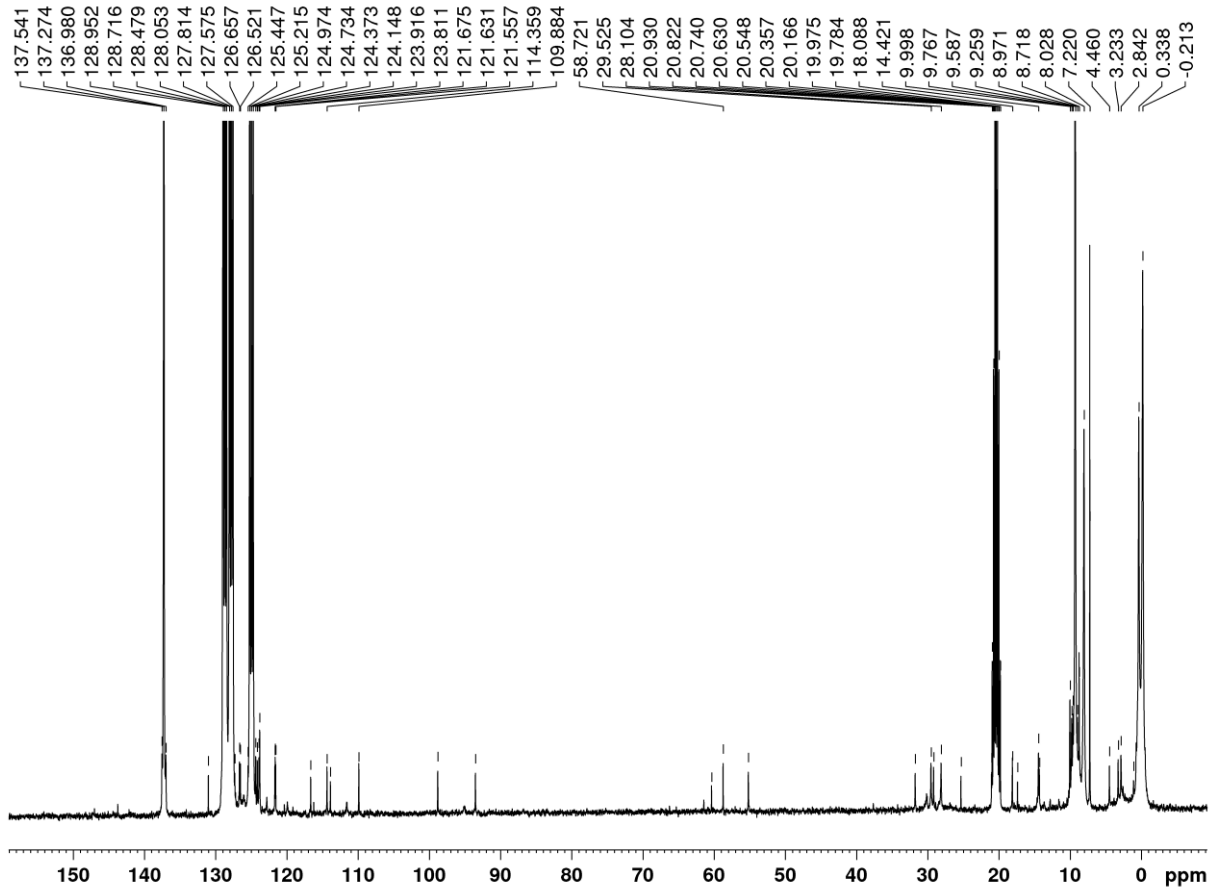
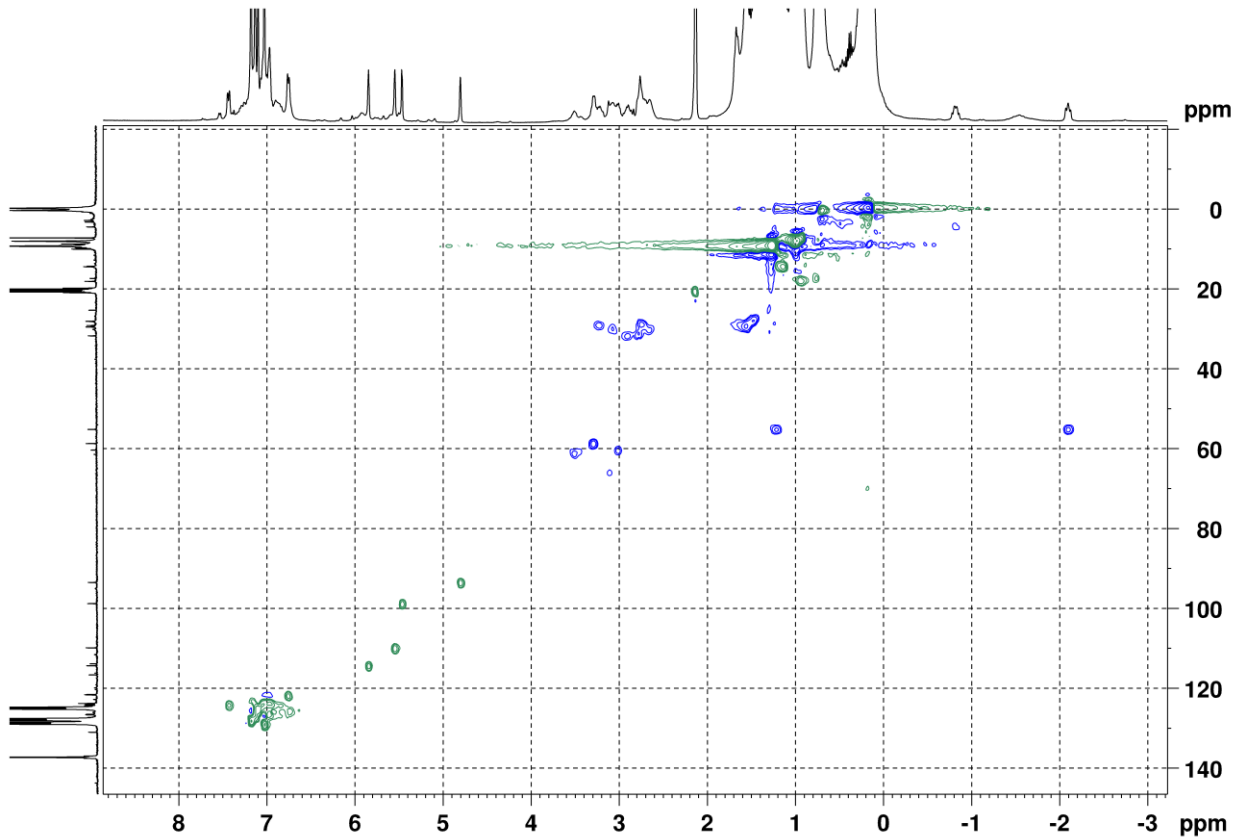
Figure S45. ^{13}C NMR of **16q** in C_7D_8 at 220 K.Figure S46. HSQC of **16q** in C_7D_8 at 220 K.

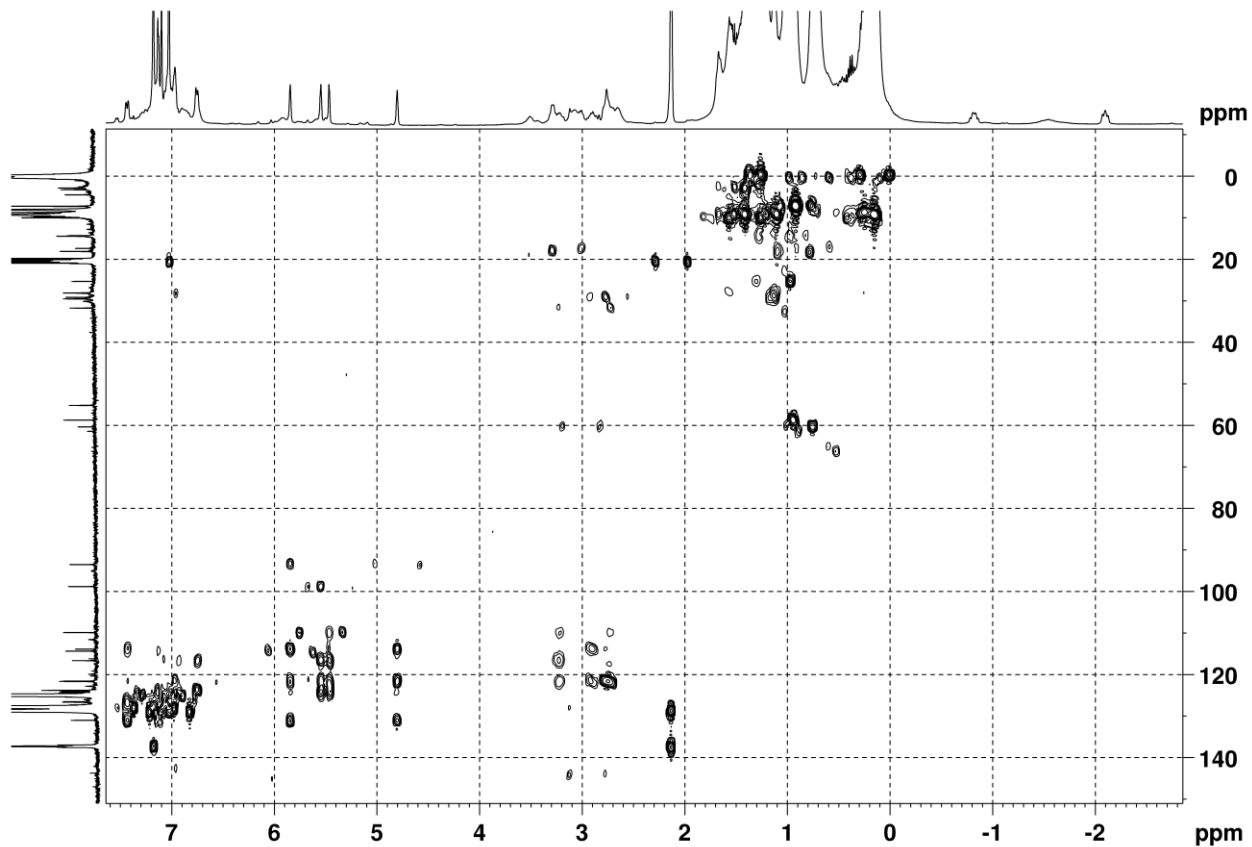
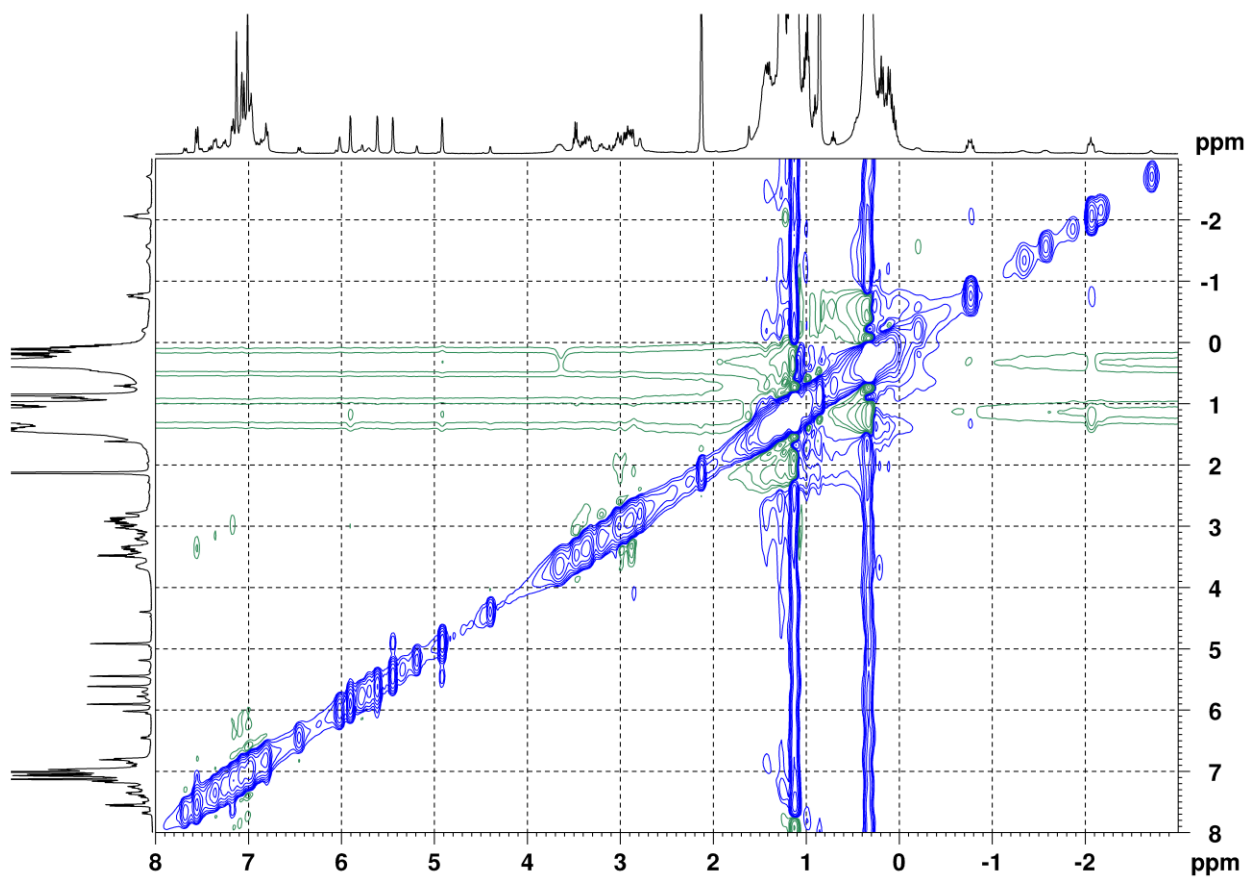
Figure S47. HMBC of **16q** in C_7D_8 at 220 K.Figure S48. EXSY of **16q** in C_7D_8 at 290 K ($\tau = 0.3$ s).

Figure S49. ^1H NMR of **16q** obtained by the reaction of **1q** with $(\text{AlEt}_3)_2$ (1:13) in CD_2Cl_2 at 285 K.

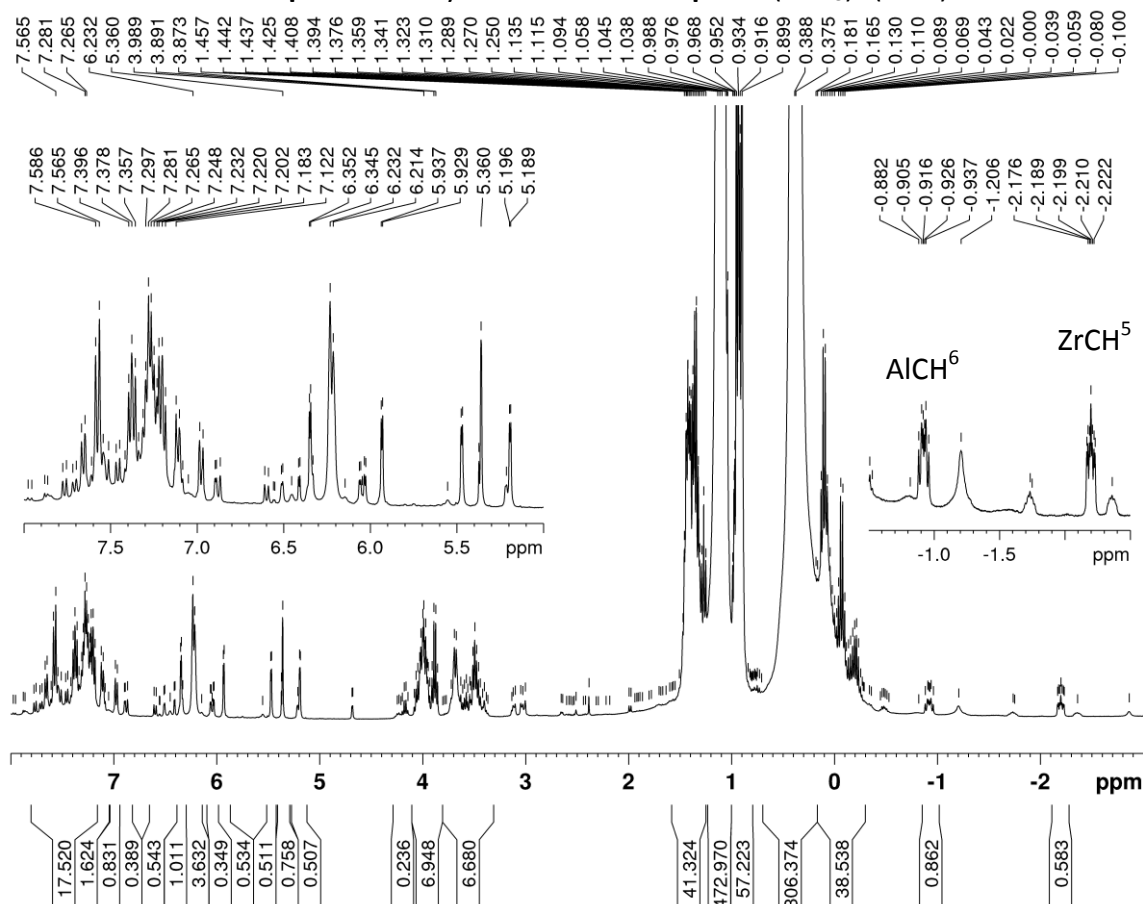


Figure S50. ^1H NMR of **17l** obtained by the reaction of **1l** with $(\text{AlEt}_3)_2$ (1:24) in C_7D_8 at 298 K.

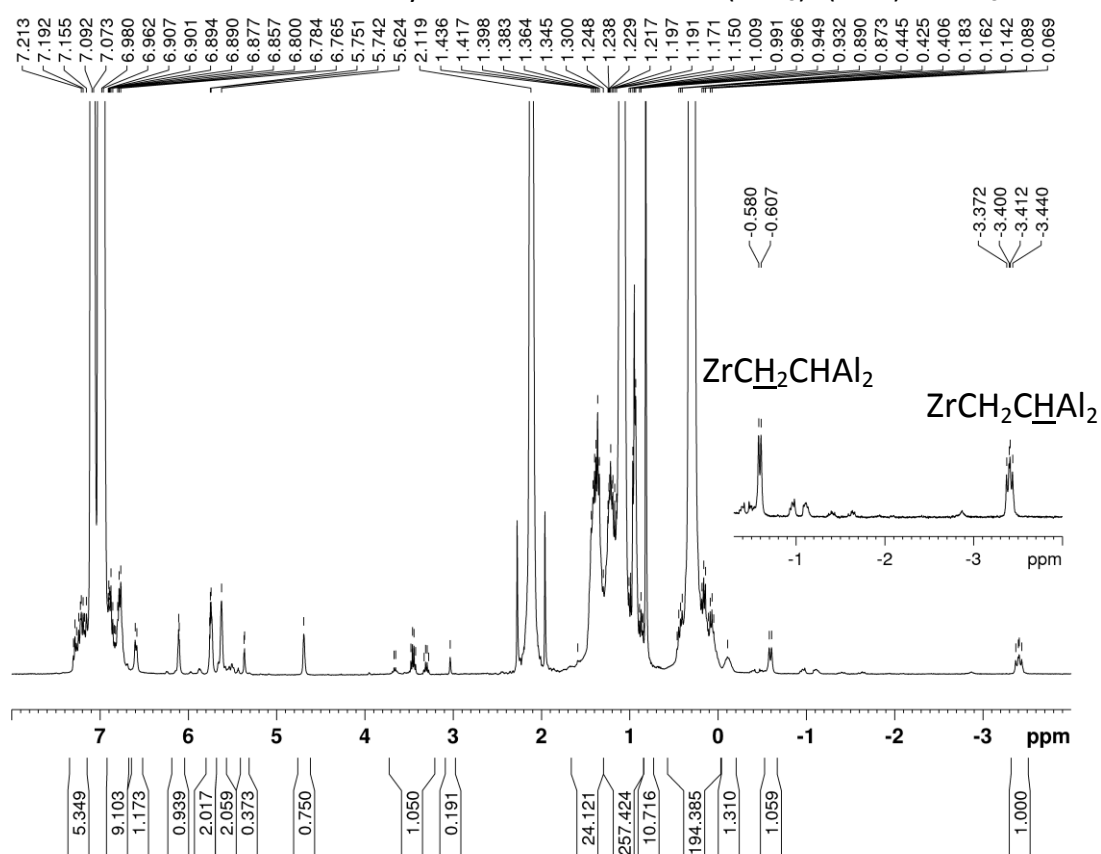


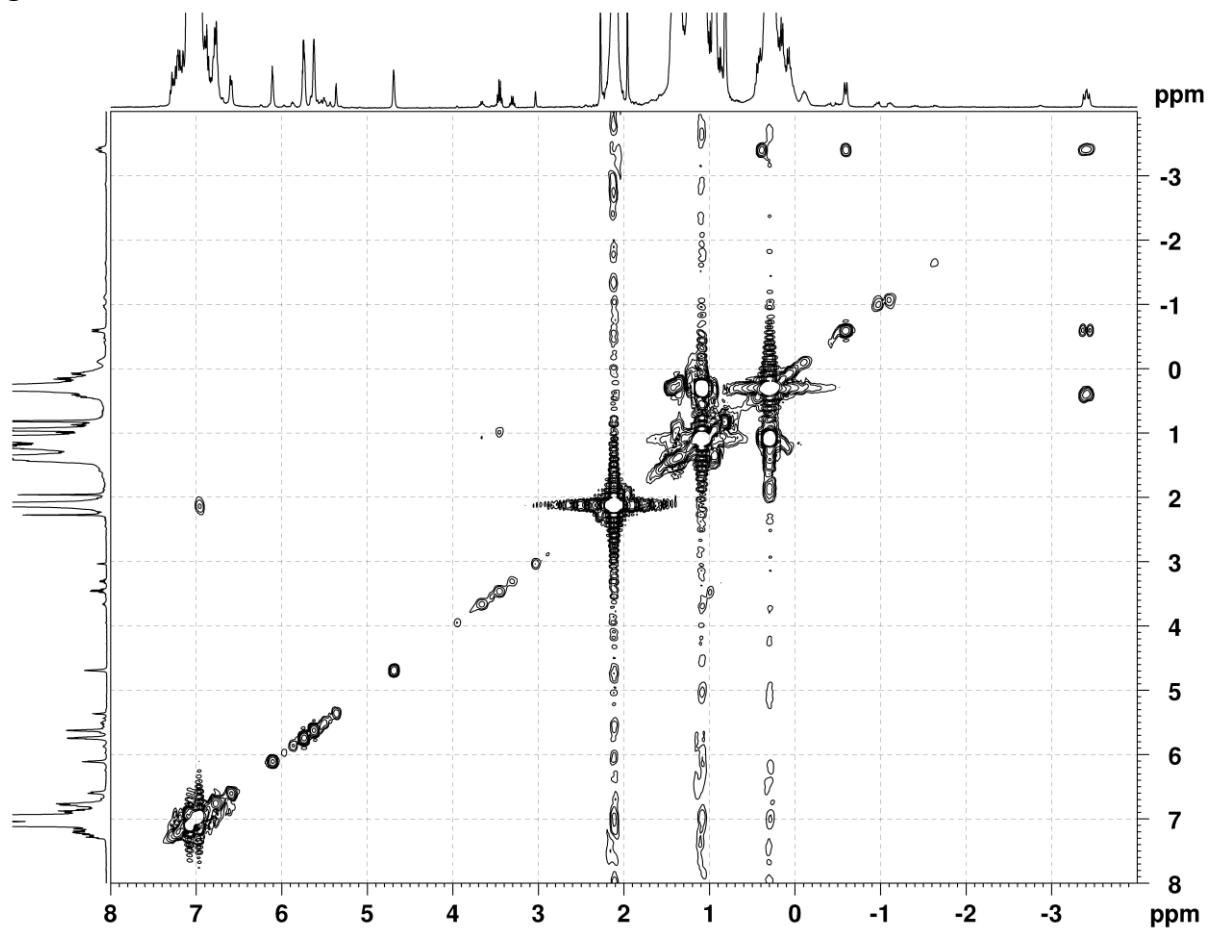
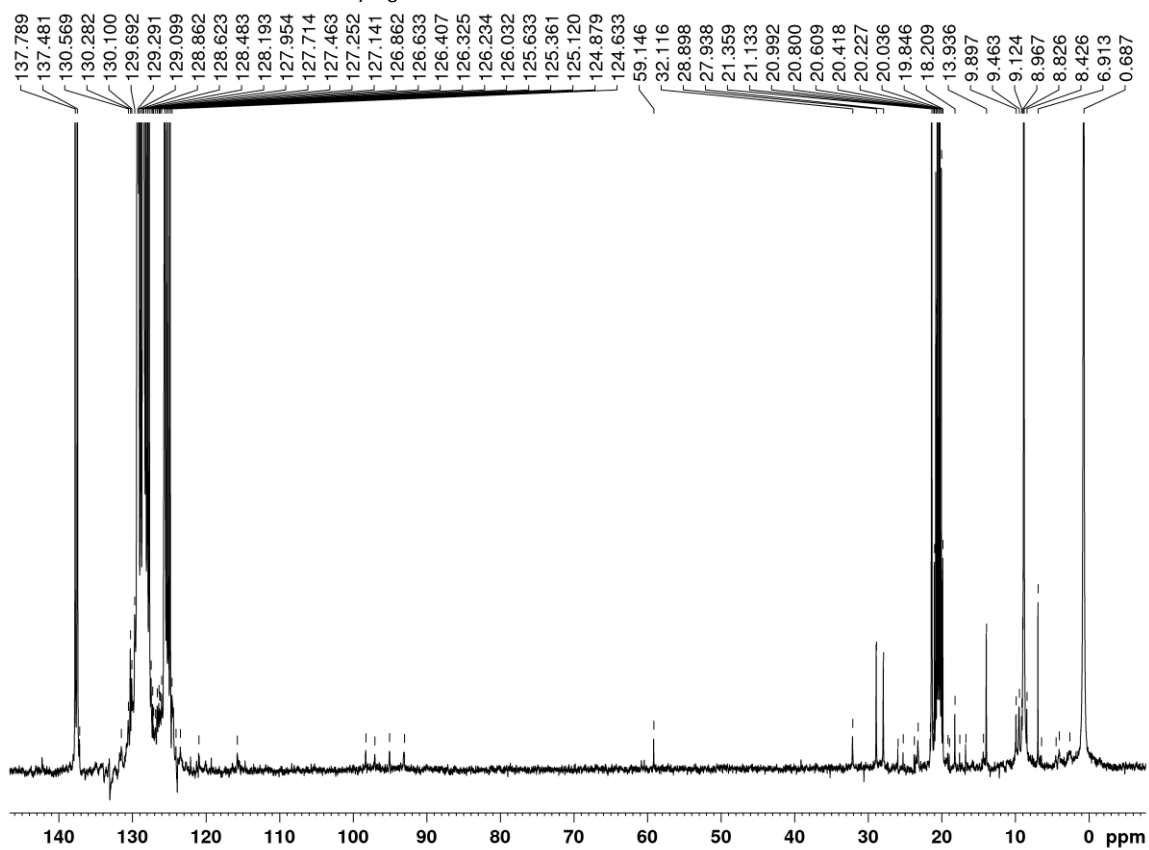
Figure S51. COSY HH of **17I** in C_7D_8 at 298 K.Figure S52. ^{13}C NMR of **17I** in C_7D_8 at 298 K.

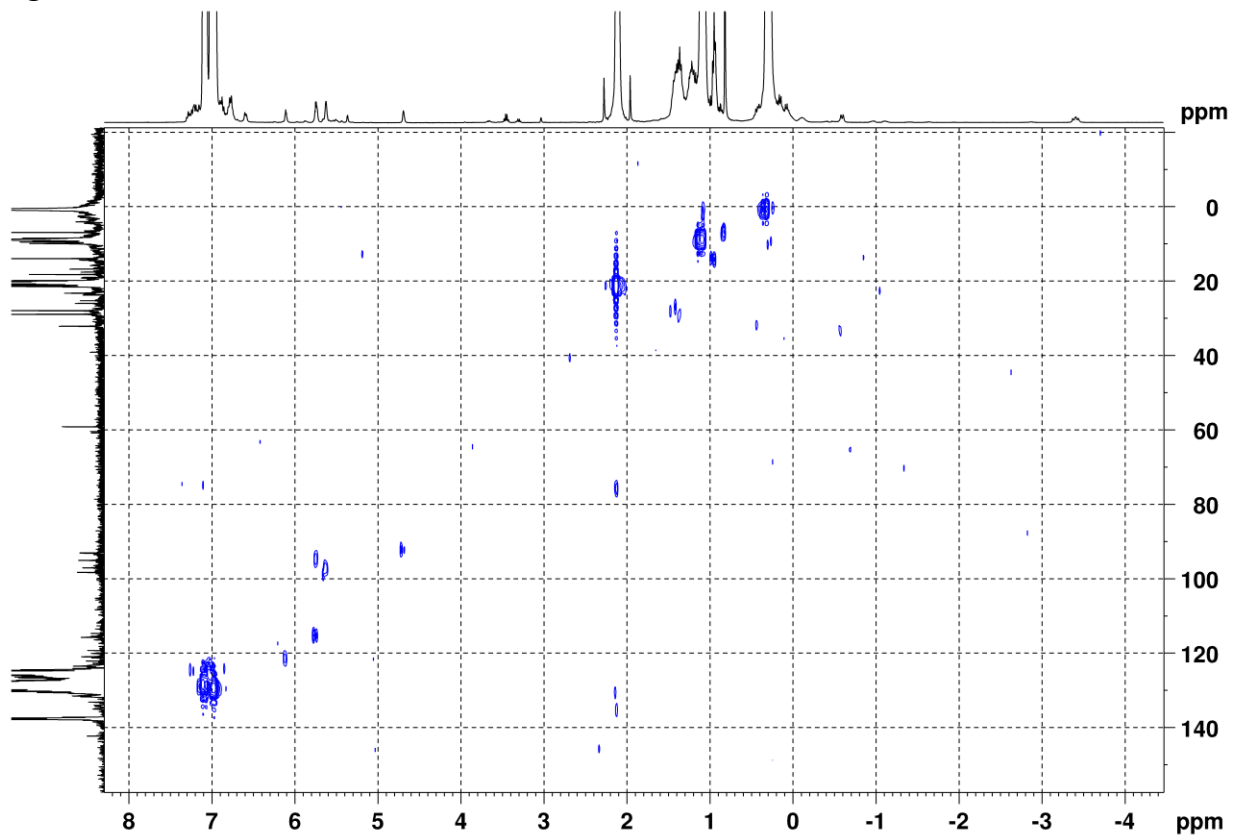
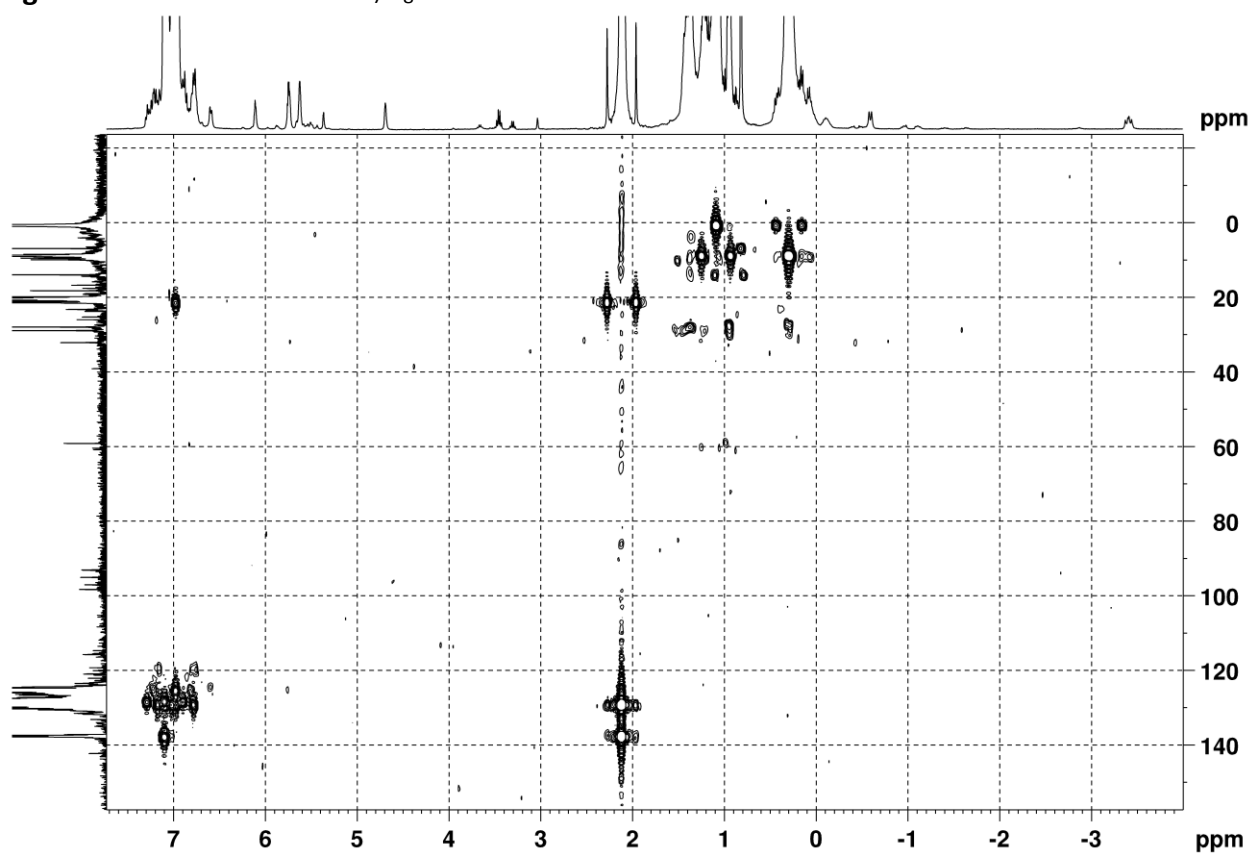
Figure S53. HSQC of **17I** in C_7D_8 at 298 K.Figure S54. HMBC of **17I** in C_7D_8 at 298 K.

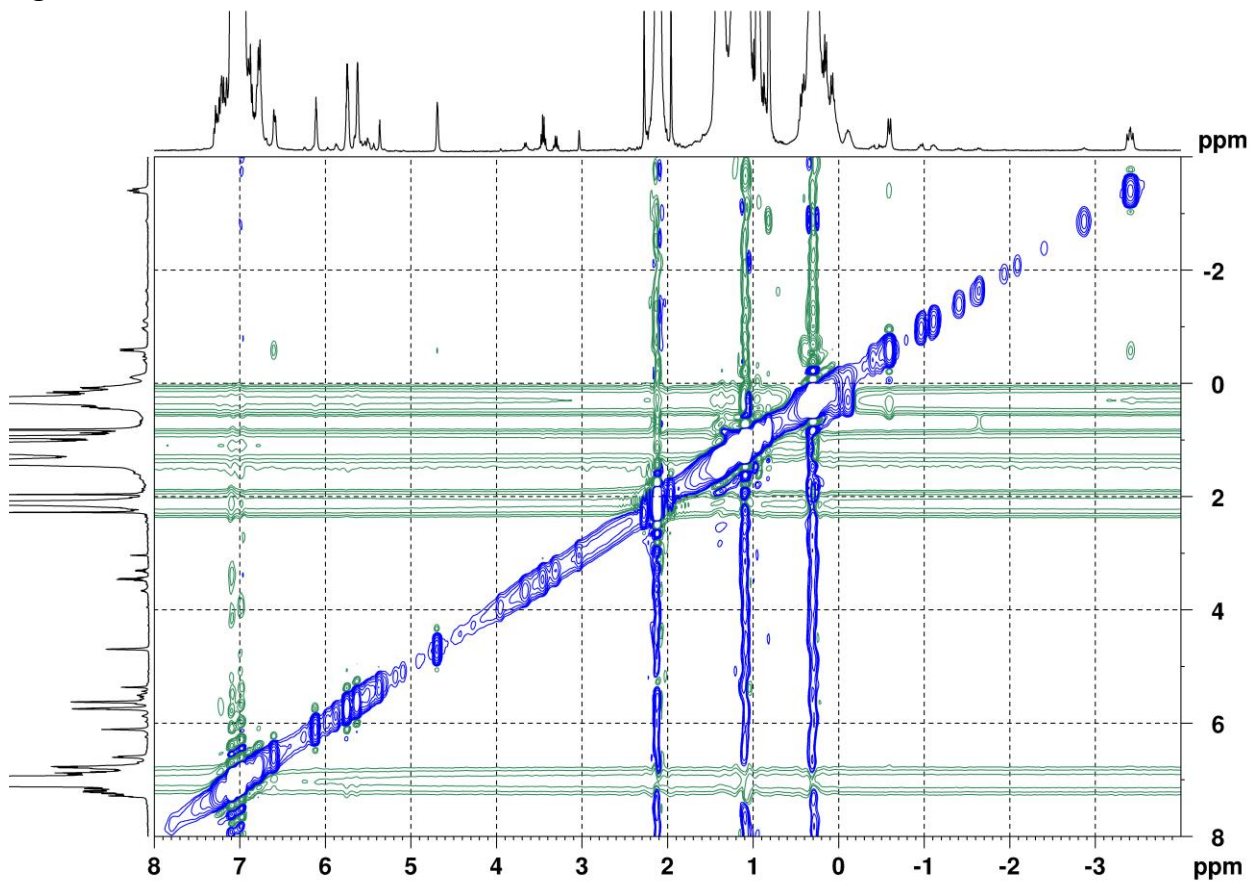
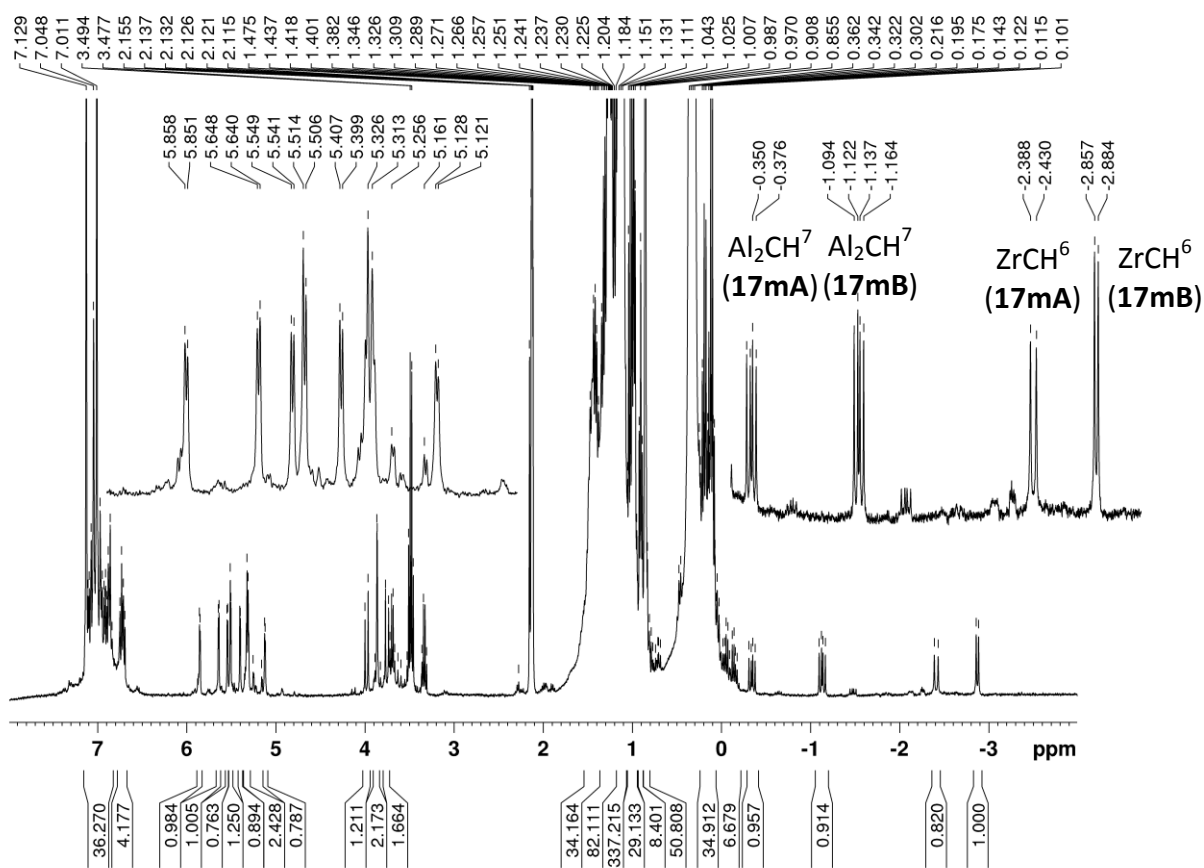
Figure S55. NOESY of **17l** in C_7D_8 at 298 K.Figure S56. 1H NMR of **17m** obtained by the reaction of **1m** with $(AlEt_3)_2$ (1:13) in C_7D_8 at 299 K.

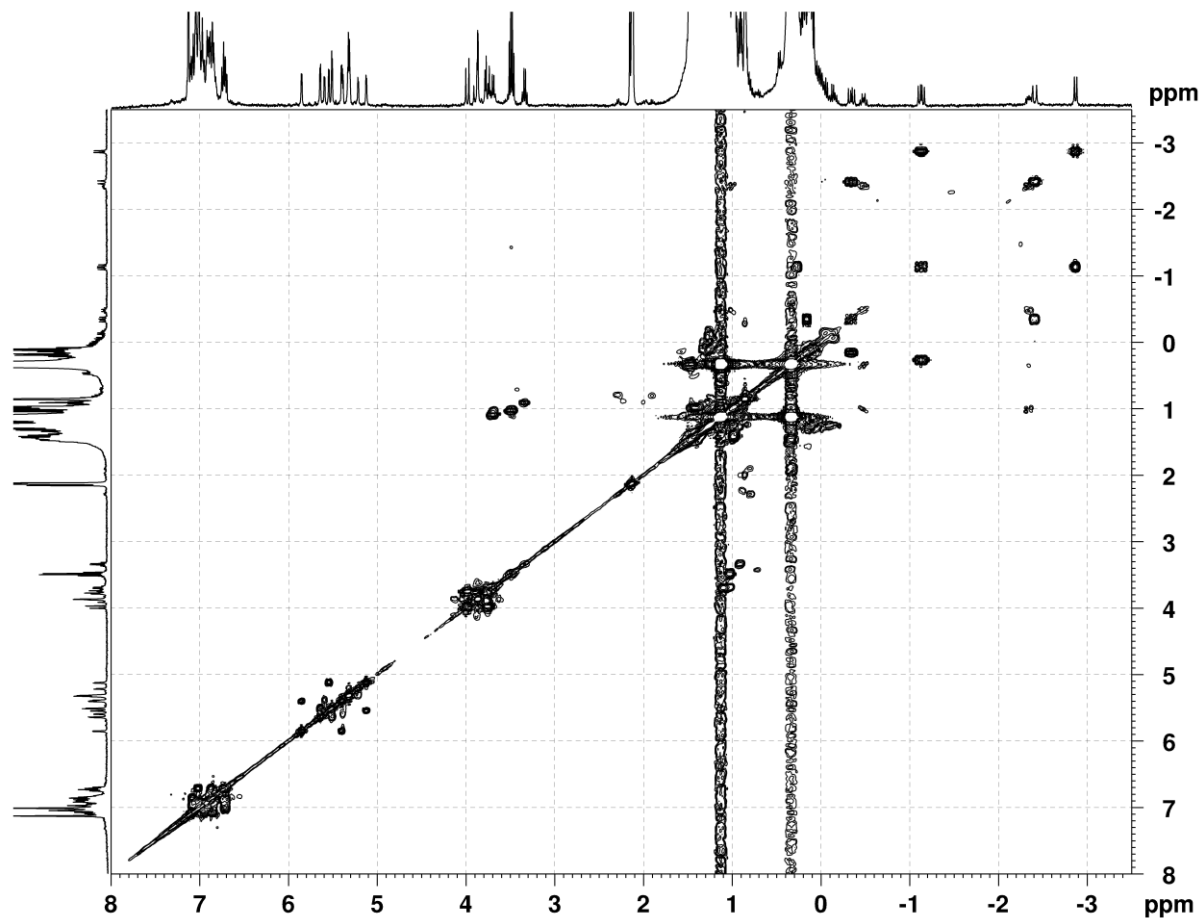
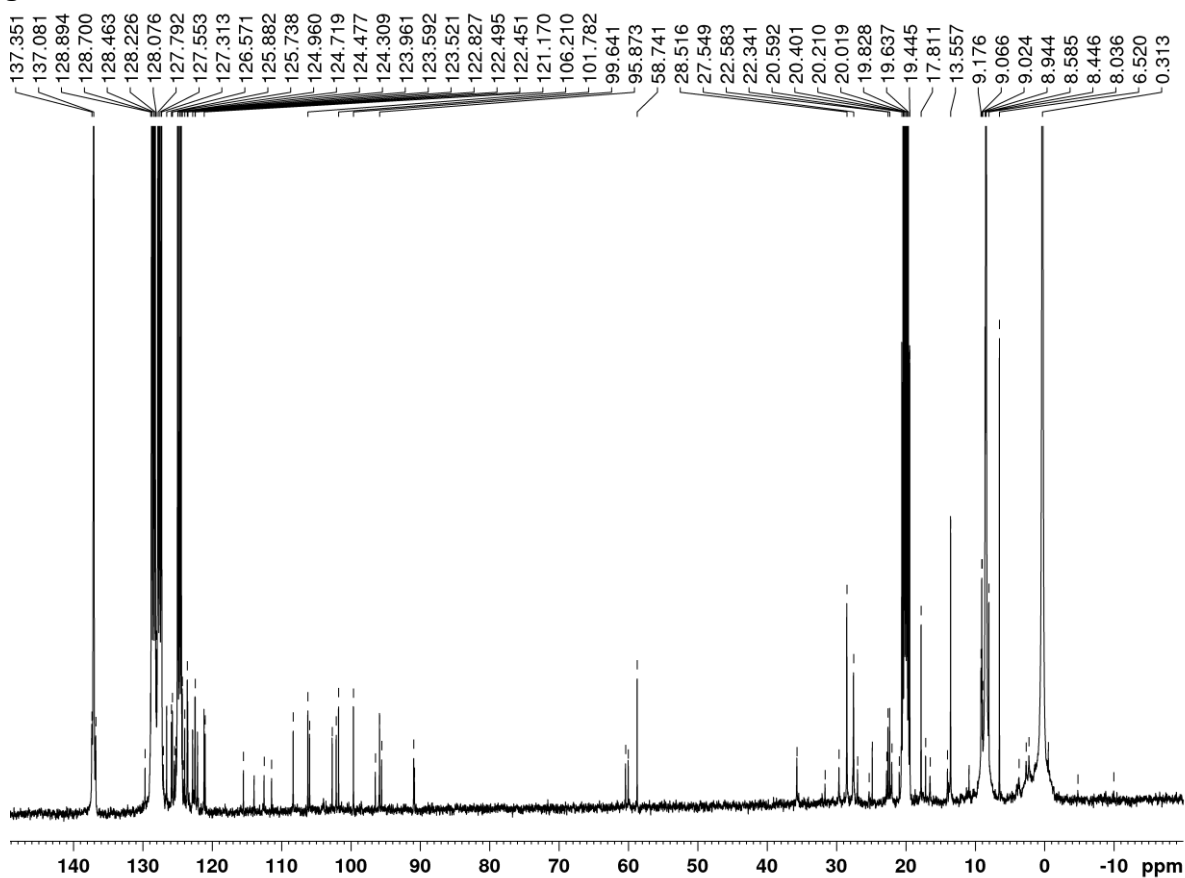
Figure S57. COSY HH of **17m** in C₇D₈ at 299 K.Figure S58. ¹³C NMR of **17m** in C₇D₈ at 299 K.

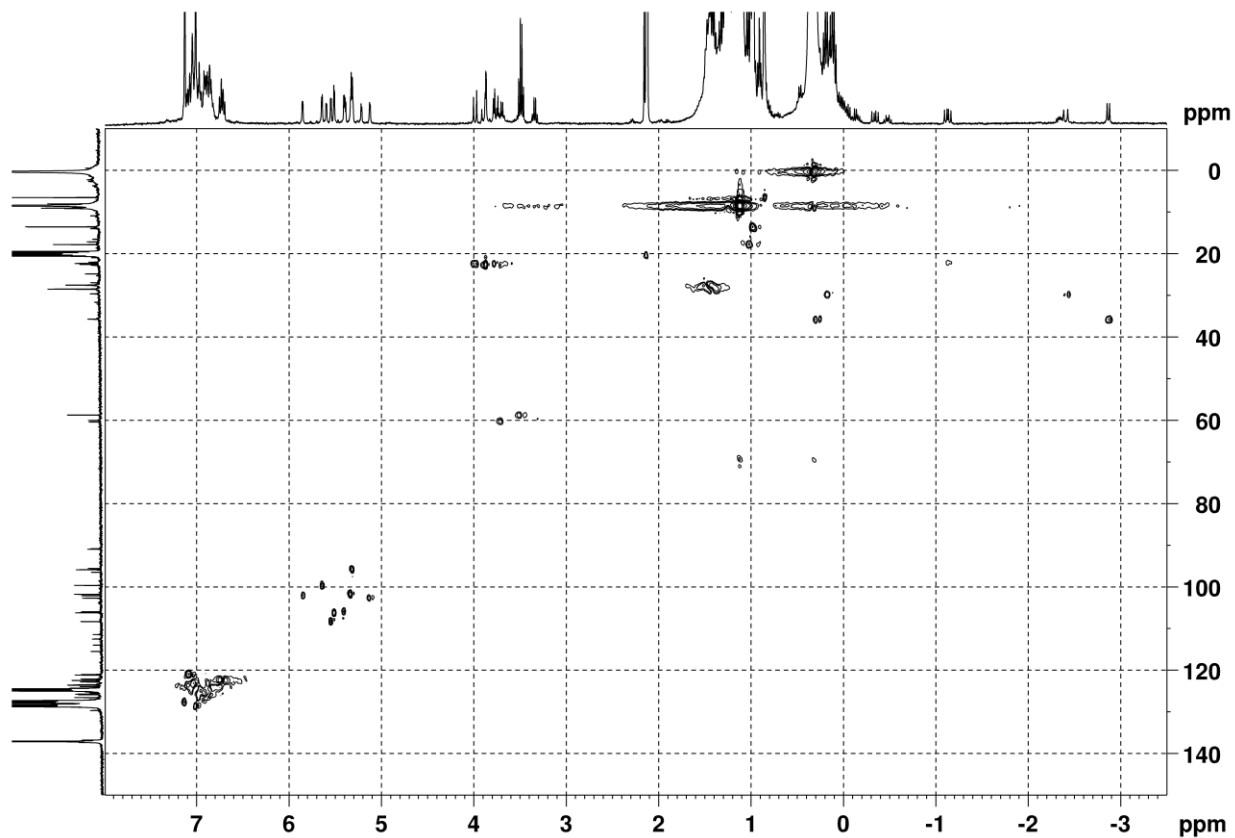
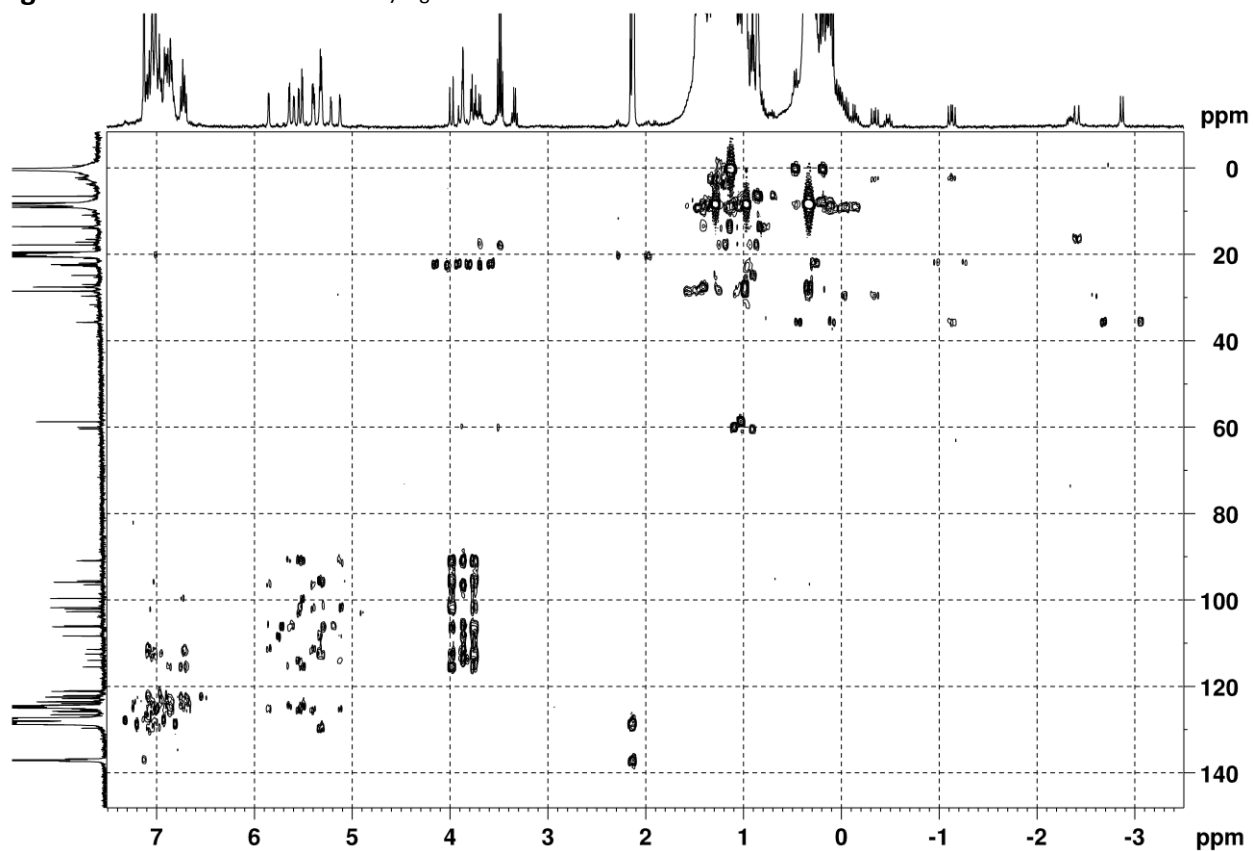
Figure S59. HSQC of **17m** in C_7D_8 at 299 K.Figure S60. HMBC of **17m** in C_7D_8 at 299 K.

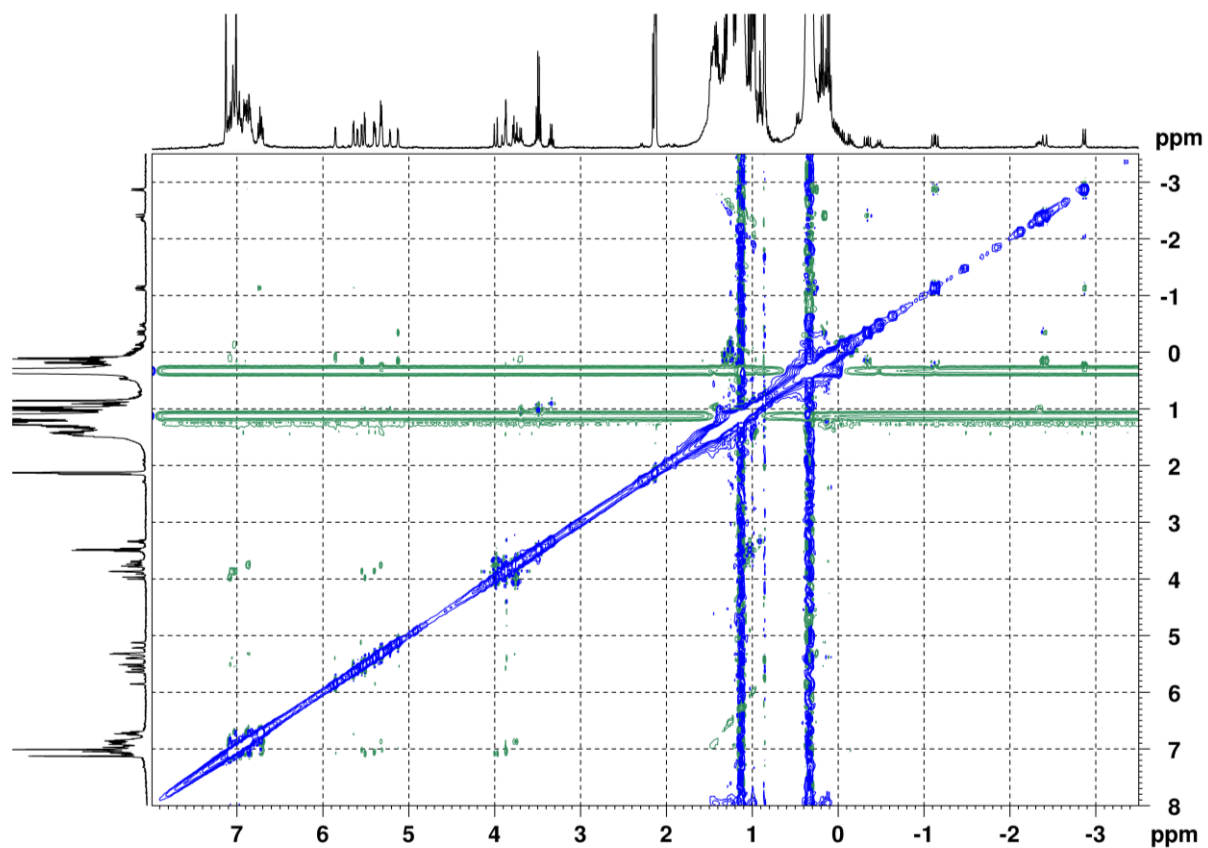
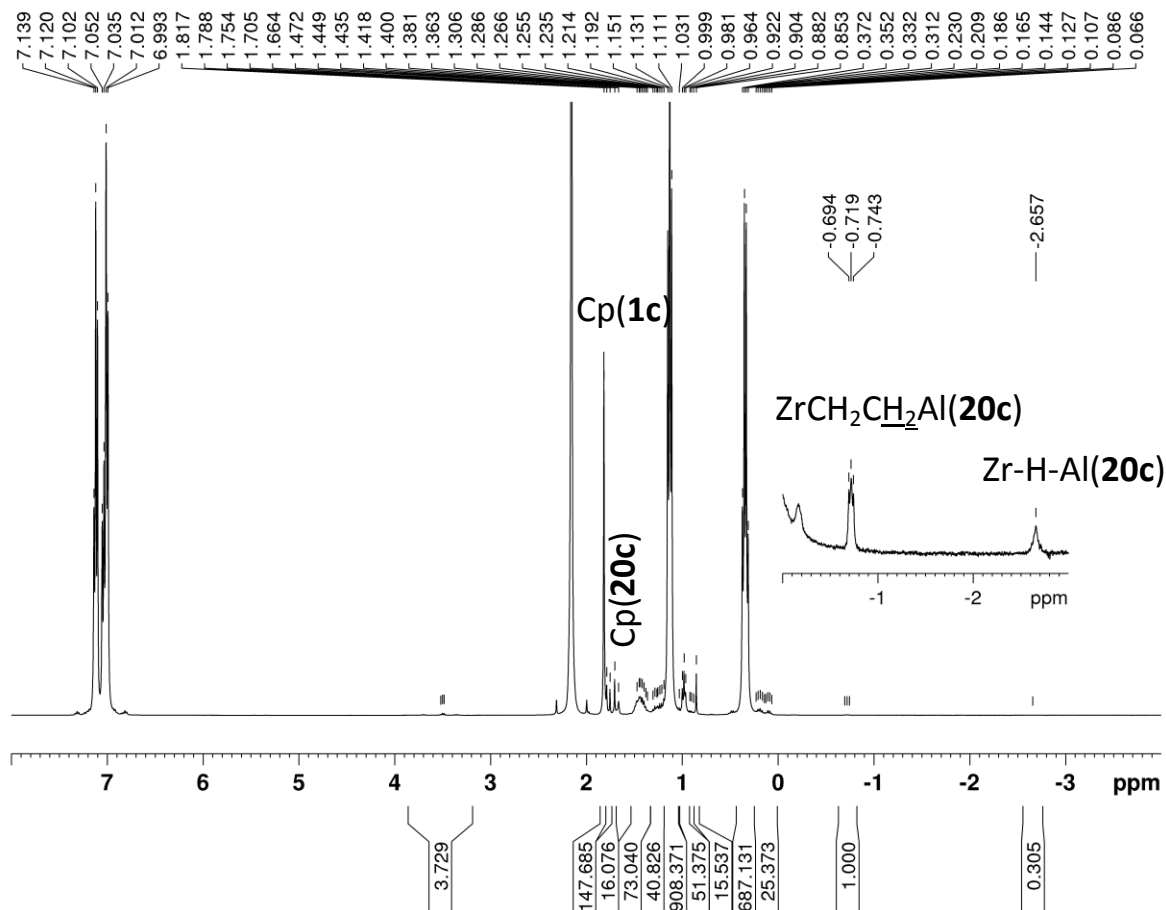
Figure S61. NOESY of **17m** in C_7D_8 at 299 K.Figure S62. 1H NMR of system $Cp^*_2ZrCl_2$ (**1c**) - $(AlEt_3)_2$ (1:20) in C_7D_8 at 299 K.

Figure S63. COSY HH of system Cp*₂ZrCl₂ (**1c**) - (AlEt₃)₂ (1:20) in C₇D₈.

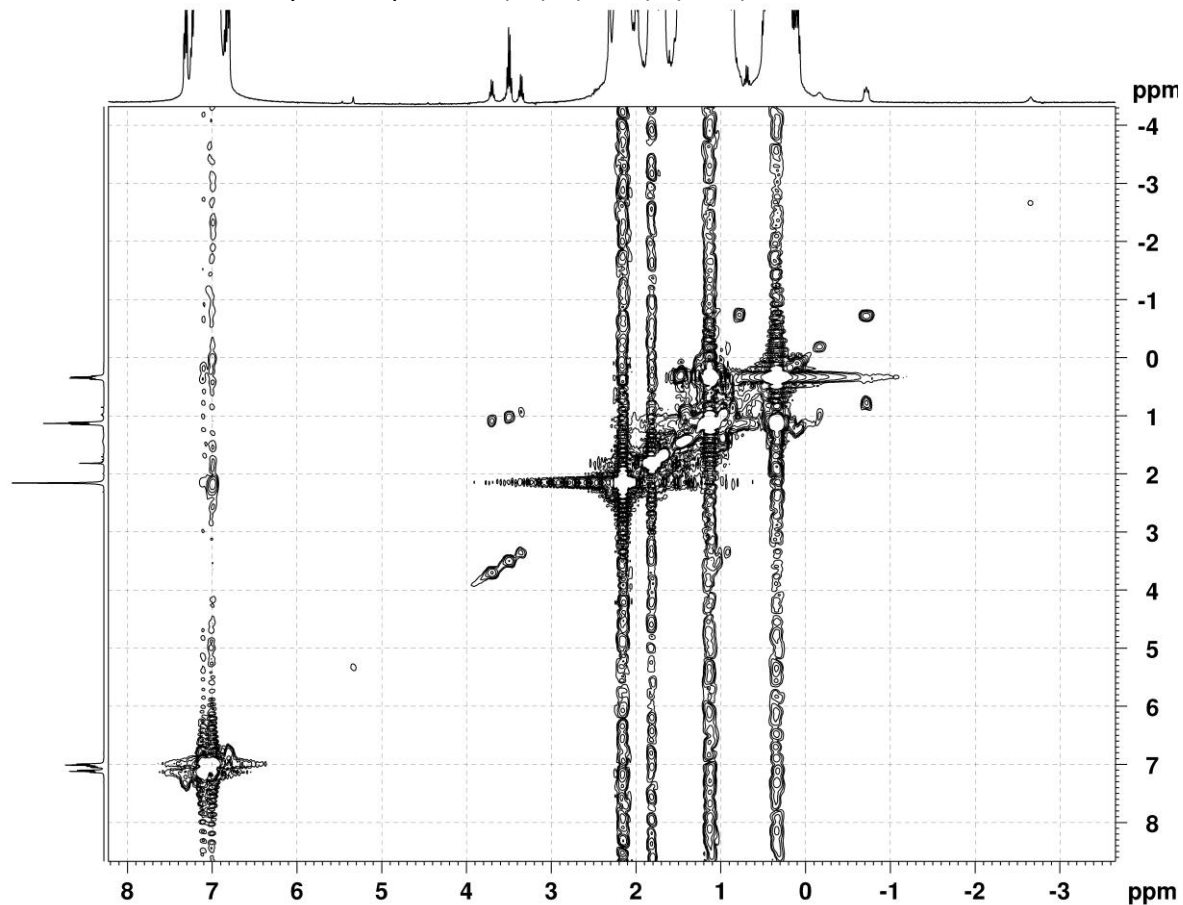


Figure S64. ¹H NMR of **20h** obtained by the reaction of **1h** with (AlEt₃)₂ (1:11) in C₇D₈ at 290 K.

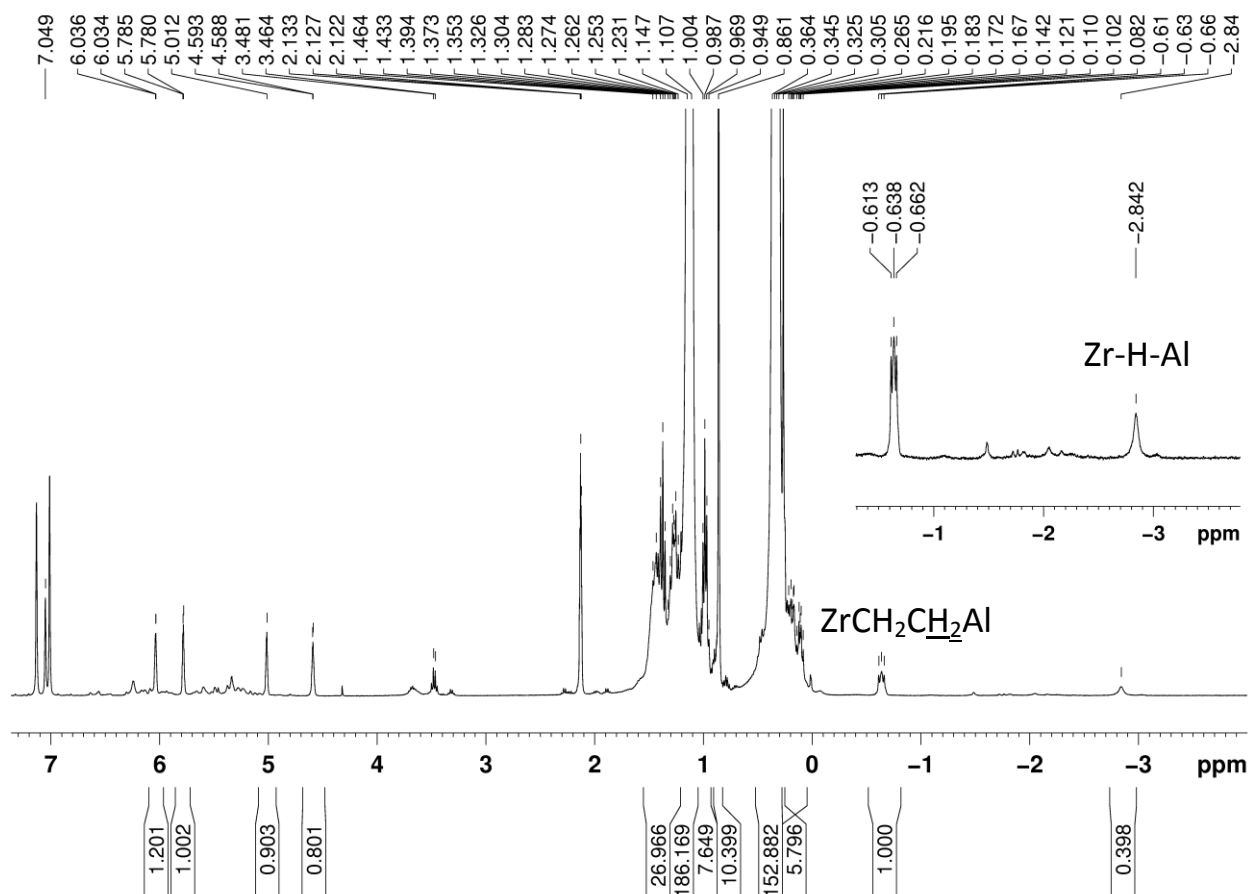


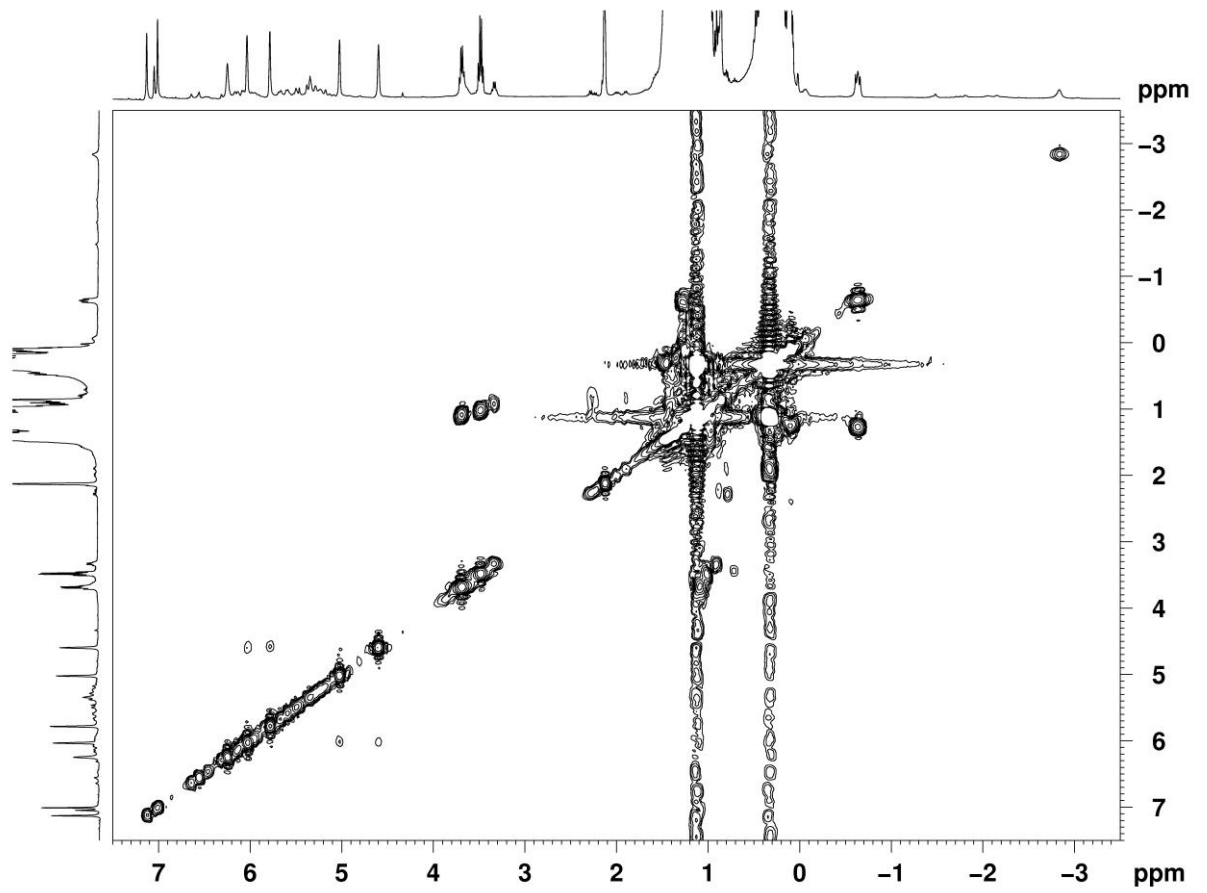
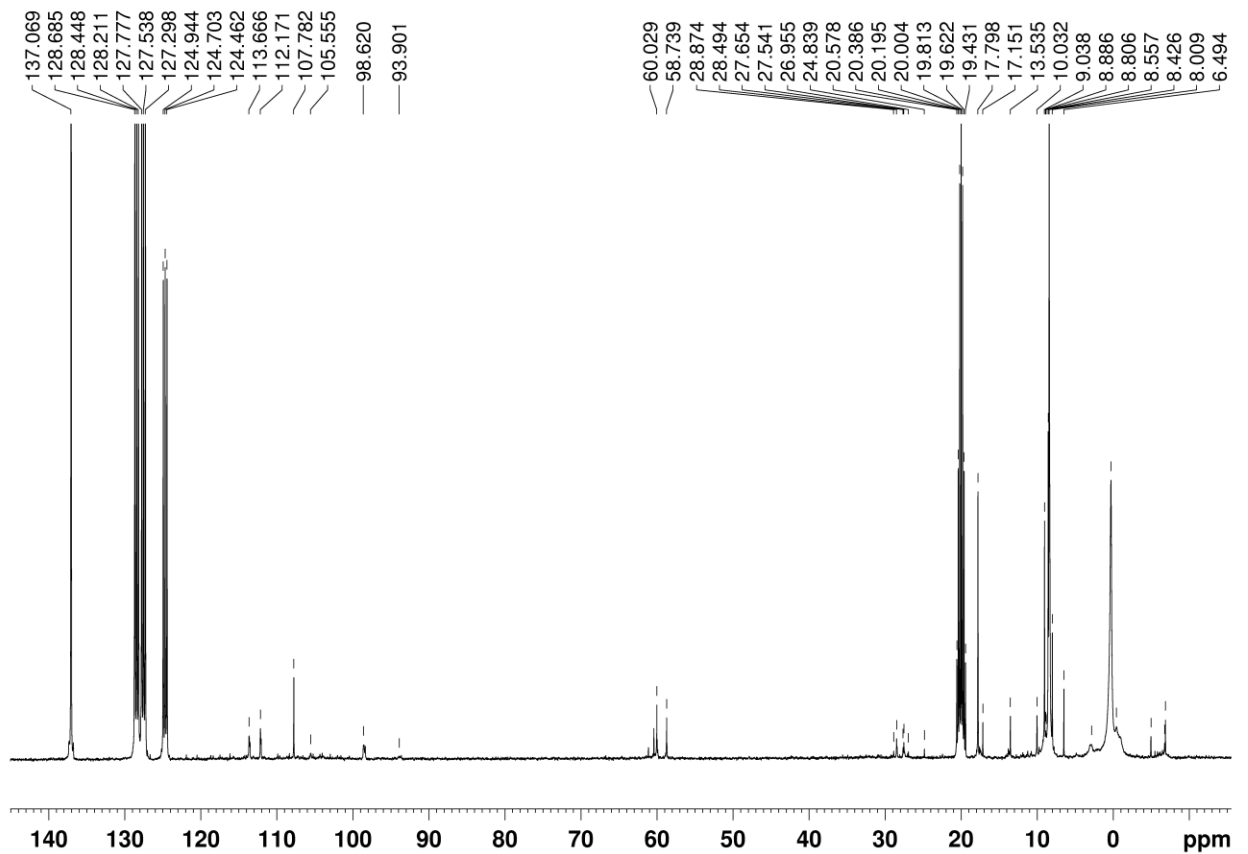
Figure S65. COSY HH of **20h** in C_7D_8 at 290 K.Figure S66. ^{13}C NMR of **20h** in C_7D_8 at 290 K.

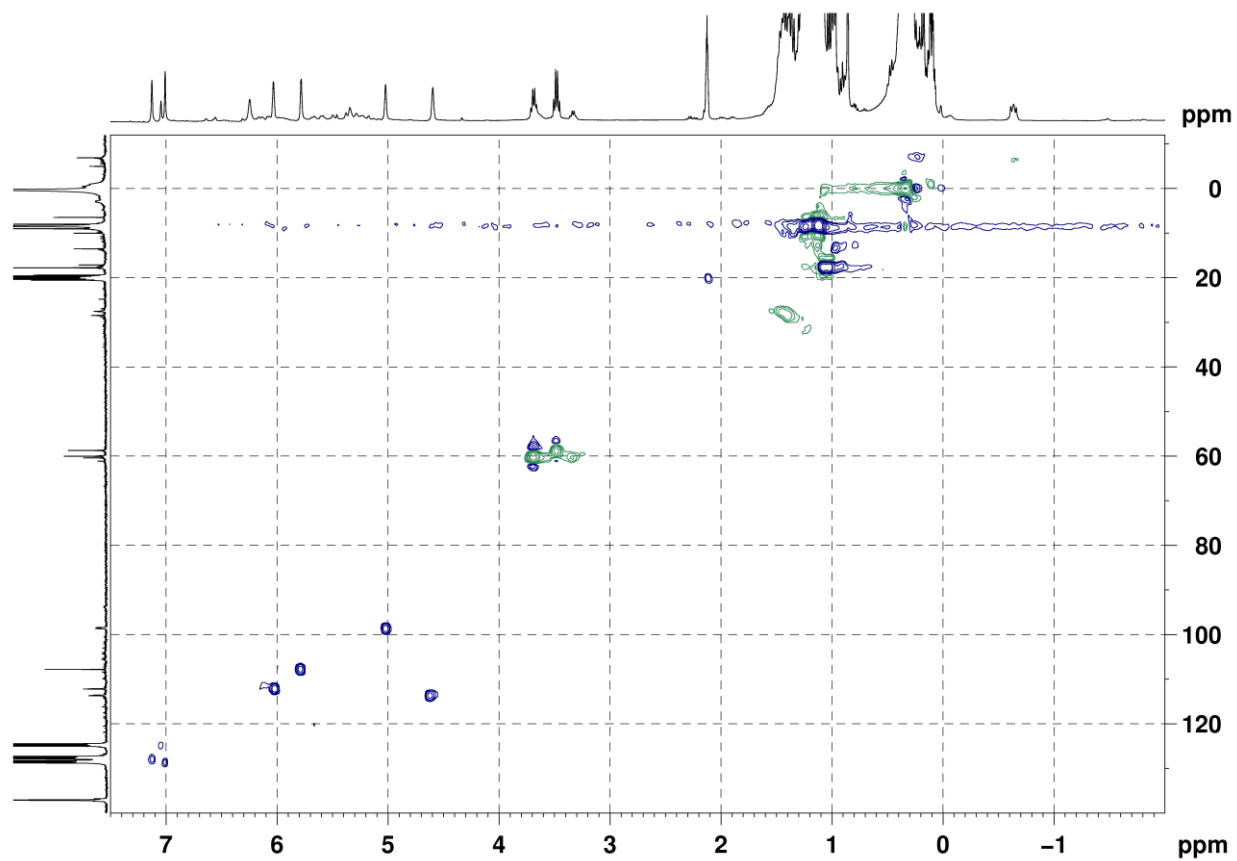
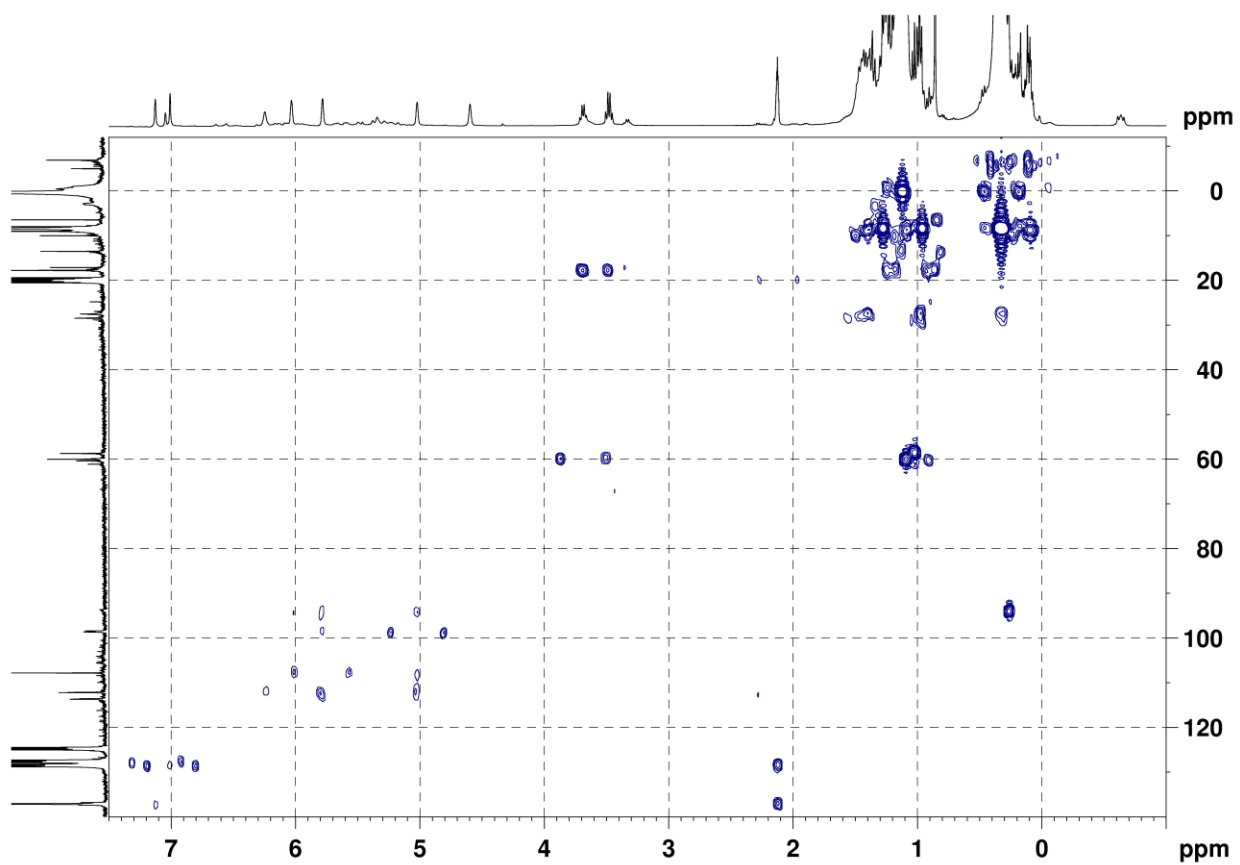
Figure S67. HSQC of **20h** in C_7D_8 at 290 K.Figure S68. HMBC of **20h** in C_7D_8 at 290 K.

Figure S69. ^1H NMR of **20p** obtained by the reaction of **1p** with $(\text{AlEt}_3)_2$ (1:13) in C_7D_8 at 305 K.

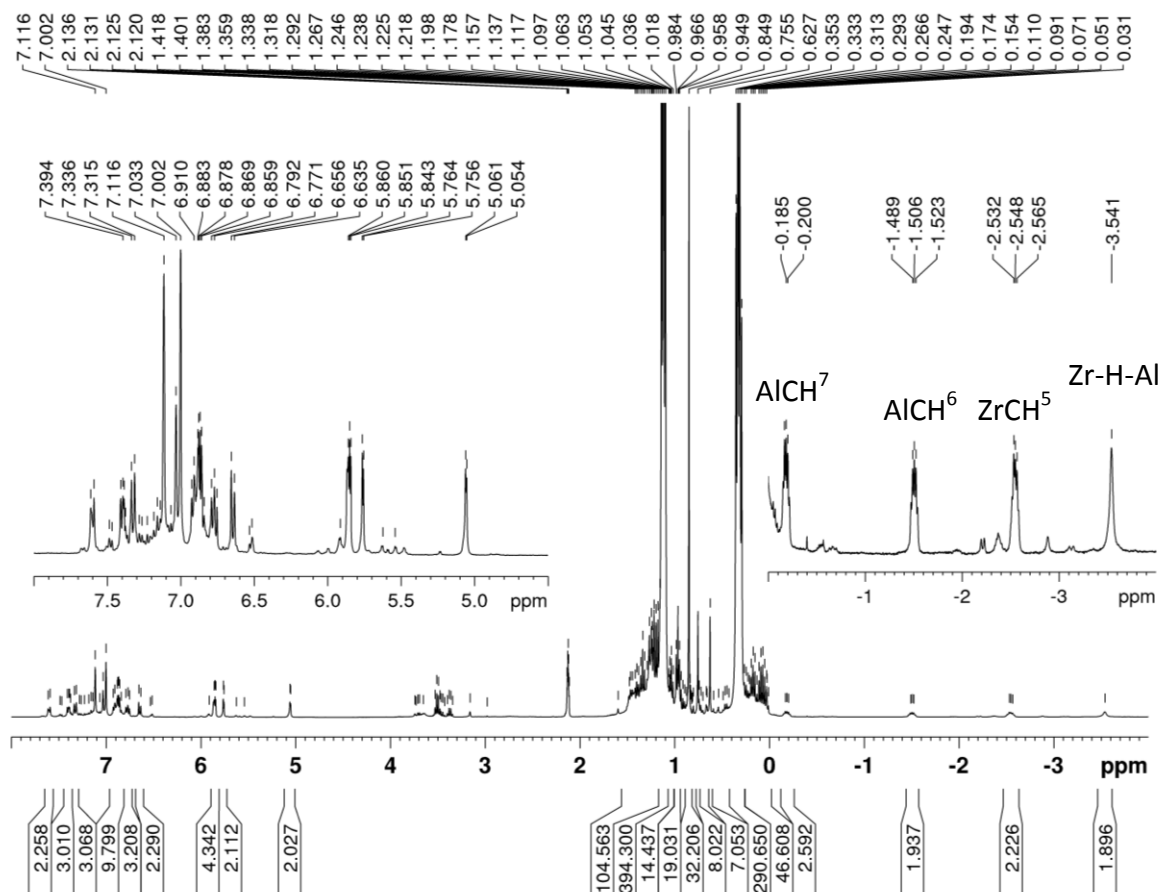


Figure S70. COSY HH of **20p** in C_7D_8 at 299 K.

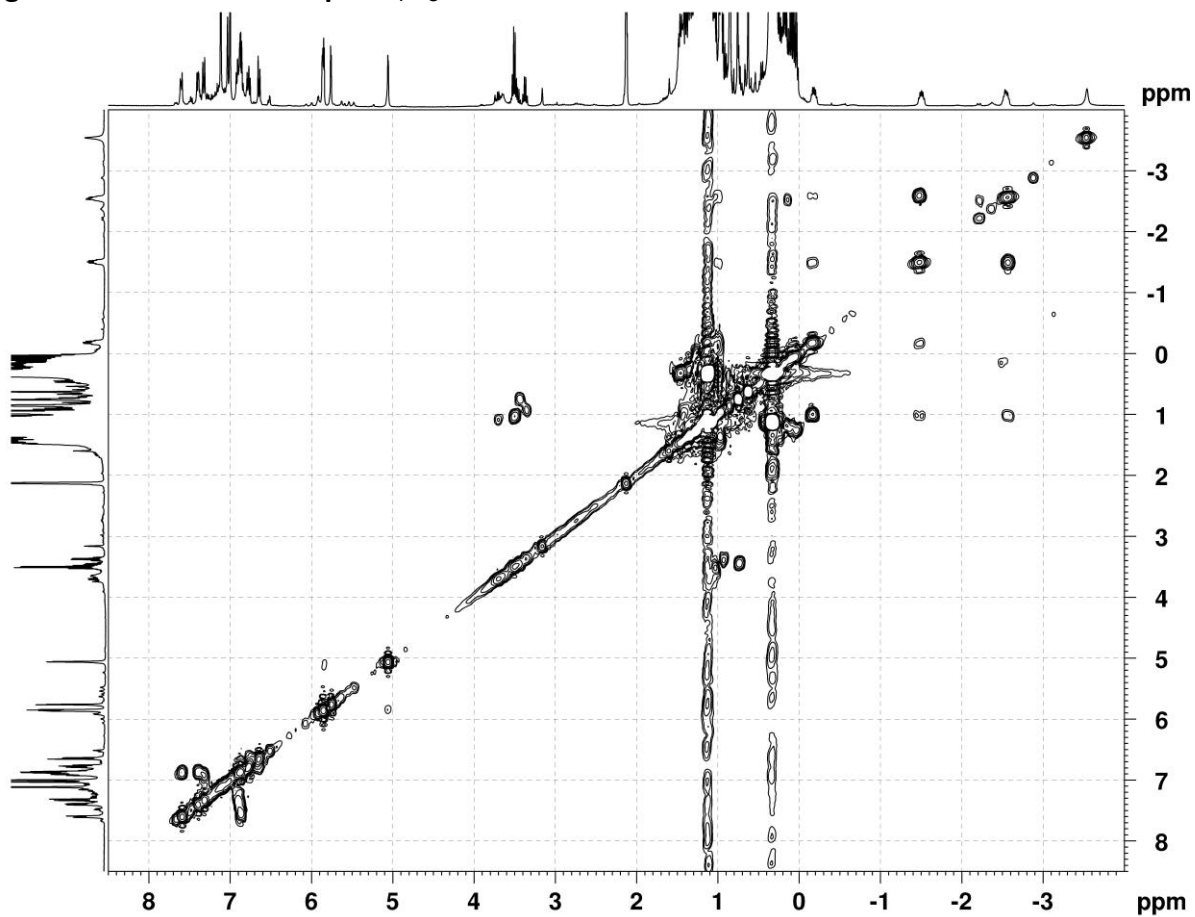


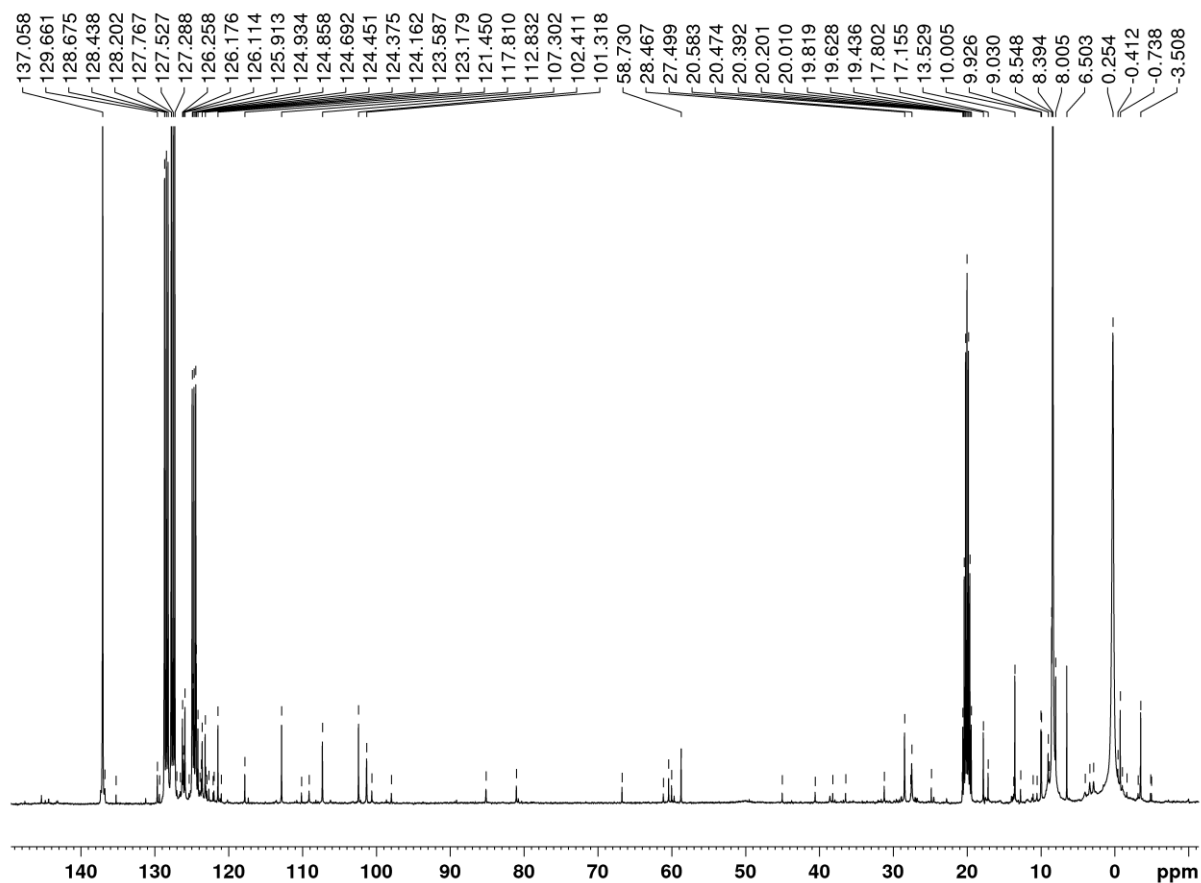
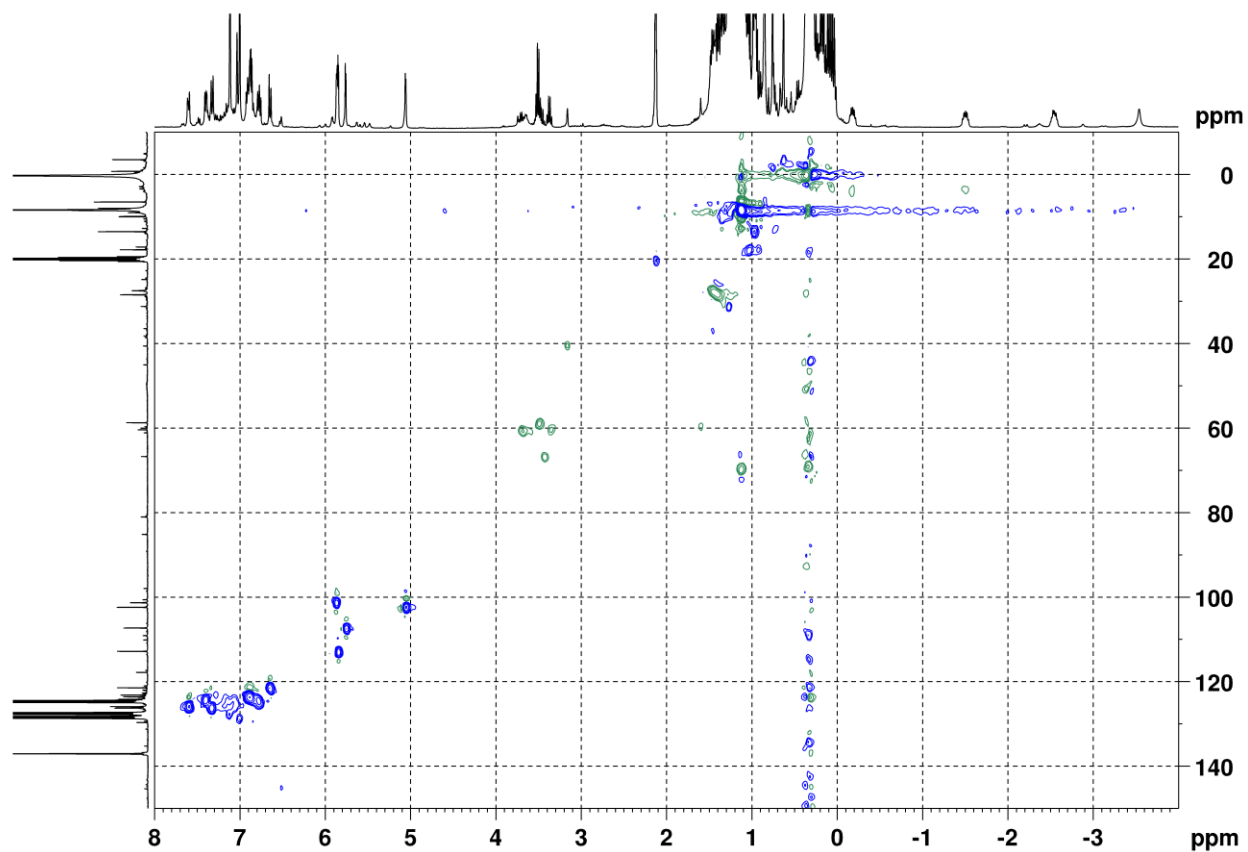
Figure S71. ^{13}C NMR of **20p** in C_7D_8 at 299 K.**Figure S72.** HSQC of **20p** in C_7D_8 at 299 K.

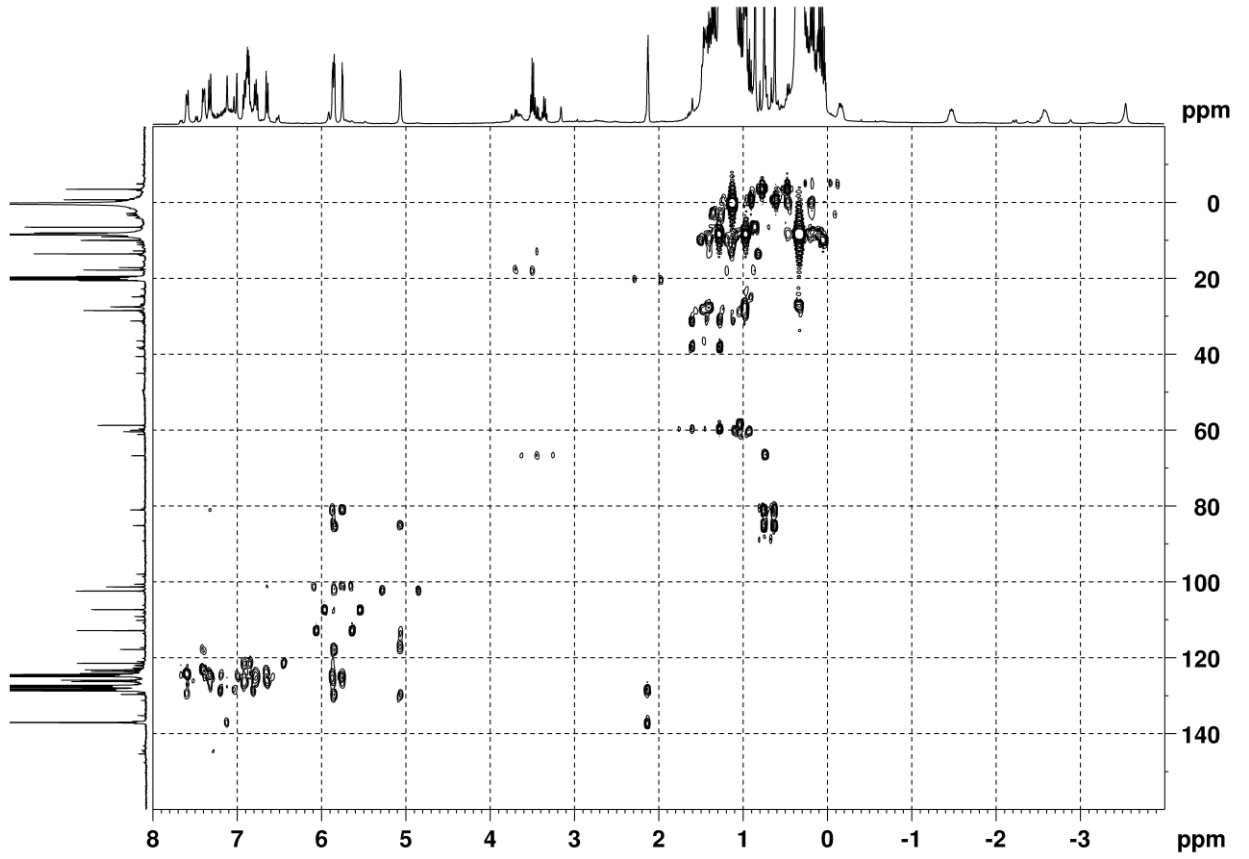
Figure S73. HMBC of **20p** in C_7D_8 at 299 K.

Figure S74. ^1H NMR of **20q** obtained by the reaction of **1q** with $(\text{AlEt}_3)_2$ (1:13) in CD_2Cl_2 at 298 K.

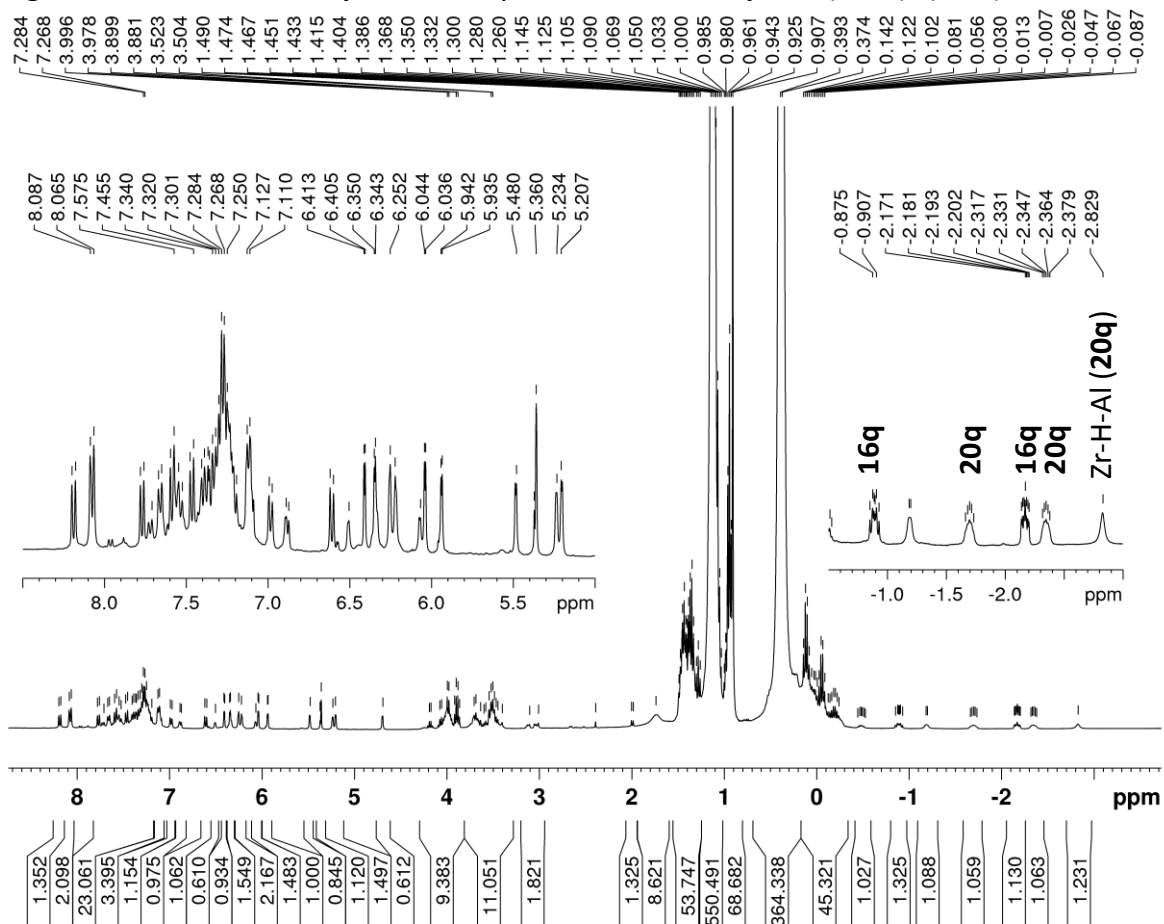


Figure S75. COSY HH of **20q** in CD_2Cl_2 at 298 K.

